



HAL
open science

Imaging in patients with cardiovascular implantable electronic devices - Part 1: Imaging before and during device implantation. A clinical consensus statement of the European Association of Cardiovascular Imaging (EACVI) and the European Heart Rhythm Association (EHRA) of the ESC

Ivan Stankovic, Jens-Uwe Voigt, Haran Burri, Denisa Muraru, L. Elif Sade, Kristina Hermann Haugaa, Joost Lumens, Mauro Biffi, Jean-Nicolas Dacher, Nina Ajmone Marsan, et al.

► **To cite this version:**

Ivan Stankovic, Jens-Uwe Voigt, Haran Burri, Denisa Muraru, L. Elif Sade, et al.. Imaging in patients with cardiovascular implantable electronic devices - Part 1: Imaging before and during device implantation. A clinical consensus statement of the European Association of Cardiovascular Imaging (EACVI) and the European Heart Rhythm Association (EHRA) of the ESC. *European Heart Journal - Cardiovascular Imaging*, 2023, 25 (1), pp.e1-e32. 10.1093/ehjci/jead272 . hal-04279107

HAL Id: hal-04279107

<https://hal.science/hal-04279107>

Submitted on 9 Jul 2024

HAL is a multi-disciplinary open access archive for the deposit and dissemination of scientific research documents, whether they are published or not. The documents may come from teaching and research institutions in France or abroad, or from public or private research centers.

L'archive ouverte pluridisciplinaire **HAL**, est destinée au dépôt et à la diffusion de documents scientifiques de niveau recherche, publiés ou non, émanant des établissements d'enseignement et de recherche français ou étrangers, des laboratoires publics ou privés.



Distributed under a Creative Commons Attribution - NonCommercial 4.0 International License

1 **Imaging in patients with cardiovascular implantable electronic devices – Part**
2 **1: Imaging before and during device implantation**

3
4 **A clinical consensus statement of the European Association of Cardiovascular Imaging (EACVI)**
5 **and the European Heart Rhythm Association (EHRA) of the ESC**

7 Ivan Stankovic¹, Jens-Uwe Voigt², Haran Burri³ (EHRA representative), Denisa Muraru^{4,5}, L. Elif
8 Sade⁶, Kristina Hermann Haugaa^{7,8}, Joost Lumens⁹, Mauro Biffi¹⁰ (EHRA representative), Jean-
9 Nicolas Dacher¹¹, Nina Ajmone Marsan¹², Elise Bakelants³ (EHRA representative), Charlotte
10 Manisty^{13,14}, Marc R Dweck¹⁵, Otto A. Smiseth¹⁶, Erwan Donal¹⁷

11 **Reviewers:** This document was reviewed by members of the 2020-2022 EACVI Scientific
12 Documents Committee: Daniele Andreini, Magnus Bäck, Philippe B. Bertrand, Niall Keenan, Danilo
13 Neglia; and by the 2020-2022 EACVI President: Bernard Cosyns.

14 1) Clinical Hospital Centre Zemun, Department of Cardiology, Faculty of Medicine, University of Belgrade, Belgrade,
15 Serbia

16 2) Department of Cardiovascular Diseases, University Hospitals Leuven / Department of Cardiovascular Sciences,
17 Catholic University of Leuven, Herestraat 49, 3000 Leuven. Belgium

18 3) Cardiac Pacing Unit, Cardiology Department, University Hospital of Geneva, Geneva, Switzerland

19 4) Department of Medicine and Surgery, University of Milano-Bicocca, Milan, Italy

20 5) Department of Cardiology, Istituto Auxologico Italiano, IRCCS, Milan, Italy

21 6) University of Pittsburgh Medical Center, Heart and Vascular Institute, Pittsburgh, PA, USA

22 7) ProCardio Center for Innovation, Department of Cardiology, Oslo University Hospital, Rikshospitalet, Norway

23 8) Faculty of Medicine Karolinska Institutet AND Cardiovascular Division, Karolinska University Hospital, Stockholm
24 Sweden

25 9) Cardiovascular Research Center Maastricht (CARIM), Maastricht University, Maastricht, Netherlands

26 10) Department of Cardiology, IRCCS, Azienda Ospedaliero Universitaria Di Bologna, Policlinico Di S.Orsola, Bologna,
27 Italy

28 11) Department of Radiology, Normandie University, UNIROUEN, INSERM U1096 - Rouen University Hospital, F 76000,
29 Rouen, France

30 12) Department of Cardiology, Heart and Lung Center, Leiden University Medical Center, The Netherlands

31 13) Department of Cardiovascular Imaging, Barts Heart Centre, Barts Health NHS Trust, London, UK

32 14) Institute of Cardiovascular Science, University College London, London, UK

- 1 15) Centre for Cardiovascular Science, University of Edinburgh, Little France Crescent, Edinburgh EH16 4SB, United
2 Kingdom
3 16) Institute for Surgical Research, Oslo University Hospital and University of Oslo, Oslo, Norway
4 17) University of Rennes, CHU Rennes, Inserm, LTSI-UMR 1099, Rennes, France
5
6

7 **Abstract**

8 More than 500,000 cardiovascular implantable electronic devices (CIED) are implanted in the
9 European Society of Cardiology countries each year. The role of cardiovascular imaging in patients
10 being considered for CIED is distinctly different from imaging in CIED recipients. In the former
11 group, imaging can help identify specific or potentially reversible causes of heart block, the
12 underlying tissue characteristics associated with malignant arrhythmias, the mechanical
13 consequences of conduction delays and can also aid challenging lead placements. On the other
14 hand, cardiovascular imaging is required in CIED recipients both for standard indications, and to
15 assess the response to device implantation, to diagnose immediate and delayed complications
16 after implantation, and to guide device optimization. The present clinical consensus statement
17 (Part 1) from the European Association of Cardiovascular Imaging, in collaboration with the
18 European Heart Rhythm Association, provides comprehensive, up-to-date and evidence-based
19 guidance to cardiologists, cardiac imagers and pacing specialists regarding the use of imaging in
20 patients undergoing implantation of conventional pacemakers, cardioverter defibrillators and
21 resynchronization therapy devices. The document summarizes the existing evidence regarding the
22 use of imaging in patient selection and during the implantation procedure and also underlines
23 gaps in evidence in the field. The role of imaging after CIED implantation is discussed in the second
24 document (Part 2).

25

26 **Keywords:** multimodality imaging, cardiovascular implantable electronic devices, pacemaker,
27 cardiac resynchronization therapy, defibrillator

28

29

1 Introduction

2 More than 500,000 pacemakers and cardiac devices are implanted in the European Society of
3 Cardiology (ESC) countries each year (1). There is strong evidence that the implantation of cardiac
4 devices improves patients' outcomes, while the evidence that cardiac imaging can improve patient
5 selection and performance of these devices is growing.

6 The role of cardiac imaging in patients being considered for cardiovascular implantable electronic
7 devices (CIED) is distinctly different from imaging in CIED recipients. In the former group, imaging
8 can help identify specific or potentially reversible causes of heart block, the underlying tissue
9 characteristics associated with malignant arrhythmias, the mechanical consequences of
10 conduction delays and can also aid challenging lead placements. Furthermore, this is an area of
11 ongoing vibrant research aimed at identifying and filling evidence gaps to improve or refine
12 strategies for selecting patients for implantation of different types of CIEDs.

13 On the other hand, cardiac imaging is required for standard indications in CIED recipients,
14 alongside to assess the response to device implantation, to diagnose immediate and delayed
15 complications after implantation, and to guide device optimization.

16 This document is the first (Part 1) of two clinical consensus statements on imaging in patients with
17 CIEDs and aims to provide comprehensive, up-to-date and evidence-based guidance to
18 cardiologists, cardiac imagers and pacing specialists regarding the use of imaging in patients
19 undergoing implantation of CIEDs: conventional antibradycardia pacemakers, implantable
20 cardioverter defibrillators (ICD) and cardiac resynchronization therapy devices (CRT). The
21 document summarizes the existing evidence regarding the use of imaging in patient selection and
22 during the implantation procedure and also underlines gaps in evidence in the field. The role of
23 imaging after device implantation is discussed in the second document (Part 2).

24

25 Methodology

26 This clinical statement statement is based on a review of the literature performed by the members
27 of the writing group. The clinical advice is based upon the evidence and/or consensus of the writing
28 group and is classified into several categories, as shown in Table 1.

29

1
2
3
4
5
6
7
8
9
10
11
12
13
14
15
16
17
18
19
20
21
22
23
24
25

I. General aspects of pre-implantation imaging

In the 2021 ESC guidelines on cardiac pacing and CRT, and 2022 ESC guidelines for the management of patients with ventricular arrhythmias (VA) and the prevention of sudden cardiac death (SCD), imaging is recognized as a crucial tool to assess cardiac function and also to detect the heterogenous conditions associated with conduction abnormalities, VA and SCD (2,3). Accurately diagnosing the underlying disease state may have an impact on decisions regarding the type of CIED that will be implanted (e.g. conventional antibradycardia pacing or ICD in hypertrophic cardiomyopathy), lead to the initiation of disease-specific treatments (e.g. for transthyretin cardiac amyloidosis or Fabry disease) or both (e.g. ICD and immunosuppression in cardiac sarcoidosis) leading to improved patient outcomes. Regardless of the underlying disease state(s), the assessment of left ventricular (LV) systolic function by measuring LV ejection fraction (LVEF) is a common step in the diagnostic work-up of patients being considered for CIED implantation. An overview of the different LVEF cut-off values proposed by the current ESC guidelines to help guide which type of CIED should be implanted in various underlying conditions is shown in **Figure 1**. It should be noted that other imaging parameters, in particular assessments of myocardial scar, can also be used to refine decision-making in patients being considered for CIED implantation, particularly when LVEF is preserved (e.g. scar burden in hypertrophic cardiomyopathy). In addition, pre-implantation cardiac imaging can also help identify the diverse, mainly anatomical reasons that might lead to challenging CIED lead placement (**Table 2**). In this introductory chapter, we discuss common aspects of pre-implantation cardiac imaging: the assessment of LV systolic function and the use of imaging in potentially challenging lead placement scenarios. Specific issues regarding the use of cardiac imaging to help guide the implantation of the different types of CIEDs will be discussed in the respective chapters of this document.

1.1 Assessment of LV systolic function

The assessment of LV size and function plays a pivotal role in patients undergoing device therapy. The general echocardiographic approach has been described in the EACVI/ASE document on chamber quantification (4). In short, LV volumes and LVEF can be measured using two- (2DE) or

1 three-dimensional echocardiography (3DE). Calculations from linear measurements (e.g.
2 Teichholz and Quinones methods) are no longer advised. The standard method for 2DE volume
3 calculations is the biplane method of disk summation (modified Simpson's rule) where LV volumes
4 are measured by tracing the endocardial borders in the apical four- and two-chamber views.
5 Although the biplane method was mostly used to assess LVEF in the landmark ICD and CRT clinical
6 trials, it is susceptible to inaccurate endocardial border tracing and contrast agents use is advised
7 to improve endocardial delineation when two or more contiguous LV segments are poorly
8 visualized in apical views (4). Without contrast use, LVEF by 2DE and cardiovascular magnetic
9 resonance (CMR, the current imaging reference standard) may differ by $\geq 10\%$ EF units in up to
10 26% of patients (5). Furthermore, (semi-) automated measurements based on speckle tracking
11 technology may be useful, as they reduce inter- and intra-observer variability. In general, caution
12 is advised to avoid foreshortening of the LV in 2DE apical views, which typically results in volume
13 underestimation and LVEF over- or underestimation (6). However, even when images are acquired
14 by experienced operators taking care to maximize the LV long axis on apical views, foreshortening
15 of the LV is frequently inevitable. LV volume quantification is further hampered by its reliance on
16 the assumption that the LV cross section can be described by a stack of ellipsoidal disks, which can
17 be inaccurate especially in the presence of local shape abnormalities such as aneurysms (7). These
18 issues are of particular relevance, given that small differences in LVEF (5%) might determine
19 whether a patient is a candidate for an ICD or not (**Figure 1**).

20 In patients with LV dysfunction undergoing ICD implantation, 3DE LVEF is an independent
21 predictor of major arrhythmic events and improves arrhythmic risk prediction, with the potential
22 to change decisions to implant an ICD in 20% of patients (most of them having 2DE LVEFs within
23 $\pm 10\%$ from the threshold) (8). Therefore, when the value of 2DE LVEF is close to the cutoff for ICD
24 implantation ($\pm 5\%$) - particularly in patients with abnormal LV shape or extensive LV wall motion
25 abnormalities - 3DE or CMR may be helpful to confirm a patient's candidacy for primary prevention
26 ICD implantation (**Figure 2**).

27
28

1 1.2 Cardiac imaging in potentially challenging lead placement scenarios

2 Cardiac imaging reports should describe findings that may complicate CIED implantation (**Table 2**).
3 Pre-procedural imaging may influence the CIED insertion approach (transvenous right- or left-
4 sided, epicardial) or help anticipate complications and define the most effective implantation
5 technique.

6 CIED implantation in patients with complex adult congenital heart disease (ACHD) may be
7 particularly technically demanding due to complex anatomy, both before and after repair
8 procedures (9). These patients require a tailored approach, which should ideally be discussed by
9 a Heart team that includes imaging and ACHD specialists.

10 On the other hand, some mild-to-moderate complexity ACHD, such as atrial septal defect (ASD),
11 persistent left superior vena cava (PLSVC), or dextrocardia may be unrecognized before the
12 conduction disorder occurs (10, 11) (**Figure 3**). While advanced screening for ACHD does not seem
13 justified, some clinical signs (e.g. heart murmur, cyanosis, digital clubbing, etc.) may raise suspicion
14 of ACHD. In this situation, if a routine TTE examination is not sufficient to confirm or rule out
15 clinically suspected ACHD, it is advisable to order appropriate imaging tests (e.g. CMR). PLSVC is
16 usually an incidental finding, and it should be suspected in the presence of a dilated coronary sinus.
17 The diagnosis is confirmed by computed tomography (CT), CMR, or by an agitated saline
18 echocardiography study through the patient's left antecubital vein if bubbles reach the coronary
19 sinus before the right heart chambers (**Figure 3**). Use can be made of historical thoracic chest CT
20 scans where these are available. In the presence of PLSVC, left-sided CIED implantation can be
21 technically demanding. A right-sided approach is advised in these cases if a right superior vena
22 cava is present without an innominate vein (12). For these reasons, it seems prudent to use
23 imaging to confirm or rule out PLSVC in patients with dilated coronary sinus before CIED
24 implantation.

25 Patent foramen ovale (PFO) and ASD do not complicate CIED implantation per se. Still, care should
26 be taken that the lead does not cross into the left heart chambers, thereby increasing the risk of
27 stroke or systemic embolization (13). In addition, PFO increases the risk of paradoxical septic
28 embolism during transvenous lead extraction in patients with CIED-related infections (14). Whilst
29 it does not seem necessary to use agitated saline study and provocative maneuvers to




1 systematically screen for PFO in patients undergoing CIED implantation, particular care should be
 2 taken in patients with known PFO or ASD, to ensure proper lead placement at implantation using
 3 multiple views.




4 Severe tricuspid regurgitation (TR) and right ventricular (RV) dilatation may interfere with lead
 5 placement and subsequent stability, while the presence of a mechanical tricuspid valve (TV)
 6 prosthesis may dictate the need for epicardial ventricular pacing or LV pacing through the coronary
 7 sinus (9, 10, 11). In a small randomized study in patients with severe TR, the ventricular lead was
 8 more easily and steadily located at the RV outflow tract septum than at the RV apex with shorter
 9 fluoroscopy time and lower incidence of intra-procedural dislodgement (15).

10 Exceptionally, prominent embryonic remnants in the right atrium may pose a challenge to
 11 pacemaker lead placement (16). A prominent Eustachian valve, Chiari network, and Thebesian
 12 valve are occasionally seen in the right atrium as fenestrated membranes, ridges or webs
 13 sometimes dividing the chamber into two cavities (**Figure 3**). On occasion, these structures may
 14 entrap a pacemaker lead within the right atrium or interfere with coronary sinus cannulation,
 15 resulting in prolonged procedure times, increased radiation exposure, failed lead implantation or
 16 the surgical management of complication (17, 18).

17 If transthoracic (TTE) cannot provide sufficient information for pre-procedural planning,
 18 transoesophageal (TOE) echocardiography, CT or CMR imaging can be used to depict complex
 19 cardiac anatomy or vascular abnormalities.

20 **Clinical advice**

It is advised to routinely assess LV systolic function in patients undergoing CIED implantation	
The echocardiographic 2D biplane method of disk summation is the standard method to calculate LVEF	
In patients with good acoustic windows, extensive LV wall motion abnormalities or borderline LVEF (i.e. $\pm 5\%$ around the cut-off for ICD implantation), 3D echocardiography, if available, is the preferred method to measure LVEF by ultrasound	

If poor echocardiographic windows preclude a reliable assessment of LVEF, contrast echocardiography or CMR are advised	
Pre-implantation cardiac imaging reports should include the description of findings that may complicate CIED implantation	
Cross-sectional imaging with CT or CMR is advised in patients with suspected persistent left-sided SVC	

1

2

3

4 II. Imaging of patients undergoing CIED implantation: RV pacing vs. CRT

5

6 In the 2021 ESC guidelines on cardiac pacing and CRT, cardiac imaging is recommended in patients
7 with symptomatic bradycardia to evaluate the presence of structural heart disease, to determine
8 left ventricular (LV) systolic function, and to diagnose potential causes of conduction disorders (2).
9 While degenerative conduction disease and coronary artery disease (CAD) are considered the
10 most frequent causes of atrioventricular block (AVB) in elderly patients (2), an underlying aetiology
11 for AVB is not identified during standard clinical pre-implantation assessment in approximately
12 half of young–middle aged patients (19). Of note, young pacemaker-treated patients with
13 atrioventricular block have a 3- to 4-fold higher rate of the composite of death, hospitalization for
14 heart failure (HF), VA or aborted SCD when compared with a cohort of matched controls (20). In
15 line with this, by the 2021 ESC guidelines, myocardial tissue characterization with multimodality
16 imaging should be considered for the diagnostic-work up of specific pathologies associated with
17 conduction disorders requiring pacemaker implantation, especially in patients younger than 60
18 years (2). This age cut-off is provisional, as some cardiac conditions associated with conduction
19 disorders may be more frequent in elderly patients (e.g. transthyretin cardiac amyloidosis).

20

1 **2.1 Assessment of structural heart disease and the potential aetiology of conduction abnormalities**

2 While echocardiography alone may be sufficient for the routine assessment of global and regional
3 LV systolic function in most patients, multimodality imaging may be needed to diagnose different
4 congenital or acquired cardiac pathologies associated with conduction disorders. **Figure 4**
5 illustrates several important roles for cardiac imaging in the assessment of patients presenting
6 with symptomatic bradycardia. Together with clinical data, a comprehensive multi-modality
7 imaging assessment may identify potentially reversible causes of conduction abnormalities (e.g.
8 acute ischemia, inflammation or infection) or previously undiagnosed cardiomyopathies or heart
9 valve disease, which may vary widely in phenotype and clinical expression. Furthermore, imaging
10 plays a role in determining the most appropriate type of CIED for a specific patient - those with
11 conduction disorders will be treated with conventional antibradycardia pacing or CRT (with or
12 without defibrillator capability) depending predominantly on LV systolic function but also on other
13 imaging parameters, in particular the extent of myocardial scar. Finally, the presence of clinical or
14 imaging red flags, regardless of LV systolic function, should trigger multimodality imaging protocols
15 to identify previously unrecognized cardiac or multisystemic diseases in patients presenting with
16 AVB thereby enabling disease-specific treatment (**Table 3**).

17 Identifying the AVB etiology should ideally be performed prior to CIED implantation, especially if
18 CMR is the part of the diagnostic algorithm. However, this may not be always possible due to time
19 constraints or limited availability of advanced imaging modalities or genetic testing; therefore,
20 diagnostic process can be completed after CIED implantation.

21 In the following, we briefly summarize the imaging approach to patients with various cardiac
22 pathologies leading to conduction abnormalities. Of note, according to the 2023 ESC guidelines
23 for the management of cardiomyopathies, contrast CMR is recommended in patients with
24 cardiomyopathy at initial assessment (21). This means that the majority of these patients will have
25 had prior imaging for review during consideration of device implantation. Further details can be
26 found in the respective ESC and EACVI scientific documents (21, 22, 23).

27
28

1
2
3
4
5
6
7
8
9
10
11
12
13
14
15
16
17
18
19
20
21
22
23
24
25
26
27
28
29

2.1.1 Acute myocardial ischemia

High-degree atrioventricular (AV) block most frequently occurs in patients with acute inferior or inferolateral myocardial infarctions, but it may also complicate anterior infarctions (24). If AV block does not resolve after revascularization or spontaneously (within a waiting period of at least 5 days), permanent cardiac pacing is indicated (2).

2.1.2 Infective endocarditis

Conduction abnormalities are uncommon complications of infective endocarditis and should always raise suspicion of perivalvular extension of the infection and an aortic root abscess (25) (**Figure 5**). Due to the proximity of the AV node to the non-coronary aortic cusp and the anterior mitral leaflet, complete AV block is most often associated with aortic or mitral valve endocarditis (25). The sensitivity of TTE for the detection of perivalvular complications of infective endocarditis is relatively low and the use of other imaging modalities, including TOE, CT, nuclear imaging positron emission tomography/computed tomography (PET/CT) and single photon emission tomography/computed tomography (SPECT/CT) is advised, particularly in patients with clinically suspected prosthetic valve endocarditis (26) (**Figure 6**).

2.1.3 Severe aortic stenosis

Conduction abnormalities are common findings in patients with aortic valve disease, particularly in the presence of extensive valve calcifications and LV dysfunction (27, 28). While permanent pacemaker implantation for conduction disturbances is relatively rare after isolated surgical aortic valve replacement (SAVR) (29), new-onset left bundle-branch block (LBBB) and advanced AV block requiring permanent pacemaker implantation are common complications of transcatheter aortic valve implantation (TAVI) (30). The risk of pacemaker dependency after TAVI is influenced by several patient- and procedure-related factors, some of which can be assessed by CT (31, 32). Anatomic factors predisposing to pacemaker dependency after TAVI include aortic valve calcification (33), a larger annulus perimeter (32), a shorter membranous septum length (34), LV outflow tract calcifications under the left coronary cusp and a difference

1 between membranous septum length and implantation depth ≥ 3 mm (31, 32). Membranous
2 septum length is measured on preprocedural CT coronal views as the perpendicular distance from
3 the annular plane to the beginning of the muscular septum, while implantation depth is measured
4 at the final aortic angiogram as the distance between the lower end of the transcatheter heart
5 valve frame and the lowest part of the noncoronary cusp (31). Lower implantation depth and
6 oversizing have been identified as procedural factors associated with an increased risk of
7 permanent pacemaker implantation following TAVI (32). There is currently no evidence to support
8 pacemaker implantation prior to TAVI or extended rhythm monitoring after SAVR/TAVI based on
9 pre-interventional imaging data.

10

11 **2.1.4 Myocarditis**

12 Patients with acute myocarditis uncommonly present with high-degree AV block. In a
13 retrospective study of >30 000 patients with acute myocarditis, the incidence of high-degree AV
14 block was 1.1% with only a minority of these (23.5%) requiring a permanent pacemaker (35).
15 However, Mobitz II or third-degree AV block can be seen in approximately 25% of patients with
16 giant cell myocarditis (36, 37, 38). Early diagnosis in patients with unexplained high-degree AV
17 block (particularly in those younger than 60 years) is worthwhile (2), as they may benefit from
18 immunosuppressive therapy.

19 The diagnosis of definite myocarditis has traditionally relied on endomyocardial biopsy. However,
20 multiparametric CMR imaging allows noninvasive tissue characterization and is now often used
21 clinically to make a diagnosis of myocarditis without the need for biopsy. According to the 2018
22 Lake Louise criteria (39), a CMR diagnosis of myocarditis is based on at least one T1-based criterion
23 (increased myocardial T1 relaxation times, extracellular volume fraction, or late gadolinium
24 enhancement, LGE) with at least one T2-based criterion (increased myocardial T2 relaxation times,
25 visible myocardial edema, or increased T2 signal intensity ratio).

26

27 **2.1.5 Cardiac sarcoidosis**

28 Cardiac sarcoidosis is usually suspected in younger patients (aged <60 years) presenting with
29 higher degree AV block (38). Whilst frequently accompanied by extracardiac features, isolated

1 cardiac sarcoidosis can also occur. Accurate diagnosis is important because it may impact the
2 choice of CIED implanted and given the potential for clinical improvement with
3 immunosuppressive therapy but also the serious adverse side effects with inappropriate steroid
4 therapy.

5 The multimodality imaging approach to patients with suspected cardiac sarcoidosis includes
6 echocardiography, CMR and 18-fluorodeoxyglucose-positron emission tomography/computed
7 tomography (¹⁸FDG PET/CT) (38). FDG PET/CT is useful in identifying active cardiac sarcoidosis
8 (**Figure 7**), and also allows the identification of extracardiac sites of active sarcoidosis. Careful
9 dietary preparation and clinical attention during reporting are required to distinguish true
10 myocardial FDG PET activity due to sarcoid from physiological FDG uptake in the normal
11 myocardium.

12

13 **2.1.6 Cardiac amyloidosis**

14 Atrial fibrillation and AV block are the most common rhythm and conduction disorders in cardiac
15 amyloidosis (CA) (40). In a retrospective cohort study of 369 patients with transthyretin (ATTR)-
16 CA, almost 10% of patients had high-grade AV block requiring pacemaker implantation at the time
17 of diagnosis, whilst an additional 10% developed high-grade AV block during a mean follow-up of
18 28 months (40). Echocardiography may reveal a typical pattern of biatrial enlargement and
19 mechanical dysfunction, a small pericardial effusion, ventricular wall and interatrial septal
20 thickening, small LV cavity and diastolic dysfunction, very reduced long-axis function and impaired
21 LV global longitudinal strain (GLS) with a basal-apical gradient (**Figure 8**). On CMR, CA presents
22 with a classic pattern of diffuse subendocardial or transmural LGE (including hyperenhancement
23 of the atrial walls), abnormal gadolinium kinetics (difficulties in nulling the myocardium) and
24 increased native T1 and extracellular volume (23, 41). Whereas these typical echocardiographic or
25 CMR findings are suggestive of CA, non-invasive diagnosis of ATTR-CA also requires bone
26 scintigraphy and increased myocardial uptake of a bisphosphonate-based radiotracer (uptake
27 equal to/greater than bone uptake) in the absence of a monoclonal gammopathy (light chain
28 amyloidosis) (**Figure 9**) (23, 41).

29

1 2.1.7 Hypertrophic cardiomyopathy

2 Registry data indicate that up to 10% of patients with hypertrophic cardiomyopathy (HCM) require
3 permanent pacemaker implantation because of conduction disorders (42). According to the 2021
4 ESC guidelines on cardiac pacing, AV sequential pacing with short AV delay may be considered in
5 patients with HCM in sinus rhythm who have other pacing or ICD indications if drug-refractory
6 symptoms or baseline or provokable LV outflow tract (LVOT) gradients ≥ 50 mmHg are present (2).
7 Further, according to the 2023 ESC guidelines on cardiomyopathies, sequential AV pacing, with
8 optimal AV interval to reduce the LV outflow tract (LVOT) gradient or to facilitate medical
9 treatment with beta-blockers and/or verapamil, may be considered in selected patients with
10 resting or provokable LVOT obstruction ≥ 50 mmHg, sinus rhythm, and drug-refractory symptoms,
11 who have contraindications for septal reduction therapies or are at high risk of developing heart
12 block following septal reduction therapies (21).

13 The mechanisms behind the beneficial effects of AV sequential pacing in HCM include
14 asynchronous LV activation and premature septal thickening, interactions with LV filling, negative
15 inotropic effects with reduced hypercontractility of the LV, limitation of abnormal mitral valve
16 motion and LV remodeling (43). Echocardiography can be used during AV delay optimization to
17 assess changes in LV outflow tract pressure gradient and LV filling patterns (**Figure 10**). Since the
18 success of the procedure depends on full ventricular capture, AV delay must be short enough to
19 fully capture the LV from the RV apex, but also long enough to allow the atrial contribution to LV
20 filling (43). In clinical practice, AV delay optimization is carried out in a step-by-step fashion using
21 surface electrocardiography (ECG) and TTE. The programmed AV delay should be changed
22 gradually until reaching an optimal value defined as the longest AV delay that preserves both full
23 ventricular capture (no fusion beats on ECG) and LV filling (no A-wave truncation on the pulsed-
24 wave Doppler of the mitral inflow).

25 The use of imaging in risk stratification for SCD in HCM will be discussed in a subsequent section
26 of this document. However, if a patient is being considered for pacing for LVOT obstruction, CMR
27 for scar assessment is advised to guide device selection (conventional pacemaker or dual chamber
28 ICD).

29

1 2.1.8 Fabry disease

2 In an international survey comprising 714 patients with Fabry disease, conduction abnormalities
3 were observed in 16% of patients, while 3% had a permanent pacemaker (44).

4 Echocardiographic features of the disease include biatrial enlargement, LV hypertrophy
5 (concentric, asymmetrical septal or apical), increased papillary muscle thickness, LV diastolic
6 dysfunction and RV hypertrophy (45) (**Figure 8**). Abnormal segmental longitudinal strain in the
7 basal and mid-inferolateral LV walls may precede thinning of these segments. On CMR, low native
8 T1 values are characteristic, whilst basal non-infarct inferolateral LGE can be observed in
9 approximately half of the patients with Fabry disease (46, 46).

10

11 2.1.9 Dilated cardiomyopathy

12 If previously unknown and unexplained LV or biventricular dilatation and systolic dysfunction
13 (EF<40%) are discovered in a patient with an indication for permanent pacemaker implantation,
14 the patient will be treated with a CRT device rather than with conventional antibradycardia pacing
15 (2). If the clinical scenario permits, then decision-making regarding the type of CIED required
16 should involve heart team discussions after a thorough diagnostic work-up and a minimum of 3
17 months of optimal medical therapy. In the pre-implantation work-up, cardiac imaging is used to
18 rule out ischaemic heart disease and also to detect the presence and extent of myocardial
19 oedema, scarring, fibrosis, and infiltration in the dysfunctional myocardium (20). According to
20 the 2022 ESC guidelines, CMR with LGE should be considered in patients with dilated
21 cardiomyopathy for assessing the aetiology and the risk of VA/SCD (3). If possible, CMR is advised
22 prior to CIED implantation to avoid artifacts and also device-related safety issues (particularly if
23 non-CMR conditional CIED will be implanted).

24

25 2.1.10 Hemochromatosis

26 Conduction disorders are seen in around 2% of hemochromatosis patients, while the most
27 common cardiovascular manifestations of hemochromatosis include arrhythmias, congestive HF
28 and pulmonary hypertension (23, 48). CMR is the method of choice for assessing patients with

1 suspected hemochromatosis, as T2-star (T2*) mapping can reliably identify and quantify
2 myocardial iron accumulation (23, 46).

3

4 **2.1.11 Chagas disease**

5 Chagas disease, caused by the protozoan *Trypanosoma cruzi*, is an important cause of
6 bradyarrhythmias and pacemaker implantation in endemic areas (49).

7 The disease is characterized by atrial and ventricular arrhythmias, conduction abnormalities, HF,
8 thromboembolic events and sudden death (49). Cardiac imaging typically reveals thinning of the
9 LV walls (most commonly seen in the basal inferolateral and lateral walls), apical ventricular
10 aneurysms (with or without thrombi), impaired LV systolic function and pericardial effusions (49).

11

12 **2.1.12 Cardiac tumors**

13 Cardiac tumors are exceedingly rare, but may cause a wide spectrum of arrhythmias and
14 conduction abnormalities, depending on the type of the tumor and the site of involvement (50).

15 For instance, cardiac fibromas have a propensity to cause VA, while cystic tumors of the AV node
16 can cause sudden death despite pacemaker implantation. Although multimodality imaging,
17 particularly noninvasive tissue characterization with CMR imaging, can provide valuable
18 information regarding the nature of the mass, histopathological characterization remains the
19 diagnostic gold standard (51). Besides CMR, a structured imaging approach to patients with a
20 possible cardiac tumor may include TTE, TOE, contrast echocardiography, CT and PET (51).

21





22 **2.2 Imaging in temporary cardiac pacing**

23 Temporary pacing wire insertion is usually performed under fluoroscopic guidance. Vascular
24 ultrasound is very useful to guide central venous access and echocardiography can be used to help
25 temporary pacing lead positioning if fluoroscopy is not available (52). Ultrasound-guided jugular
26 vein puncture involves identification of the internal jugular vein (confirmed by compressibility of
27 the vessel), puncture of the vein and confirmation of the correct position of the wire in the internal
28 jugular vein lumen (**Figure 11**). Echocardiography-guided temporary pacing lead positioning is

1 ideally performed from the subcostal window by continuous echo-monitoring of the catheter
2 pathway, from the right atrium through the tricuspid valve to the RV apex (**Figure 11**).

3

4 **Clinical advice**

If clinical data or pre-implantation TTE raise suspicion of structural heart disease or specific cardiomyopathy, it is advised to evaluate the patient using the ESC guideline-proposed diagnostic algorithms	
If CMR is the part of the diagnostic algorithm, it is advised to perform this examination prior to CIED implantation	
Echocardiography and ECG are useful during AV delay optimization to assess changes in LV outflow tract pressure gradient and LV filling patterns in patients with hypertrophic obstructive cardiomyopathy and AV sequential pacing	
Vascular ultrasound is useful to guide central venous access and echocardiography can be used to help pacing lead positioning if fluoroscopy is not available.	

5

6

7 **III. Imaging of patients undergoing implantation of cardioverter defibrillators**

8 Sudden cardiac death may be the first manifestation of previously unrecognized CAD or
9 cardiomyopathies, and multimodality imaging has an essential role in the evaluation of structural
10 heart disease of survivors. Most survivors will receive ICD therapy for secondary prevention unless
11 a reversible cause of SCD is clearly identified (3). On the other hand, although the causes of SCD
12 vary from frequent cardiomyopathies to rare channelopathies, decisions regarding primary
13 prevention ICD therapy were almost solely based on reduced LVEF. The undeniable role of LVEF
14 originates from the landmark ICD trials in which $LVEF \leq 35\%$, usually assessed by 2D
15 echocardiography, was the main inclusion criterion (53). However, it has a modest predictive
16 accuracy, especially in patients with non-ischemic cardiomyopathies (54) and in the 2022 ESC
17 guidelines, a balanced, more personalized approach combining clinical, imaging and genetic data
18 was proposed (3). Various cardiac imaging modalities allow visualization of tissue characteristics

1 (often myocardial scar/fibrosis) that can be associated with VA in a broad spectrum of
2 cardiomyopathies, but the lack of data from randomized trials currently limits their routine use for
3 the prediction and prevention of VA and SCD. Using CMR scar as a risk indication tool in non-
4 ischemic cardiomyopathy with LVEF \leq 35% (on any imaging modality) is being tested in the ongoing
5 BRITISH randomized controlled trial (ClinicalTrials.gov Identifier: NCT05568069).

6
7

8 **3.1 Imaging for identifying tissue characteristics that can be associated with ventricular arrhythmia**

9 Assessment of myocardial scar and fibrosis, mechanical dispersion, inflammation, denervation and
10 impaired perfusion have all shown superiority to LVEF measurements in risk-stratifying patients
11 for SCD in observational studies (**Figure 12**). LGE on CMR represents the non-invasive reference
12 standard for the visualization and quantification of replacement myocardial fibrosis. The presence
13 and extent of LGE are strongly associated with VA in both ischemic and non-ischemic
14 cardiomyopathies (55, 56). Furthermore, in patients with ischemic cardiomyopathy, the size of the
15 peri-infarct grey (border) zone, composed of a mixture of normal myocardium and fibrosis, is
16 independently associated with VA, even after accounting for total myocardial scar burden (57).
17 Non-focal, diffuse myocardial fibrosis, often encountered in non-ischemic cardiomyopathies,
18 quantified by myocardial native T1 mapping and extracellular volume calculation, is also predictive
19 of VA even in the setting of normal LVEF and in the absence of LGE (58). The superiority of a CMR-
20 guided management strategy for ICD insertion in patients with LVEF 36-50%, based on the
21 presence of scar or fibrosis, to the current strategy based around an LVEF \leq 35% is being tested in
22 the ongoing CMR GUIDE trial (59).

23 The presence of myocardial scar or fibrosis can be indirectly evaluated by assessing their functional
24 consequences using myocardial strain and mechanical dispersion on speckle-tracking strain
25 echocardiography or less often by CMR feature tracking analysis. GLS was independently
26 associated with an increased risk of VA and the first appropriate ICD therapy in an unselected
27 cohort of ICD patients with structural heart disease (60). The ability of mechanical dispersion to
28 predict VAs has been shown in patients with long QT syndrome (61), post-myocardial infarction
29 (62, 63) and familial dilated cardiomyopathy (64). There are currently no randomized controlled

1 trials reported or in progress to provide evidence for the superiority of either GLS or mechanical
2 dispersion over LVEF in VA or SCD prediction.

3 Nuclear imaging techniques have the ability to depict sympathetic denervation, perfusion defects
4 and cardiac inflammation, and thus identify the risk for VA and SCD. Cardiac scintigraphy with the
5 ¹²³I-iodine-labeled meta-iodobenzylguanidine (¹²³I-MIBG), an analogue of noradrenaline, allows
6 evaluation of cardiac sympathetic activity (65). A heart-to-mediastinum ratio <1.6, calculated as
7 ¹²³I-MIBG accumulation in the heart divided by that in the mediastinum, has been identified as a
8 risk factor for VA and SCD in both ischemic and non-ischemic cardiomyopathies (66). Similarly, in
9 ischemic cardiomyopathy, sympathetic denervation assessed using ¹¹C-metahydroxyephedrine PET predicted SCD independently of LVEF and infarct volume (67). Among
10 patients with CAD and LVEF>35%, the extent of stress perfusion defects on single-photon emission
11 computed tomography (SPECT) myocardial perfusion imaging was associated with an increased
12 risk of SCD (68). Myocardial perfusion defects in patients with cardiac sarcoidosis can represent
13 areas of scar or inflammation, while ¹⁸F-FDG PET identifies areas of pathologic glucose uptake and
14 myocardial inflammation (38). Patients with cardiac sarcoidosis with both focal perfusion defects
15 and corresponding areas of inflammation (FDG uptake) were at higher risk of death or ventricular
16 tachycardia (VT) than those with either perfusion defects or inflammation alone (69).

17 Recently, cardiac CT (CCT) has emerged as a promising method for identifying the substrate of
18 malignant arrhythmias and in planning radiofrequency catheter ablation (RFCA) for refractory VT
19 (70, 71). In patients with contraindication to CMR, CCT identification of myocardial fibrosis was
20 feasible and accurate versus EAM electro-anatomical mapping during RFCA procedure (72).
21 Finally, a pilot study suggested that CCT might be a useful tool for planning, guidance and follow-
22 up of external stereotactic radioablation for the treatment of VT (73).

24

25 **3.2 Valvular heart disease**

26 In patients with valvular heart disease (VHD), VA and SCD may occur due to VHD-induced LV
27 dysfunction, hypertrophy and fibrosis, but also due to coexisting triggers (e.g. CAD in elderly
28 patients with aortic stenosis) (74). Whether surgical or interventional correction of VHD lowers
29 the risk of SCD remains uncertain although in aortic stenosis the burden of irreversible myocardial

1 fibrosis appears to increase rapidly (with a relative annual progression of midwall LGE of 78%) until
2 valve replacement occurs and is closely related to long-term prognosis (75). Primary prevention
3 ICD implantation is indicated for patients who satisfy general guideline-proposed criteria (3). With
4 the exception of mitral valve prolapse, there is currently no solid data on the ability of cardiac
5 imaging to improve risk stratification for VA and SCD in patients with VHD.

6

7 **3.2.1 Arrhythmogenic mitral valve prolapse and mitral annular disjunction**

8 MVP is characterized by >2 mm displacement of 1 or both mitral valve leaflets above the annulus
9 within the left atrium in end-systole (76) in the parasternal or apical long-axis views (**Figure 13**),
10 while MAD is defined as a separation between the annulus (i.e. left atrium wall-mitral valve
11 junction) and the LV wall (77). CMR is important for confirmation and for better visualization of
12 MAD, its location, quantification of MAD length, and most importantly, for detection of associated
13 LGE in the inferolateral wall and in the papillary muscles (78). Of note, MAD is a common finding
14 on CMR and it appears that only inferolateral disjunction warrants consideration of further
15 investigation (79).

16 The criteria for primary prevention ICD implantation in patients with AMVP are not established.
17 Risk markers for severe VA include arrhythmic syncope, frequent PVCs and non-sustained VTs,
18 reduced LVEF, presence of MAD, and papillary muscle or inferolateral LGE (78). Reduced LVEF has
19 repeatedly been reported as a risk marker for severe arrhythmic events in patients with AMVP.
20 However, the changes in LV function are often subtle, even occurring within the normal range of
21 LVEF. The presence of LGE is an important risk marker for events, and CMR is useful in patients
22 with MVP and an arrhythmic phenotype (78). A recent study showed that CMR T1 mapping was
23 associated with T-wave inversion on the ECG and with VA (80). These results indicated that diffuse
24 fibrosis may explain such ECG changes and may be promising for risk stratification in AMVP.

25

26 **3.3 Inflammatory conditions**

27 it has been shown that the burden, location and pattern of LGE may improve risk stratification in
28 myocarditis, including amongst patients with preserved LVEF (81). Patients with midwall
29 anteroseptal LGE have worse prognosis, in terms of cardiac death, appropriate ICD therapy,

1 resuscitated cardiac arrest, and hospitalization for HF, than those with other patterns or without
2 LGE (81). However, a prognostic threshold for LGE burden has not been defined; moreover, there
3 are no randomized trials showing the superiority of LGE over LVEF to facilitate decision-making for
4 primary prevention ICD therapy. In patients with cardiac sarcoidosis, LVEF<35% predicts
5 unfavorable outcomes, but VA can also occur in patients with preserved LVEF (82). Based on data
6 demonstrating that patients with LGE had more VA than those without it (83), the 2022 ESC
7 Guidelines inform that an ICD implantation should be considered in patients with cardiac
8 sarcoidosis who have a LVEF>35% but significant LGE at CMR after resolution of acute
9 inflammation (3). While the threshold for significant LGE extent was not specified, a recent study
10 suggested that a value of >5.7% had good accuracy for predicting a composite of SCD, significant
11 ventricular VA and appropriate ICD therapy (84). Also, LGE affecting $\geq 20\%$ of the LV mass has been
12 associated with arrhythmic events in previous reports (85, 86). A widely accepted definition of
13 significant LGE is not available, partly due to the challenges of precise quantification of LGE burden.
14 In the absence of robust data, it seems prudent to use a lower LGE cutoff (>6%) for the prediction
15 of SCD or VA in patients with cardiac sarcoidosis (85, 87). Further studies are needed to refine
16 quantification and to determine the optimal cutoff.

17

18 **3.4 Hypertrophic cardiomyopathy**

19 Imaging is crucial for making a diagnosis of HCM, risk stratification and for decisions on primary
20 prevention ICDs. According to the ESC guidelines, a complete TTE study and CMR with LGE should
21 be performed in all patients with HCM (3, 21). Contrast echocardiography, 3DE and CMR may
22 increase the sensitivity of conventional TTE to detect apical HCM and apical aneurysms (88) (**Figure**
23 **14**). The ESC HCM risk calculator (89) is commonly used for estimating individual risk for VA. The
24 parameters in this risk calculator include age, maximum ventricular wall thickness, left atrial size,
25 maximum LV outflow gradient, family history of SCD, previous non-sustained VT, and unexplained
26 syncope. The prevalence of VA correlates not only with LV wall thickness, but also independently
27 with the presence of LGE on CMR (90). LGE has not been included in the ESC HCM SCD risk
28 calculator, but significant amounts of fibrosis favour ICD implantation (3, 91, 92). According to the
29 2022 ESC Guidelines, in patients with HCM and LV systolic dysfunction (LVEF<50%), or extensive

1 LGE on CMR (usually defined as $\geq 15\%$ of LV mass) or LV apical aneurysms, ICD should be or may
2 be considered if an estimated 5-year risk of SCD is intermediate or low, respectively (3).

3

4 **3.5 Arrhythmogenic right ventricular cardiomyopathy (ARVC)**

5 Imaging has an important role in risk stratification and planning for device implantation. Whilst
6 life-threatening arrhythmias can occur without overt structural changes in the myocardium (93),
7 the presence of structural abnormalities highly increases the risk of VA (94, 95, 96). RV structural
8 changes, particularly RV dilatation and RV dysfunction, indicate increased arrhythmic risk.
9 According to the 2022 ESC Guidelines, in patients with severe RV dysfunction (RV fractional area
10 change $\leq 17\%$ or RVEF $\leq 35\%$), an ICD should be considered (3). Importantly, any LV involvement
11 and dysfunction is associated with increased arrhythmic risk (97). In a risk calculation model
12 (arvcrisk.com), only RVEF by CMR was included as an imaging parameter (98, 99). Two recent
13 papers indicated added prognostic value may be provided by strain echocardiography in these
14 patients (96, 100).

15 Unfortunately, inappropriate shocks are frequent in ARVC patients and one third of patients
16 experience lead-related complications (101). Special ICD-related concerns in ARVC, compared to
17 other cardiomyopathies, include the younger age of patients at initial ICD implantation and their
18 higher level of physical activity. Most importantly, there are issues related to electrical contact of
19 the RV lead where areas of fibrosis and poor intracardiac signals may be prominent. Low sensing
20 values in the RV may exist already at the time of implantation whilst loss of sense values and
21 increased pacing threshold may also develop over time (102). In a recent study, no non-invasive
22 imaging parameters could predict lead complications (101).

23

24 **3.6 Left ventricular hypertrabeculation (left ventricular non-compaction)**

25 Classical clinical manifestations associated with non-compaction include LV dilatation and systolic
26 dysfunction, ventricular arrhythmias and thromboembolic episodes from the spongy left
27 ventricle (103). Risk stratification for primary prevention ICD follow those for heart failure (104).

28

1
2
3
4
5
6
7
8
9
10
11
12
13
14
15
16
17
18
19
20
21
22
23
24


3.7 Lamin A/C cardiomyopathy





Arrhythmic events are frequent in Lamin A/C cardiomyopathy and frequently occur before LVEF is severely reduced (105). LGE on CMR is typically located in the interventricular septum and is probably associated with AV conduction disease (105). Importantly, patients in need of pacemaker due to AV block, should receive a 2-chamber ICD due to the increased risk of VA (3). The 2022 ESC guidelines inform that CRT-D should be considered if the patient has AV-block and LVEF <50% and a high frequency of ventricular pacing is expected (3). When a CRT is indicated for the treatment of HF, patients with lamin AC cardiomyopathy demonstrate a good response rate to biventricular pacing (106).

3.8 Brugada syndrome

Imaging has a limited role in risk stratification and device implantation in patients with Brugada syndrome. However, there are preclinical reports and clinical case studies indicating a potential overlap between ARVC and Brugada syndrome, with the RV outflow tract (RVOT) area as a common region of arrhythmogenicity (107, 108, 109). A recent study confirmed that a dilated RVOT was associated with VA on top of a spontaneous Brugada type 1 ECG pattern (107). By contrast, a normal RVOT diameter (<32 mm or indexed RVOT diameter <18 mm/m²) was associated with the absence of arrhythmic events in patients with Brugada syndrome with a spontaneous type 1 ECG and previous syncope (109). These findings may indicate a possible clinical value of repeated imaging assessments in risk stratification for ventricular arrhythmias.

Clinical advice

<p>Cardiac imaging reports in patients with HCM must contain parameters included in the ESC risk calculator: maximum wall thickness, maximum LVOT pressure gradient and LA diameter</p>	
---	---

<p>CMR LGE is useful to help decision making regarding primary prevention ICDs in patients with HCM at intermediate and low risk</p>	
<p>CMR is useful to help risk stratification in patients with MVP/MAD and an arrhythmic phenotype</p>	
<p>Assessing RV structure and function by CMR in patients with arrhythmogenic cardiomyopathy is useful for risk assessment and selection for primary prevention ICDs</p>	
<p>In patients with cardiac sarcoidosis and LVEF >35%, myocardial scar assessment by CMR or PET is useful to improve risk stratification of VA and SCD and selection of patients for primary prevention ICDs</p>	

1

2

3

4 **IV. Imaging of patients undergoing cardiac resynchronization therapy (CRT)**

5 CRT is an established therapy for patients with HF, reduced LVEF and a wide QRS complex who
6 remain symptomatic despite optimal medical treatment (104). Unfortunately, the rate of patients
7 without volumetric response to CRT remains stable in the range of 30-40% despite technical
8 improvements and accumulating experience (110). Current selection criteria are based on patient
9 symptoms, QRS width and morphology and LVEF (2, 104). In the 2010 focused update of the ESC
10 guidelines on device therapy in HF, mechanical dyssynchrony, assessed by time-to-peak velocity
11 parameters, was considered a useful tool for CRT patient selection in subgroups less likely to
12 respond to this treatment (e.g. a QRS width 120-150 ms) (111). However, its use has been refuted
13 by the disappointing results of a multicenter, observational study that questioned both the
14 accuracy and reproducibility of this approach (112). Furthermore, in the subsequent Echo-CRT
15 randomized controlled trial, mechanical dyssynchrony-driven CRT implantation not only failed to
16 reduce the rate of death or hospitalization for HF, but might even have increased mortality in

1 patients with narrow QRS complexes (113). Over the past decade, the superiority of novel
2 approaches for mechanical dyssynchrony assessment over time-to-peak parameters, and their
3 favourable association with CRT outcome has been repeatedly shown in observational studies
4 (114, 115, 116, 117, 118). However, guideline recommendations for CRT patient selection are not
5 likely be refined before the accuracy and reproducibility of novel parameters are supported by
6 evidence from randomized controlled trials. Finally, the response to CRT is no longer considered a
7 binary variable, since patients who either improve or stabilize after CRT fare better than those
8 with disease progression despite CRT (119, 120, 121, 122).

9 In the following section we discuss all potentially useful imaging parameters, acknowledging that
10 several are beyond current guideline criteria and also revisit the relationship of different response
11 metrics with patient outcomes after CRT.

12

13 **4.1 Assessment of the mechanical consequences of conduction delays**

14 **4.1.1 Atrioventricular dyssynchrony**

15 Prolonged AV conduction can lead to impaired LV diastolic filling and thereby reduced LV preload
16 and stroke volume. This type of dyssynchrony can be assessed with pulsed-wave-Doppler
17 echocardiographic recordings of the mitral valve inflow, typically characterized by reduced LV
18 filling time leading to fusion of the early (E) and late (A) diastolic waves (**Figure 15**), which
19 nevertheless is also favoured by higher heart rate in normal individuals. An LV filling time <40% of
20 the total cardiac length denotes significant AV dyssynchrony (123). CRT allows control of the
21 atrioventricular interplay which contributes in part to the favourable effects of CRT via improved
22 AV coupling (124), but also by allowing optimal beta-blocker treatment while avoiding AV block.
23 Of note, the AV delay can also be programmed in dual chamber pacing.

24

25 **4.1.2 Interventricular dyssynchrony**

26 The time difference between RV and LV ejection defines interventricular mechanical dyssynchrony
27 and can be determined from pulsed-wave-Doppler traces as the time elapsed between the onset
28 of flow in the RV and LV outflow tract (**Figure 15**). A time delay >40 ms is considered a significant

1 interventricular mechanical delay, but does not predict CRT response with sufficient accuracy for
2 clinical use (112).

3

4 **4.1.3 Intraventricular dyssynchrony**

5 Intraventricular dyssynchrony refers to the dyssynchronous motion or deformation of the
6 different regions of the left ventricle. Alternatively, the term “LV mechanical dyssynchrony” is used
7 to distinguish it from the electrical phenomena seen on the ECG. Intraventricular dyssynchrony is
8 not well defined and many, mainly echocardiographic parameters have been proposed for its
9 measurement. Early dyssynchrony parameters were mostly based on time-to-peak tissue velocity
10 or strain measurements and could sensitively detect mechanical dyscoordination among the
11 different regions of the LV and were therefore sensitive criteria for the detection of LV mechanical
12 dyssynchrony (125, 126, 127, 128). However, time-to-peak measurements demonstrated poor
13 specificity (129) and therefore failed to selectively identify patients who would benefit from CRT
14 and did not provide added value beyond established guideline criteria (112, 113). In order to
15 improve patient selection by cardiac imaging, it is therefore important to find selection criteria
16 which are not only sensitive, but also specific and to identify motion or deformation patterns that
17 are amenable by CRT (**Figure 16**).

18

19 **4.1.3.1 Intraventricular dyssynchrony amenable to resynchronization**

20 Typical LBBB causes early activation of the septum and delayed activation of the lateral wall (**Figure**
21 **16**). The septal activation ends diastole when the cavity pressure and the load on the septal
22 myocardium is low. The delayed contraction of the lateral wall then bears the main work load of
23 systolic ejection while the septum is stretched (**Figure 16**). The septal stretching can be observed
24 as a short “notching” in the strain curve of a still functioning septum in early stages of
25 cardiomyopathy, but may become holosystolic when the septum is thin and weak in more
26 advanced states of LV remodeling (130, 131). In animal models, the imbalance in loading of the
27 septum and lateral wall has been shown to lead to progressive atrophy of the septum, hypertrophy
28 of the lateral wall and dilatation of the LV (132, 133), changes which can also be observed in
29 patients (132). Furthermore, the uncoordinated contraction and relaxation pattern of the LV

1 myocardium causes a slower LV pressure rise and decay and hence longer isovolumic contraction
2 and relaxation times, respectively. As a consequence, LBBB shortens LV filling time and impairs LV
3 function in a similar way as described above for AV dyssynchrony (**Figure 15**).

4 Regional LV deformation patterns in LBBB have to be distinguished from those caused by
5 myocardial ischemia or scar. In ischemic and scarred myocardium, a reduced shortening in systole
6 and a delayed shortening peak after aortic valve closure (post-systolic shortening) are common
7 findings (134). If only the temporal occurrence of myocardial deformation peaks is considered, a
8 ventricle with scar shows a “dispersion” of shortening peaks across affected segments which are
9 not recruitable and cannot be therefore resynchronized (**Figure 17**). LV dispersion has been shown
10 to be related to the risk of life-threatening arrhythmia (62). However, mechanical dispersion
11 should not be used in the context of dyssynchrony assessments, since it is sensitive to both
12 ischemic and conduction disease substrates (135).

13 In ischemic cardiomyopathy with conduction delay, the typical LBBB pattern of intraventricular
14 dyssynchrony may be complicated by regional dysfunction due to scar (136). Such hearts show a
15 mechanical dyssynchrony, but not all patterns of dyssynchrony may be improved by CRT. It is
16 therefore of utmost importance that imaging parameters used to identify potential CRT
17 responders are specific enough to identify dyssynchrony patterns which are amenable by CRT
18 (114). Several novel parameters of mechanical dyssynchrony have been successfully tested in
19 observational studies (115, 116, 117), but all are lacking supportive evidence from prospective,
20 randomized trials. Mechanical dyssynchrony as a selection criterion for CRT is currently being
21 tested in the ongoing randomized AMEND-CRT trial (ClinicalTrials.gov Identifier: NCT04225520).

22

23 **4.1.4 Other imaging modalities to detect LV mechanical dyssynchrony**

24 In theory, any imaging modality with sufficient temporal and spatial resolution may be used to
25 identify the typical deformation patterns described above. Modern 3D echocardiography can
26 reach a sufficient temporal resolution, and can provide time-aligned information on the
27 deformation of all segments of the LV within one acquisition. Obtaining speckle tracking
28 echocardiographic 3D data sets with good regional quality, however, is challenging, has low
29 feasibility and reproducibility and, in its current form, limited added value over 2D approaches

1 (137). CMR sequences with sufficient frame rate are available and tracking methods can be applied
2 similar to echocardiographic images. However, regional tracking with CMR demonstrates poor
3 reproducibility and must be used with caution (138, 139). Radial tracking, tagging approaches and
4 velocity-encoded imaging sequences may provide better results but require cumbersome post-
5 processing. CT data, when acquired throughout the entire cardiac cycle with ECG-tagging, may
6 also have sufficient temporal and spatial resolution to assess LV dyssynchrony (140), but the
7 disadvantage of ionizing radiation. Whilst scintigraphic methods have limited temporal and spatial
8 resolution, they can provide dyssynchrony information through analysis of the amplitude
9 (reflecting wall thickening) and phase (reflecting the timing of regional wall motion) of tracer
10 uptake. Studies have suggested the use of the standard deviation of phase-related parameters as
11 a potential criterion (141, 142). Of note, scintigraphy also has the disadvantage of ionizing
12 radiation.

13

14 **4.2 Assessment of heart failure aetiology**

15 Current ESC guidelines (2) give common recommendations for CRT implantation regardless of HF
16 aetiology, since randomized clinical trials showed similar benefit in terms of mortality and HF
17 hospitalizations between patients with ischemic or non-ischemic HF. However, the same ESC
18 guidelines recognize that patients with an ischaemic aetiology have less improvement in LV
19 function after CRT, probably due to presence of myocardial scar tissue, which is less likely to be
20 associated with favourable remodelling. Nonetheless, guideline-proposed recommendations to
21 consider implantation of CRT-D rather than CRT-P are based on individual risk assessment that
22 includes, among other factors, ischemic aetiology of HF and the presence of myocardial fibrosis
23 (2). Echocardiography represents the first-line imaging modality for the characterization of LV
24 function, and may give important suggestions regarding HF aetiology. However, CMR with LGE is
25 considered the reference standard assessment of cardiac structure and function as well as
26 uniquely providing information on myocardial scar pattern, extent and location. Such scar is
27 typically subendocardial or transmural in patients with ischemic heart disease, as compared to the
28 mid-wall or subepicardial scar in patients with non-ischemic cardiomyopathy. In a prospective,

1 observational study, pre-implantation scar assessment by CMR was predictive of appropriate ICD
2 therapies and SCD in CRT patients (143) while data from randomized studies are currently lacking.
3 Pre-implantation stress imaging (including echocardiography, and nuclear or CMR perfusion
4 imaging) may be used for the assessment of inducible ischaemia and viability in those being
5 considered for coronary revascularization. The integrated use of different imaging modalities may
6 therefore help optimise patient selection for CRT and maximise cost-effectiveness.

7

8 **4.3 Assessment of scar burden and localization**

9 Approximately half of patients referred for CRT have an ischemic aetiology of HF. The presence,
10 location and extent of scar tissue determines response to CRT. Lateral scar is an impediment for
11 efficient LV free wall pacing. It reduces CRT response and increases the risk of HF, hospitalization
12 and death (144, 145). When analysing mechanical dyssynchrony in patients with LBBB, lateral scar
13 leads to pseudo-normalization of septal deformation patterns (146). Septal strain curves therefore
14 always need to be interpreted in the context of the lateral curves (117). Septal scar reduces the
15 chances of septal functional recovery and can therefore also be detrimental to successful CRT
16 (147). LV lead deployment over non-scarred myocardium, as assessed by LGE-CMR, was associated
17 with a higher percentage of LV reverse remodeling and better clinical outcomes after CRT (148,
18 149). However, randomized trials have not unequivocally demonstrated that the guidance of LV
19 lead implantation based on imaging (assessing myocardial scar or site of latest mechanical
20 activation) is superior to an electrically guided CRT strategy (2, 150, 151).

21 Perfusion defects at rest on single photon emission computed tomography (SPECT) or positron
22 emission tomography (PET) generally indicate the presence of scar tissue. However, in the
23 presence of dyssynchrony, reduced septal tracer-uptake may also be caused by partial volume
24 effects in the thinned septum as well as the lower work and reduced metabolism in this LV region.
25 The extensive LV contraction abnormalities induced by LBBB cause regional myocardial metabolic
26 and structural remodeling, even in the absence of reductions in blood flow. Therefore, reduced
27 septal tracer uptake does not necessarily indicate scar and the accuracy of nuclear methods to
28 identify scar tissue is reduced in patients with LV dyssynchrony (**Figure 18**) (152, 153). However, a

1 matched perfusion/metabolism defect on PET imaging can detect true scar in patient with LBBB
2 (154).

3
4

5 4.4 Response to CRT

6 4.4.1 Definitions of response

7 Favorable effects of CRT can be observed immediately as well as over the mid- and the long-terms
8 (Table 4).

9 Correction of conduction abnormality can immediately translate into favorable hemodynamic
10 changes such as increases in blood pressure, cardiac output, dP/dt, LV filling period, as well as
11 decreases in mitral regurgitation (MR) and signs of dyssynchrony (117, 155). Mid to long term
12 effects of successful resynchronization include LV reverse remodeling (156, 157), decreased MR
13 (158), increased EF, improved LV diastolic function (159), LA function (160) and RV function (161),
14 as well as reductions in both VA (156, 162) and atrial fibrillation (160). Overall, these effects
15 improve the well-being and functional capacity of patients and reduce the need for diuretics, the
16 rate of recurrent hospitalizations, cardiac and overall mortality.

17 CRT response rate is however challenging to assess and varies significantly based on the definition
18 of response, and which of the above parameters are included (163, 164). Response rate based on
19 clinical endpoints (such as New York Heart Association class or quality of life scores) is higher than
20 the response rate based on LV reverse remodeling assessed by imaging (165). Changes in
21 echocardiographic markers of reverse remodeling remain the most commonly used surrogate
22 endpoints of CRT response (157). LV reverse remodeling is usually defined by a decrease in end-
23 systolic volume (ESV) of >15% compared to baseline or by an absolute increase in LVEF of >5-10%.
24 On this basis, nonresponse has been detected in 30-40% of patients (157, 163, 165). However,
25 the agreement between improved patient functional status and these markers of reverse
26 remodeling is only modest (163, 166, 167). Reverse remodeling most likely translates into
27 favorable outcomes, but lack of reverse remodeling is not equivalent to non-response in all
28 patients (119, 120). In some patients LV volume “stabilization” (i.e. no further volume expansion)
29 after CRT may already be a favorable effect providing a survival benefit (167, 168, 169) as many
30 assumed non-responders demonstrate a deterioration in cardiac performance when their device

1 is switched off (121) (**Figure 19**). In addition, repeat echocardiography is not well suited to
2 detecting more subtle changes in cardiac structure and function due to the inherent variability in
3 echocardiographic biplane volume measurements. Furthermore, it remains difficult to define the
4 optimal time point at which to evaluate the response to treatment, given the continuous
5 remodeling and dynamic nature of heart failure (168). In the recent ADVANCE CRT registry,
6 recurrence of clinical heart failure was a stronger marker of a poor prognosis than a lack of
7 echocardiographic reverse remodeling among patients with LBBB receiving CRT (169). From that
8 perspective, it is challenging to dichotomize response to CRT using LV reverse remodeling or any
9 other standalone marker as a surrogate of clinical outcome.

10 Composite clinical scores (CCS) may be a more appropriate tool to evaluate the effect of CRT (119,
11 122, 170) because slowing down the progression of the disease is a positive outcome and is not
12 necessarily associated with reverse remodeling. This is particularly evident in patients with
13 ischemic cardiomyopathy who manifest less reverse remodeling but demonstrate a similar risk
14 reduction after CRT for HF admissions and death as the non-ischemic group (171).

15 In a subset of patients, super-response is observed. This is usually defined as LVEF increase above
16 50% together with a decrease in ESV of >15%, although a universal definition of super response to
17 CRT does not exist. Independent of the definition, however, super responders with pronounced
18 LV reverse remodeling do demonstrate superior clinical outcomes (162, 172).

19

20 **4.4.2 Imaging predictors of response**

21 Several imaging parameters have been developed recently to predict response to CRT (115, 116,
22 173). Accumulated evidence from several non-randomized studies suggests that these
23 parameters, discussed below, could be a useful addition for CRT patient selection.

24

25 **4.4.2.1 Visual echocardiographic analysis**

26 Early activation of the septum in LBBB causes a short and rapid inward motion of the septum which
27 is commonly referred to as “septal flash” (**Figure 16**) (173). Septal flash is a very sensitive
28 parameter, but may lack some specificity as it may appear even if relevant parts of the septum are
29 ischemic scar. Nevertheless, it has been shown to identify CRT responders with good accuracy

1 (115, 173). A low dose dobutamine challenge increases mechanical dyssynchrony and can help to
2 unmask septal flash in a minority of difficult cases (174, 175). “Apical rocking” describes the typical
3 LV motion pattern caused by LBBB conduction delay. Early septal contraction at end-diastole pulls
4 the LV apex towards the septum, whilst lateral wall contraction then causes pronounced lateral
5 motion of the apex during the ejection phase (176). Detecting this apical rocking pattern has been
6 demonstrated in several studies to be both sensitive and specific for CRT response and strongly
7 associated with successful outcome after CRT (115, 177). Apical rocking is also related to
8 favourable outcome in patients undergoing upgrade from regular pacing to CRT and in CRT
9 recipients with a QRS <150 ms (115, 178). Apical rocking is diminished in the presence of scar,
10 which is advantageous in the assessment of CRT candidates with ischemic cardiomyopathy (147).
11 Both septal flash and apical rocking are relatively simple markers that can be obtained by visual
12 inspection of routine 2-dimensional cine-loops, and do not require any further quantitative off-
13 line analysis. These visual phenomena are consistent with studies of more quantitative measures
14 of systolic stretch by strain imaging, and likely relate to the same electromechanical
15 pathophysiology (**Figure 16**).

16

17 **4.4.2.2 Quantitative echocardiographic analysis of the LV**

18 Echocardiographic strain imaging enables quantification of LV segmental deformation and is
19 therefore a useful aid for the analysis of global as well as regional LV mechanical function. An
20 increased baseline value of absolute GLS, an integral measure of apex-to-base myocardial
21 deformation, has been shown to be strongly associated with LV reverse remodelling and clinical
22 outcome after CRT (117, 179).

23 Several studies have analyzed septal strain patterns as predictors for CRT response (130, 180, 181).

24 In early disease, the delayed lateral wall contraction causes a short “notching” in the septal strain
25 curve, while in advanced disease, the septum shows systolic stretching (**Figure 16**). It has recently
26 been suggested that systolic septal stretching increases over time, reflecting LBBB-induced
27 ventricular remodelling (157). This may explain why dyssynchrony indices incorporating septal
28 stretch are sensitive and specific for volumetric response and strongly associated with clinical
29 outcome after CRT (117, 134, 180, 181, 182).

1 More recently, the calculation of segmental myocardial work has been suggested. For this,
2 segmental pressure-strain- (or stress-strain-) loops are constructed utilising echocardiographic
3 speckle tracking strain and an estimate of the LV pressure (183) (**Figure 20**). Regional work
4 distribution is associated with LV remodelling in LBBB (184) and reverse-remodelling after CRT
5 implantation (185) and has been suggested as a predictor of CRT response (186, 187). In a recent
6 observational prospective multicentre trial, the LV lateral wall to septal work difference as a single
7 parameter proved to have similarly good predictive value as visual analysis by septal flash and
8 apical rocking (116). When either method is combined with assessment of septal scar by CMR, CRT
9 response is predicted with significantly higher accuracy than the former approaches alone (116,
10 188).

11

12 **4.4.2.3 Left atrial function**

13 Although most of the studies investigating the role of imaging in CRT response prediction focussed
14 on LV function, a recent study has demonstrated that baseline left atrial reservoir function,
15 assessed with echocardiographic strain imaging, is independently associated with volumetric CRT
16 response (159). Furthermore, imaging studies have shown that left atrial reverse remodeling is
17 independently predictive of long-term survival after CRT implantation (189, 190).

18

19 **4.4.2.4 RV function**

20 RV function is an independent prognostic marker in CRT recipients (191, 192) and should be
21 routinely assessed before and after device implantation. Although simple echocardiographic
22 parameters, such as tricuspid annular plane systolic excursion, were predictive of all-cause
23 mortality in patients undergoing CRT (193), it appears that RV free wall strain provides incremental
24 prognostic value over conventional RV function parameters in CRT recipients (161, 194). However,
25 it should be noted that improvement in RV function may occur in parallel with the improvement
26 in LV function after CRT, identifying patients with the best prognosis (195).

27

1
2
3
4
5
6
7
8
9
10
11
12
13
14
15
16
17
18
19
20
21
22
23
24
25
26
27
28
29




4.5 Coronary venous anatomy assessment

The coronary venogram is a key step for CRT implantation, and selecting the optimal site for LV lead placement. This is performed during fluoroscopy at the time of CRT implantation. The placement of a lead dedicated to LV stimulation occurs most commonly via the coronary veins, targeting the LV free wall. It is thus mandatory to have precise knowledge of the coronary venous anatomy to guide lead placement and to troubleshoot potential barriers in achieving a stable lead position. The coronary sinus drains the blood collected by the network of coronary veins into the right atrium (**Figure 21**). The length and size of the coronary sinus is highly variable, depending on the preferential development of certain coronary veins with respect to others during the embryonic phase. Moreover, LV or biventricular dilatation and hemodynamic overload due to the underlying cardiac disease may also change the size and length of the coronary veins, displacing the atrioventricular plane, and further influencing the unique anatomic pattern of the coronary venous circulation in each patient. Thus, when planning LV lead placement, it is more clinically useful to consider the vein to be targeted based on the region of the left ventricle where the LV lead should be located, rather than any anatomic classification based on the take-off point of the vein at the CS junction (**Figure 21**). Based on the electromechanical delay imposed by LBBB, the mid-basal lateral, antero- or postero-lateral veins are the preferential lead locations (196). The anatomical representation of these regions is obtained by recording a coronary venogram in RAO 20-30° and LAO 40-60°. The RAO view (similar to the two chamber view on imaging) displays the LV regions and the coronary veins course in full length from base to apex of the heart, thereby enabling the visualization of its basal, mid and distal segments, and the location of the junctions between the coronary veins and the coronary sinus from the middle cardiac vein inferiorly to the anterior interventricular vein and great cardiac vein superiorly (**Figure 21**). The LAO view (similar to the short axis view on imaging) enables distinction of the anterior, lateral, posterior, and inferior segments of the LV (**Figure 21**). Separation of the LV and RV pacing leads is therefore well appreciated on this view. It is well known that coronary veins may have several connections between each other creating a venous network that spreads from the apex to the base of the heart and which ultimately drains into the coronary sinus and right atrium (**Figure 21**).

1 Anatomical variants of the thoracic venous system are not rare, with persistence of the Marshall
 2 vein or the left superior vena cava being the most common (*Supplementary material online*)
 3 (**Figure 3**). This latter variant makes LV lead placement challenging, especially in the absence of a
 4 right superior vena cava (197). Anatomic variants are more frequent in patients with congenital
 5 cardiac disease. Pre-operative cardiac imaging in these congenital heart disease patients with
 6 echocardiography, CMR and CT scans are mandatory for proper planning of CRT procedures, to
 7 balance different opportunities during implantation. Indeed, in the event of atresia of the coronary
 8 sinus ostium (*Supplementary material online*), or lack of suitable veins leading to the targeted LV
 9 location, alternative strategies such as His bundle pacing or left bundle branch area pacing may be
 10 considered before resorting to a leadless CRT implantation or to epicardial LV lead placement
 11 (198). Intraoperative integration of three dimensional imaging with the coronary venogram in
 12 theatre can improve targeting of the most mechanically delayed and viable myocardial segments,
 13 and can enhance patients' outcome (**Figure 22**) (149, 199, 200, 201). Of note, electrical delay to
 14 the LV lead (Q-LV interval) has also been shown to be associated with favorable outcome, and may
 15 be simpler to measure than mechanical dyssynchrony parameters (202).

16

17 Clinical advice

Imaging is useful to assess LV mechanical dyssynchrony, myocardial scar extent and location and RV function to obtain prognostic information in patients undergoing CRT	
Patients with CRT should be categorized as “improved” “unchanged,” and “worsened” on the basis of composite clinical score rather than dichotomized as “responders” and “non-responders” by LV reverse remodeling or any other standalone imaging marker	
Intraoperative and in certain cases pre-operative imaging of the coronary venous anatomy is advisable for targeted LV lead placement	

18

19

1 **CONCLUSIONS**

2 In patients undergoing CIED implantation, imaging is pivotal to assess cardiac function and to
3 potentially detect disorders causing conduction abnormalities or malignant arrhythmias. Imaging
4 can also provide crucial information for deciding the most appropriate type of CIED and avoid
5 problems with challenging lead placements. Randomized controlled trials are eagerly awaited to
6 inform whether novel imaging parameters could further improve risk stratification for primary
7 prevention ICD implantation and refine criteria for CRT patient selection.

8

9

10 **CONFLICTS OF INTEREST**

11

12 IS: Speaker fees and software support from GE Healthcare; JUV: Speaker fees from and collaboration
13 with GE Healthcare and Philips Ultrasound; HB: None; DM: Collaboration with GE Healthcare; LES:
14 Collaboration with GE Healthcare; KHH: None; JL: None; MB: None; JND: None; NAM: Speaker fees
15 from GE Healthcare and Abbott Vascular and member of Medical Advisory Board of Philips Ultrasound;
16 EB: None; MRD: None; OAS is the co-inventor of the ‘Method for myocardial segment work
17 analysis’ and has filed patent on ‘Estimation of blood pressure in the heart’, one speaker fee from
18 GE Healthcare; ED: Collaboration with GE Healthcare and Abbott vascular.

19

20

21 **DATA AVAILABILITY STATEMENT**

22 No new data were generated or analysed in support of this research.

23

24 **REFERENCES**

25

26 1. Raatikainen MJP, Arnar DO, Merkely B, Nielsen JC, Hindricks G, Heidbuchel H, et al. A Decade of Information on the
27 Use of Cardiac Implantable Electronic Devices and Interventional Electrophysiological Procedures in the European
28 Society of Cardiology Countries: 2017 Report from the European Heart Rhythm Association. *Europace*.
29 2017;19(suppl_2):ii1-ii90.

30

31 2. Glikson M, Nielsen JC, Kronborg MB, Michowitz Y, Auricchio A, Barbash IM, et al; ESC Scientific Document Group.
32 2021 ESC Guidelines on cardiac pacing and cardiac resynchronization therapy. *Europace*. 2022;24(1):71-164.

33

34 3. Zeppenfeld K, Tfelt-Hansen J, de Riva M, Winkel BG, Behr ER, Blom NA, et al; ESC Scientific Document Group. 2022
35 ESC Guidelines for the management of patients with ventricular arrhythmias and the prevention of sudden cardiac
36 death. *Eur Heart J*. 2022;43(40):3997-4126.

- 1
- 2 4. Lang RM, Badano LP, Mor-Avi V, Afilalo J, Armstrong A, Ernande L, et al. Recommendations for cardiac chamber
- 3 quantification by echocardiography in adults: an update from the American Society of Echocardiography and the
- 4 European Association of Cardiovascular Imaging. *Eur Heart J Cardiovasc Imaging*. 2015;16(3):233-70.
- 5
- 6 5. Malm S, Frigstad S, Sagberg E, Larsson H, Skjaerpe T. Accurate and reproducible measurement of left ventricular
- 7 volume and ejection fraction by contrast echocardiography: a comparison with magnetic resonance imaging. *J Am*
- 8 *Coll Cardiol*. 2004;44(5):1030-5.
- 9
- 10 6. Ünlü S, Duchenne J, Mirea O, Pagourelis ED, Bézy S, Cvijic M, et al; EACVI-ASE Industry Standardization Task Force.
- 11 Impact of apical foreshortening on deformation measurements: a report from the EACVI-ASE Strain Standardization
- 12 Task Force. *Eur Heart J Cardiovasc Imaging*. 2020;21(3):337-343.
- 13
- 14 7. Muraru D, Cecchetto A, Cucchini U, Zhou X, Lang RM, Romeo G, et al. Intervendor Consistency and Accuracy of Left
- 15 Ventricular Volume Measurements Using Three-Dimensional Echocardiography. *J Am Soc Echocardiogr*.
- 16 2018;31(2):158-168.e1.
- 17
- 18 8. Rodríguez-Zanella H, Muraru D, Secco E, Boccacini F, Azzolina D, Aruta P, et al. Added Value of 3- Versus 2-
- 19 Dimensional Echocardiography Left Ventricular Ejection Fraction to Predict Arrhythmic Risk in Patients With Left
- 20 Ventricular Dysfunction. *JACC Cardiovasc Imaging*. 2019;12(10):1917-1926.
- 21
- 22 9 Hernández-Madrid A, Paul T, Abrams D, Aziz PF, Blom NA, Chen J, et al; ESC Scientific Document Group. Arrhythmias
- 23 in congenital heart disease: a position paper of the European Heart Rhythm Association (EHRA), Association for
- 24 European Paediatric and Congenital Cardiology (AEPC), and the European Society of Cardiology (ESC) Working Group
- 25 on Grown-up Congenital heart disease, endorsed by HRS, PACES, APHRS, and SOLAECE. *Europace*. 2018;20(11):1719-
- 26 1753.
- 27
- 28 10. Albouaini K, Rao A, Ramsdale D. Pacing in patients with congenital heart disease: part 1. *Br J Cardiol* 2013;20:117–
- 29 20.
- 30
- 31 11. Albouaini K, Rao A, Ramsdale D. Pacing in patients with congenital heart disease: part 2. *Br J Cardiol* 2013;20:151–
- 32 3.
- 33
- 34 12. Burri H, Starck C, Auricchio A, Biffi M, Burri M, D'Avila A, et al. EHRA expert consensus statement and practical
- 35 guide on optimal implantation technique for conventional pacemakers and implantable cardioverter-defibrillators:
- 36 endorsed by the Heart Rhythm Society (HRS), the Asia Pacific Heart Rhythm Society (APHRS), and the Latin-American
- 37 Heart Rhythm Society (LAHRS). *Europace*. 2021 ;23(7):983-1008.
- 38
- 39 13. DeSimone CV, Friedman PA, Noheria A, Patel NA, DeSimone DC, Bdeir S, et al. Stroke or transient ischemic attack
- 40 in patients with transvenous pacemaker or defibrillator and echocardiographically detected patent foramen ovale.
- 41 *Circulation*. 2013;128(13):1433-41.
- 42
- 43 14. Lee JZ, Agasthi P, Pasha AK, Tarin C, Tseng AS, Diehl NN, et al. Stroke in patients with cardiovascular implantable
- 44 electronic device infection undergoing transvenous lead removal. *Heart Rhythm*. 2018;15(11):1593-1600.
- 45
- 46 15. Wang J, MD; Chen H, MD; Su Y, MD, Ge J. Pacing lead is more easily located at RVOT septum in patients with
- 47 severe tricuspid regurgitation. *Acta Cardiol* 2016; 71(6): 730-736.
- 48
- 49 16. Moral S, Ballesteros E, Huguet M, Panaro A, Palet J, Evangelista A. Differential Diagnosis and Clinical Implications
- 50 of Remnants of the Right Valve of the Sinus Venosus. *J Am Soc Echocardiogr*. 2016;29(3):183-94.
- 51
- 52 17. Dissmann R, Schröder J, Völler H, Behrens S. Entrapment of pacemaker lead by a large net-like Eustachian valve
- 53 within the right atrium. *Clin Res Cardiol*. 2006;95(4):241-3.

- 1
2 18. Dissmann R, Wolthoff U, Zabel M. Double left ventricular pacing following accidental malpositioning of the right
3 ventricular electrode during implantation of a cardiac resynchronization therapy device. *J Cardiothorac Surg.*
4 2013;8:162.
5
6 19. Rudbeck-Resdal J, Christiansen MK, Johansen JB, Nielsen JC, Bundgaard H, Jensen HK. Aetiologies and temporal
7 trends of atrioventricular block in young patients: a 20-year nationwide study. *Europace.* 2019;21(11):1710-1716.
8
9 20. Dideriksen JR, Christiansen MK, Johansen JB, Nielsen JC, Bundgaard H, Jensen HK. Long-term outcomes in young
10 patients with atrioventricular block of unknown aetiology. *Eur Heart J.* 2021;42(21):2060-2068.
11
12 21. Arbelo E, Protonotarios A, Gimeno JR, Arbustini E, Barriales-Villa R, Basso C, et al; ESC Scientific Document Group.
13 2023 ESC Guidelines for the management of cardiomyopathies. *Eur Heart J.* 2023 Aug 25:ehad194. doi:
14 10.1093/eurheartj/ehad194. Epub ahead of print. PMID: 37622657.
15
16 22. Donal E, Delgado V, Bucciarelli-Ducci C, Galli E, Haugaa KH, Charron P, et al; 2016–18 EACVI Scientific Documents
17 Committee. Multimodality imaging in the diagnosis, risk stratification, and management of patients with dilated
18 cardiomyopathies: an expert consensus document from the European Association of Cardiovascular Imaging. *Eur*
19 *Heart J Cardiovasc Imaging.* 2019;20(10):1075-1093.
20
21 23. Habib G, Bucciarelli-Ducci C, Caforio ALP, Cardim N, Charron P, Cosyns B, et al; EACVI Scientific Documents
22 Committee; Indian Academy of Echocardiography. Multimodality Imaging in Restrictive Cardiomyopathies: An EACVI
23 expert consensus document In collaboration with the "Working Group on myocardial and pericardial diseases" of the
24 European Society of Cardiology Endorsed by The Indian Academy of Echocardiography. *Eur Heart J Cardiovasc*
25 *Imaging.* 2017;18(10):1090-1121.
26
27 24. Auffret V, Loirat A, Leurent G, Martins RP, Filippi E, Coudert I, et al. High-degree atrioventricular block complicating
28 ST segment elevation myocardial infarction in the contemporary era. *Heart.* 2016;102(1):40-9.
29
30 25. Anguera I, Miro JM, Evangelista A, Cabell CH, San Roman JA, Vilacosta I, et al. Periannular complications in infective
31 endocarditis involving native aortic valves. *Am J Cardiol* 2006;98:1254–1260.
32
33 26. Delgado V, Ajmone Marsan N, de Waha S, Bonaros N, Brida M, Burri H, et al; ESC Scientific Document Group. 2023
34 ESC Guidelines for the management of endocarditis. *Eur Heart J.* 2023 Aug 25:ehad193. doi:
35 10.1093/eurheartj/ehad193. Epub ahead of print. PMID: 37622656.
36
37 27. Dhingra RC, Amat-y-Leon F, Pietras RJ, Wyndham C, Deedwania PC, Wu D, et al. Sites of conduction disease in
38 aortic stenosis: significance of valve gradient and calcification. *Ann Intern Med.* 1977;87(3):275-80.
39
40 28. Thompson R, Mitchell A, Ahmed M, Towers M, Yacoub M. Conduction defects in aortic valve disease. *Am Heart J.*
41 1979;98(1):3-10.
42
43 29. Hwang YM, Kim J, Lee JH, Kim M, Hwang J, Kim JB, et al. Conduction disturbance after isolated surgical aortic valve
44 replacement in degenerative aortic stenosis. *J Thorac Cardiovasc Surg.* 2017;154(5):1556-1565.e1.
45
46 30. Auffret V, Puri R, Urena M, Chamandi C, Rodriguez-Gabella T, Philippon F, et al. Conduction Disturbances After
47 Transcatheter Aortic Valve Replacement: Current Status and Future Perspectives. *Circulation.* 2017;136(11):1049-
48 1069.
49
50 31. Nai Fovino L, Cipriani A, Fabris T, Massussi M, Scotti A, Lorenzoni G, et al. Anatomical Predictors of Pacemaker
51 Dependency After Transcatheter Aortic Valve Replacement. *Circ Arrhythm Electrophysiol.* 2021;14(1):e009028.
52

- 1 32. Maier O, Piayda K, Afzal S, Polzin A, Westenfeld R, Jung C, et al. Computed tomography derived predictors of
2 permanent pacemaker implantation after transcatheter aortic valve replacement: A meta-analysis. *Catheter*
3 *Cardiovasc Interv.* 2021;98(6):E897-E907.
4
- 5 33. Sharma E, McCauley B, Ghosalkar DS, Atalay M, Collins S, Parulkar A, et al. Aortic Valve Calcification as a Predictor
6 of Post-Transcatheter Aortic Valve Replacement Pacemaker Dependence. *Cardiol Res.* 2020;11(3):155-167.
7
- 8 34. Maeno Y, Abramowitz Y, Kawamori H, Kazuno Y, Kubo S, Takahashi N, et al. A Highly Predictive Risk Model for
9 Pacemaker Implantation After TAVR. *JACC Cardiovasc Imaging.* 2017;10(10 Pt A):1139-1147.
10
- 11 35. Ogunbayo GO, Elayi SC, Ha LD, Olorunfemi O, Elbadawi A, Saheed D, et al. Outcomes of Heart Block in Myocarditis:
12 A Review of 31,760 Patients. *Heart Lung Circ.* 2019;28(2):272-276.
13
- 14 36. Kandolin R, Lehtonen J, Kupari M. Cardiac sarcoidosis and giant cell myocarditis as causes of atrioventricular block
15 in young and middle-aged adults. *Circ Arrhythm Electrophysiol.* 2011;4(3):303-9.
16
- 17 37. Cooper LT Jr, Blauwet LA. When should high-grade heart block trigger a search for a treatable cardiomyopathy?
18 *Circ Arrhythm Electrophysiol.* 2011;4(3):260-1.
19
- 20 38. Slart RHJA, Glaudemans AWJM, Lancellotti P, Hyafil F, Blankstein R, Schwartz RG, et al; Document Reading Group;
21 A joint procedural position statement on imaging in cardiac sarcoidosis: from the Cardiovascular and Inflammation &
22 Infection Committees of the European Association of Nuclear Medicine, the European Association of Cardiovascular
23 Imaging, and the American Society of Nuclear Cardiology. *Eur Heart J Cardiovasc Imaging.* 2017;18(10):1073-1089.
24
- 25 39. Ferreira VM, Schulz-Menger J, Holmvang G, Kramer CM, Carbone I, Sechtem U, et al. Cardiovascular Magnetic
26 Resonance in Nonischemic Myocardial Inflammation: Expert Recommendations. *J Am Coll Cardiol.* 2018;72(24):3158-
27 3176.
28
- 29 40. Donnellan E, Wazni OM, Saliba WI, Hanna M, Kanj M, Patel DR, et al. Prevalence, Incidence, and Impact on
30 Mortality of Conduction System Disease in Transthyretin Cardiac Amyloidosis. *Am J Cardiol.* 2020;128:140-146.
31
- 32 41. Garcia-Pavia P, Rapezzi C, Adler Y, Arad M, Basso C, Brucato A, et al. Diagnosis and treatment of cardiac
33 amyloidosis: a position statement of the ESC Working Group on Myocardial and Pericardial Diseases. *Eur Heart J.*
34 2021;42(16):1554-1568.
35
- 36 42. Cardim N, Brito D, Rocha Lopes L, Freitas A, Araújo C, Belo A, et al; participating centres. The Portuguese Registry
37 of Hypertrophic Cardiomyopathy: Overall results. *Rev Port Cardiol (Engl Ed).* 2018;37(1):1-10.
38
- 39 43. Daubert C, Gadler F, Mabo P, Linde C. Pacing for hypertrophic obstructive cardiomyopathy: an update and future
40 directions. *Europace.* 2018;20(6):908-920.
41
- 42 44. Linhart A, Kampmann C, Zamorano JL, Sunder-Plassmann G, Beck M, Mehta A, et al; European FOS Investigators.
43 Cardiac manifestations of Anderson-Fabry disease: results from the international Fabry outcome survey. *Eur Heart J.*
44 2007;28(10):1228-35.
45
- 46 45. Rapezzi C, Aimo A, Barison A, Emdin M, Porcari A, Linhart A, et al. Restrictive cardiomyopathy: definition and
47 diagnosis. *Eur Heart J.* 2022;43(45):4679-4693.
48
- 49 46. Menghoum N, Vos JL, Pouleur AC, Nijveldt R, Gerber BL. How to evaluate cardiomyopathies by cardiovascular
50 magnetic resonance parametric mapping and late gadolinium enhancement. *Eur Heart J Cardiovasc Imaging.*
51 2022;23(5):587-589.
52

- 1 47. Militaru S, Gingham C, Popescu BA, Saftoiu A, Linhart A, Jurcut R. Multimodality imaging in Fabry cardiomyopathy:
2 from early diagnosis to therapeutic targets. *Eur Heart J Cardiovasc Imaging*. 2018;19(12):1313-1322.
3
- 4 48. Udani K, Chris-Olaiya A, Ohadugha C, Malik A, Sansbury J, Paari D. Cardiovascular manifestations in hospitalized
5 patients with hemochromatosis in the United States. *Int J Cardiol*. 2021;342:117-124.
6
- 7 49. Nunes MCP, Badano LP, Marin-Neto JA, Edvardsen T, Fernández-Golfín C, Bucciarelli-Ducci C, et al. Multimodality
8 imaging evaluation of Chagas disease: an expert consensus of Brazilian Cardiovascular Imaging Department (DIC) and
9 the European Association of Cardiovascular Imaging (EACVI). *Eur Heart J Cardiovasc Imaging*. 2018;19(4):459-460n.
10
- 11 50. Jayaprakash S. Clinical presentations, diagnosis, and management of arrhythmias associated with cardiac tumors.
12 *J Arrhythm*. 2018;34(4):384-393.
13
- 14 51. Tyebally S, Chen D, Bhattacharyya S, Mughrabi A, Hussain Z, Manisty C, et al. Cardiac Tumors: JACC CardioOncology
15 State-of-the-Art Review. *JACC CardioOncol*. 2020;2(2):293-311.
16
- 17 52. Ferri LA, Farina A, Lenatti L, Ruffa F, Tiberti G, Piatti L, et al. Emergent transvenous cardiac pacing using ultrasound
18 guidance: a prospective study versus the standard fluoroscopy-guided procedure. *Eur Heart J Acute Cardiovasc Care*.
19 2016;5(2):125-9.
20
- 21 53. Bardy GH, Lee KL, Mark DB, Poole JE, Packer DL, Boineau R, et al; Sudden Cardiac Death in Heart Failure Trial (SCD-
22 HeFT) Investigators. Amiodarone or an implantable cardioverter-defibrillator for congestive heart failure. *N Engl J*
23 *Med*. 2005;352(3):225-37.
24
- 25 54. Køber L, Thune JJ, Nielsen JC, Haarbo J, Videbæk L, Korup E, et al; DANISH Investigators. Defibrillator Implantation
26 in Patients with Nonischemic Systolic Heart Failure. *N Engl J Med*. 2016;375(13):1221-30.
27
- 28 55. Watanabe E, Abbasi SA, Heydari B, Coelho-Filho OR, Shah R, Neilan TG, et al. Infarct tissue heterogeneity by
29 contrast-enhanced magnetic resonance imaging is a novel predictor of mortality in patients with chronic coronary
30 artery disease and left ventricular dysfunction. *Circ Cardiovasc Imaging*. 2014;7(6):887-894.
31
- 32 56. Roes SD, Borleffs CJ, van der Geest RJ, Westenberg JJ, Marsan NA, Kaandorp TA, et al. Infarct tissue heterogeneity
33 assessed with contrast-enhanced MRI predicts spontaneous ventricular arrhythmia in patients with ischemic
34 cardiomyopathy and implantable cardioverter-defibrillator. *Circ Cardiovasc Imaging*. 2009;2(3):183-90.
35
- 36 57. Disertori M, Rigoni M, Pace N, Casolo G, Masè M, Gonzini L, et al. Myocardial Fibrosis Assessment by LGE Is a
37 Powerful Predictor of Ventricular Tachyarrhythmias in Ischemic and Nonischemic LV Dysfunction: A Meta-Analysis.
38 *JACC Cardiovasc Imaging*. 2016;9(9):1046-1055.
39
- 40 58. Soslow JH, Damon SM, Crum K, Lawson MA, Slaughter JC, Xu M, et al. Increased myocardial native T1 and
41 extracellular volume in patients with Duchenne muscular dystrophy. *J Cardiovasc Magn Reson*. 2016;18:5.
42
- 43 59. Selvanayagam JB, Hartshorne T, Billot L, Grover S, Hillis GS, Jung W, et al. Cardiovascular magnetic resonance-
44 GUIDEd management of mild to moderate left ventricular systolic dysfunction (CMR GUIDE): Study protocol for a
45 randomized controlled trial. *Ann Noninvasive Electrocardiol*. 2017;22(4):e12420.
46
- 47 60. Guerra F, Malagoli A, Contadini D, Baiocco E, Menditto A, Bonelli P, et al. Global Longitudinal Strain as a Predictor
48 of First and Subsequent Arrhythmic Events in Remotely Monitored ICD Patients With Structural Heart Disease. *JACC*
49 *Cardiovasc Imaging*. 2020;13(1 Pt 1):1-9.
50

- 1 61. Haugaa KH, Amlie JP, Berge KE, Leren TP, Smiseth OA, Edvardsen T. Transmural differences in myocardial
2 contraction in long-QT syndrome: mechanical consequences of ion channel dysfunction. *Circulation*.
3 2010;122(14):1355-63.
4
- 5 62. Haugaa KH, Smedsrud MK, Steen T, Kongsgaard E, Loennechen JP, Skjaerpe T, et al. Mechanical dispersion assessed
6 by myocardial strain in patients after myocardial infarction for risk prediction of ventricular arrhythmia. *JACC*
7 *Cardiovasc Imaging*. 2010;3(3):247-56.
8
- 9 63. Muser D, Tioni C, Shah R, Selvanayagam JB, Nucifora G. Prevalence, Correlates, and Prognostic Relevance of
10 Myocardial Mechanical Dispersion as Assessed by Feature-Tracking Cardiac Magnetic Resonance After a First ST-
11 Segment Elevation Myocardial Infarction. *Am J Cardiol*. 2017;120(4):527-533.
12
- 13 64. Haugaa KH, Hasselberg NE, Edvardsen T. Mechanical dispersion by strain echocardiography: a predictor of
14 ventricular arrhythmias in subjects with lamin A/C mutations. *JACC Cardiovasc Imaging*. 2015;8(1):104-106.
15
- 16 65. Gimelli A, Liga R, Agostini D, Bengel FM, Ernst S, Hyafil F, et al. The role of myocardial innervation imaging in
17 different clinical scenarios: an expert document of the European Association of Cardiovascular Imaging and
18 Cardiovascular Committee of the European Association of Nuclear Medicine. *Eur Heart J Cardiovasc Imaging*.
19 2021;22(5):480-490.
20
- 21 66. Al Badarin FJ, Wimmer AP, Kennedy KF, Jacobson AF, Bateman TM. The utility of ADMIRE-HF risk score in predicting
22 serious arrhythmic events in heart failure patients: incremental prognostic benefit of cardiac 123I-mIBG scintigraphy.
23 *J Nucl Cardiol*. 2014;21(4):756-62; quiz 753-55, 763-5.
24
- 25 67. Fallavollita JA, Heavey BM, Luisi AJ Jr, Michalek SM, Baldwa S, Mashtare TL Jr, et al. Regional myocardial
26 sympathetic denervation predicts the risk of sudden cardiac arrest in ischemic cardiomyopathy. *J Am Coll Cardiol*.
27 2014;63(2):141-9.
28
- 29 68. Piccini JP, Starr AZ, Horton JR, Shaw LK, Lee KL, Al-Khatib SM, et al. Single-photon emission computed tomography
30 myocardial perfusion imaging and the risk of sudden cardiac death in patients with coronary disease and left
31 ventricular ejection fraction >35%. *J Am Coll Cardiol*. 2010;56(3):206-14.
32
- 33 69. Blankstein R, Osborne M, Naya M, Waller A, Kim CK, Murthy VL, et al. Cardiac positron emission tomography
34 enhances prognostic assessments of patients with suspected cardiac sarcoidosis. *J Am Coll Cardiol*. 2014;63(4):329-
35 36.
36
- 37 70. Andreini D, Conte E, Mushtaq A, Melotti E, Gigante C, Mancini ME, et al. Comprehensive Evaluation of Left
38 Ventricle Dysfunction by a New Computed Tomography Scanner: The E-PLURIBUS Study. *JACC Cardiovasc Imaging*.
39 2023;16(2):175-188.
40
- 41 71. Conte E, Mushtaq S, Carbucicchio C, Piperno G, Catto V, Mancini ME, et al. State of the art paper: Cardiovascular
42 CT for planning ventricular tachycardia ablation procedures. *J Cardiovasc Comput Tomogr*. 2021;15(5):394-402.
43
- 44 72. Conte E, Carbucicchio C, Catto V, Kochi AN, Mushtaq S, De Luliis PG, et al. Live integration of comprehensive cardiac
45 CT with electroanatomical mapping in patients with refractory ventricular tachycardia. *J Cardiovasc Comput Tomogr*.
46 2022;16(3):262-265.
47
- 48 73. Carbucicchio C, Andreini D, Piperno G, Catto V, Conte E, Cattani F, et al. Stereotactic radioablation for the
49 treatment of ventricular tachycardia: preliminary data and insights from the STRA-MI-VT phase Ib/II study. *J Interv*
50 *Card Electrophysiol*. 2021;62(2):427-439.

- 1
2 **74.** Kubala M, de Chillou C, Bohbot Y, Lancellotti P, Enriquez-Sarano M, Tribouilloy C. Arrhythmias in Patients With
3 Valvular Heart Disease: Gaps in Knowledge and the Way Forward. *Front Cardiovasc Med.* 2022;9:792559.
4
5 **75.** Everett RJ, Tastet L, Clavel MA, Chin CWL, Capoulade R, Vassiliou VS, et al. Progression of Hypertrophy and
6 Myocardial Fibrosis in Aortic Stenosis: A Multicenter Cardiac Magnetic Resonance Study. *Circ Cardiovasc Imaging.*
7 2018;11(6):e007451.
8
9 **76.** Levine RA, Triulzi MO, Harrigan P, Weyman AE. The relationship of mitral annular shape to the diagnosis of mitral
10 valve prolapse. *Circulation.* 1987;75(4):756-767.
11
12 **77.** Hutchins GM, Moore DKS. The association of floppy mitral valve with disjunction of the mitral annulus fibrosus. *N*
13 *Engl J Med.* 1986;314(9):535-540.
14
15 **78.** Sabbag A, Essayagh B, Barrera JDR, Basso C, Berni A, Cosyns B, et al. EHRA expert consensus statement on
16 arrhythmic mitral valve prolapse and mitral annular disjunction complex in collaboration with the ESC Council on
17 valvular heart disease and the European Association of Cardiovascular Imaging endorsed cby the Heart Rhythm
18 Society, by the Asia Pacific Heart Rhythm Society, and by the Latin American Heart Rhythm Society. *Europace.*
19 2022;24(12):1981-2003.
20
21 **79.** Zugwiz D, Fung K, Aung N, Rauseo E, McCracken C, Cooper J, et al. Mitral Annular Disjunction Assessed Using CMR
22 Imaging: Insights From the UK Biobank Population Study. *JACC Cardiovasc Imaging.* 2022;15(11):1856-1866.
23
24 **80.** Chivulescu M, Aabel WE, Gjertsen E, Hopp E, Scheirlynck E, Cosyns B, et al. Electrical markers and arrhythmic risk
25 associated with myocardial fibrosis in mitral valve prolapse. *Europace.* 2022;24(7):1156-1163.
26
27 **81.** Aquaro GD, Perfetti M, Camastra G, Monti L, Dellegrottaglie S, Moro C, et al; Cardiac Magnetic Resonance Working
28 Group of the Italian Society of Cardiology. Cardiac MR With Late Gadolinium Enhancement in Acute Myocarditis With
29 Preserved Systolic Function: ITAMY Study. *J Am Coll Cardiol.* 2017;70(16):1977-1987.
30
31 **82.** Al-Khatib SM, Stevenson WG, Ackerman MJ, Bryant WJ, Callans DJ, Curtis AB, et al. 2017 AHA/ACC/HRS Guideline
32 for Management of Patients With Ventricular Arrhythmias and the Prevention of Sudden Cardiac Death: A Report of
33 the American College of Cardiology/American Heart Association Task Force on Clinical Practice Guidelines and the
34 Heart Rhythm Society. *J Am Coll Cardiol.* 2018;72(14):e91-e220.
35
36 **83.** Coleman GC, Shaw PW, Balfour PC Jr, Gonzalez JA, Kramer CM, Patel AR, et al. Prognostic Value of Myocardial
37 Scarring on CMR in Patients With Cardiac Sarcoidosis. *JACC Cardiovasc Imaging.* 2017;10(4):411-420.
38
39 **84.** Kazmirczak F, Chen KA, Adabag S, von Wald L, Roukoz H, Benditt DG, et al. Assessment of the 2017 AHA/ACC/HRS
40 Guideline Recommendations for Implantable Cardioverter-Defibrillator Implantation in Cardiac Sarcoidosis. *Circ*
41 *Arrhythm Electrophysiol.* 2019;12(9):e007488.
42
43 **85.** Ekström K, Lehtonen J, Hänninen H, Kandolin R, Kivistö S, Kupari M. Magnetic Resonance Imaging as a Predictor
44 of Survival Free of Life-Threatening Arrhythmias and Transplantation in Cardiac Sarcoidosis. *J Am Heart Assoc.*
45 2016;5(5):e003040.
46
47 **86.** Ise T, Hasegawa T, Morita Y, Yamada N, Funada A, Takahama H, et al. Extensive late gadolinium enhancement on
48 cardiovascular magnetic resonance predicts adverse outcomes and lack of improvement in LV function after steroid
49 therapy in cardiac sarcoidosis. *Heart.* 2014;100(15):1165-72.
50
51 **87.** Crawford T, Mueller G, Sarsam S, Prasitdumrong H, Chaiyen N, Gu X, et al. Magnetic resonance imaging for
52 identifying patients with cardiac sarcoidosis and preserved or mildly reduced left ventricular function at risk of
53 ventricular arrhythmias. *Circ Arrhythm Electrophysiol.* 2014;7(6):1109-15.

- 1
2 **88.** Guta AC, Badano LP, Ochoa-Jimenez RC, Genovese D, Previtero M, Civera S, et al. Three-dimensional
3 echocardiography to assess left ventricular geometry and function. *Expert Rev Cardiovasc Ther.* 2019;17(11):801-815.
4
5 **89.** Elliott PM, Anastasakis A, Borger MA, Borggrefe M, Cecchi F, Charron P, et al. 2014 ESC Guidelines on diagnosis
6 and management of hypertrophic cardiomyopathy: the Task Force for the Diagnosis and Management of Hypertrophic
7 Cardiomyopathy of the European Society of Cardiology (ESC). *Eur Heart J.* 2014;35(39):2733-79.
8
9 **90.** Monserrat L, Elliott PM, Gimeno JR, Sharma S, Penas-Lado M, McKenna WJ. Non-sustained ventricular tachycardia
10 in hypertrophic cardiomyopathy: an independent marker of sudden death risk in young patients. *J Am Coll Cardiol.*
11 2003 Sep 3;42(5):873-9.
12
13 **91.** Chan RH, Maron BJ, Olivotto I, Pencina MJ, Assenza GE, Haas T, et al. Prognostic value of quantitative contrast-
14 enhanced cardiovascular magnetic resonance for the evaluation of sudden death risk in patients with hypertrophic
15 cardiomyopathy. *Circulation.* 2014;130(6):484-95.
16
17 **92.** Mentias A, Raeisi-Giglou P, Smedira NG, Feng K, Sato K, Wazni O, et al. Late Gadolinium Enhancement in Patients
18 With Hypertrophic Cardiomyopathy and Preserved Systolic Function. *J Am Coll Cardiol.* 2018;72(8):857-870.
19
20 **93.** Haugaa KH, Bundgaard H, Edvardsen T, Eschen O, Gilljam T, Hansen J, et al. Management of patients with
21 Arrhythmogenic Right Ventricular Cardiomyopathy in the Nordic countries. *Scand Cardiovasc J.* 2015;49(6):299-307.
22
23 **94.** Leren IS, Saberniak J, Haland TF, Edvardsen T, Haugaa KH. Combination of ECG and Echocardiography for
24 Identification of Arrhythmic Events in Early ARVC. *JACC Cardiovasc Imaging.* 2017;10(5):503-513.
25
26 **95.** Lie ØH, Rootwelt-Norberg C, Dejgaard LA, Leren IS, Stokke MK, Edvardsen T, et al. Prediction of Life-Threatening
27 Ventricular Arrhythmia in Patients With Arrhythmogenic Cardiomyopathy: A Primary Prevention Cohort Study. *JACC*
28 *Cardiovasc Imaging.* 2018;11(10):1377-1386.
29
30 **96.** Kirkels FP, Lie ØH, Cramer MJ, Chivulescu M, Rootwelt-Norberg C, Asselbergs FW, et al. Right Ventricular Functional
31 Abnormalities in Arrhythmogenic Cardiomyopathy: Association With Life-Threatening Ventricular Arrhythmias. *JACC*
32 *Cardiovasc Imaging.* 2021;14(5):900-910.
33
34 **97.** Corrado D, Leoni L, Link MS, Della Bella P, Gaita F, Curnis A, et al. Implantable cardioverter-defibrillator therapy
35 for prevention of sudden death in patients with arrhythmogenic right ventricular cardiomyopathy/dysplasia.
36 *Circulation.* 2003;108(25):3084-91.
37
38 **98.** Cadrin-Tourigny J, Bosman LP, Nozza A, Wang W, Tadros R, Bhonsale A, et al. A new prediction model for
39 ventricular arrhythmias in arrhythmogenic right ventricular cardiomyopathy. *Eur Heart J.* 2019;40(23):1850-1858.
40
41 **99.** Cadrin-Tourigny J, Bosman LP, Wang W, Tadros R, Bhonsale A, Bourfiss M, et al. Sudden Cardiac Death Prediction
42 in Arrhythmogenic Right Ventricular Cardiomyopathy: A Multinational Collaboration. *Circ Arrhythm Electrophysiol.*
43 2021;14(1):e008509.
44
45 **100.** Taha K, Kirkels FP, Teske AJ, Asselbergs FW, van Tintelen JP, Doevendans PA, et al. Echocardiographic
46 Deformation Imaging for Early Detection of Genetic Cardiomyopathies: JACC Review Topic of the Week. *J Am Coll*
47 *Cardiol.* 2022;79(6):594-608.
48
49 **101.** Christensen AH, Platonov PG, Svensson A, Jensen HK, Rootwelt-Norberg C, Dahlberg P, et al. Complications of
50 implantable cardioverter-defibrillator treatment in arrhythmogenic right ventricular cardiomyopathy. *Europace.*
51 2022;24(2):306-312.
52

- 1 102. Mugnai G, Tomei R, Dugo C, Tomasi L, Morani G, Vassanelli C. Implantable cardioverter-defibrillators in patients
2 with arrhythmogenic right ventricular cardiomyopathy: the course of electronic parameters, clinical features, and
3 complications during long-term follow-up. *J Interv Card Electrophysiol*. 2014;41(1):23-9.
4
- 5 103. Gati S, Rajani R, Carr-White GS, Chambers JB. Adult left ventricular noncompaction: reappraisal of current
6 diagnostic imaging modalities. *JACC Cardiovasc Imaging*. 2014;7(12):1266-75.
7
- 8 104. McDonagh TA, Metra M, Adamo M, Gardner RS, Baumbach A, Böhm M, et al; ESC Scientific Document Group.
9 2021 ESC Guidelines for the diagnosis and treatment of acute and chronic heart failure. *Eur Heart J*. 2021;42(36):3599-
10 3726.
11
- 12 105. Hasselberg NE, Edvardsen T, Petri H, Berge KE, Leren TP, Bundgaard H, et al. Risk prediction of ventricular
13 arrhythmias and myocardial function in Lamin A/C mutation positive subjects. *Europace*. 2014;16(4):563-71.
14
- 15 106. Sidhu K, Castrini AI, Parikh V, Reza N, Owens A, Tremblay-Gravel M, et al. The response to cardiac
16 resynchronization therapy in LMNA cardiomyopathy. *Eur J Heart Fail*. 2022;24(4):685-693.
17
- 18 107. Scheirlynck E, Chivulescu M, Lie ØH, Motoc A, Koulalis J, de Asmundis C, et al. Worse Prognosis in Brugada
19 Syndrome Patients With Arrhythmogenic Cardiomyopathy Features. *JACC Clin Electrophysiol*. 2020;6(11):1353-1363.
20
- 21 108. Corrado D, Zorzi A, Cerrone M, Rigato I, Mongillo M, Bauce B, et al. Relationship Between Arrhythmogenic Right
22 Ventricular Cardiomyopathy and Brugada Syndrome: New Insights From Molecular Biology and Clinical Implications.
23 *Circ Arrhythm Electrophysiol*. 2016r;9(4):e003631.
24
- 25 109. Scheirlynck E, Van Malderen S, Motoc A, Lie ØH, de Asmundis C, Sieira J, et al. Contraction alterations in Brugada
26 syndrome; association with life-threatening ventricular arrhythmias. *Int J Cardiol*. 2020;299:147-152.
27
- 28 110. Beela AS, Ünlü S, Duchenne J, Ciarka A, Daraban AM, Kotrc M, et al. Assessment of mechanical dyssynchrony can
29 improve the prognostic value of guideline-based patient selection for cardiac resynchronization therapy. *Eur Heart J*
30 *Cardiovasc Imaging*. 2019;20(1):66-74.
31
- 32 111. Dickstein K, Vardas PE, Auricchio A, Daubert JC, Linde C, McMurray J, et al; ESC Committee for Practice Guidelines
33 (CPG). 2010 Focused Update of ESC Guidelines on device therapy in heart failure: an update of the 2008 ESC Guidelines
34 for the diagnosis and treatment of acute and chronic heart failure and the 2007 ESC guidelines for cardiac and
35 resynchronization therapy. Developed with the special contribution of the Heart Failure Association and the European
36 Heart Rhythm Association. *Eur Heart J*. 2010;31(21):2677-87.
37
- 38 112. Chung ES, Leon AR, Tavazzi L, Sun JP, Nihoyannopoulos P, Merlino J, et al. Results of the Predictors of Response
39 to CRT (PROSPECT) trial. *Circulation* 2008;117:2608-16.
40
- 41 113. Ruschitzka F, Abraham WT, Singh JP, Bax JJ, Borer JS, Brugada J, et al; EchoCRT Study Group. Cardiac-
42 resynchronization therapy in heart failure with a narrow QRS complex. *N Engl J Med*. 2013;369(15):1395-405.
43
- 44 114. Szulik M, Tillekaerts M, Vangeel V, Ganame J, Willems R, Lenarczyk R, et al. Assessment of apical rocking: a new,
45 integrative approach for selection of candidates for cardiac resynchronization therapy. *Eur J Echocardiogr*.
46 2010;11(10):863-9.
47
- 48 115. Stankovic I, Prinz C, Ciarka A, Daraban AM, Kotrc M, Aarones M, et al. Relationship of visually assessed apical
49 rocking and septal flash to response and long-term survival following cardiac resynchronization therapy (PREDICT-
50 CRT). *Eur Heart J Cardiovasc Imaging*. 2016;17(3):262-9.
51

- 1 116. Aalen JM, Donal E, Larsen CK, Duchenne J, Lederlin M, Cvijic M, et al. Imaging predictors of response to cardiac
2 resynchronization therapy: left ventricular work asymmetry by echocardiography and septal viability by cardiac
3 magnetic resonance. *Eur Heart J*. 2020;41(39):3813-3823.
4
- 5 117. Gorcsan J 3rd, Anderson CP, Tayal B, Sugahara M, Walmsley J, Starling RC, et al. Systolic Stretch Characterizes the
6 Electromechanical Substrate Responsive to Cardiac Resynchronization Therapy. *JACC Cardiovasc Imaging*.
7 2019;12(9):1741-1752.
8
- 9 118. Risum N, Jons C, Olsen NT, Fritz-Hansen T, Bruun NE, Hojgaard MV, et al. Simple regional strain pattern analysis
10 to predict response to cardiac resynchronization therapy: rationale, initial results, and advantages. *Am Heart J*.
11 2012;163(4):697-704.
12
- 13 119. Chung ES, Gold MR, Abraham WT, Young JB, Linde C, Anderson C, et al. The importance of early evaluation after
14 cardiac resynchronization therapy to redefine response: Pooled individual patient analysis from 5 prospective studies.
15 *Heart Rhythm*. 2022;19(4):595-603.
16
- 17 120. Stankovic I, Belmans A, Prinz C, Ciarka A, Daraban AM, Kotrc M, et al. The association of volumetric response and
18 long-term survival after cardiac resynchronization therapy. *Eur Heart J Cardiovasc Imaging*. 2017;18(10):1109-1117.
19
- 20 121. Mullens W, Verga T, Grimm RA, Starling RC, Wilkoff BL, Tang WH. Persistent hemodynamic benefits of cardiac
21 resynchronization therapy with disease progression in advanced heart failure. *J Am Coll Cardiol* 2009;53:600-607.
22
- 23 122. Packer M. Proposal for a new clinical end point to evaluate the efficacy of drugs and devices in the treatment of
24 chronic heart failure. *J Card Fail*. 2001;7:176-82.
25
- 26 123. Cazeau S, Leclercq C, Lavergne T, Walker S, Varma C, Linde C, et al. Effects of multisite biventricular pacing in
27 patients with heart failure and intraventricular conduction delay. *N Engl J Med* 2001;344:873-80.
28
- 29 124. Jones S, Lumens J, Sohaib SMA, Finegold JA, Kanagaratnam P, Tanner M, et al; BRAVO Investigators. Cardiac
30 resynchronization therapy: mechanisms of action and scope for further improvement in cardiac function. *Europace*.
31 2017;19(7):1178-1186.
32
- 33 125. Gorcsan J, III, Oyenuga O, Habib PJ, Tanaka H, Adelstein EC, Hara H, et al. Relationship of echocardiographic
34 dyssynchrony to long-term survival after cardiac resynchronization therapy. *Circulation* 2010;122:1910-8.
35
- 36 126. Delgado V, Van Bommel RJ, Bertini M, Borleffs CJ, Marsan NA, Arnold CT, et al. Relative merits of left ventricular
37 dyssynchrony, left ventricular lead position, and myocardial scar to predict long-term survival of ischemic heart failure
38 patients undergoing cardiac resynchronization therapy. *Circulation* 2011;123:70-8.
39
- 40 127. Richardson M, Freemantle N, Calvert MJ, Cleland JG, Tavazzi L. Predictors and treatment response with cardiac
41 resynchronization therapy in patients with heart failure characterized by dyssynchrony: a pre-defined analysis from
42 the CARE-HF trial. *Eur Heart J* 2007;28:1827-34.
43
- 44 128. Zhang Q, van Bommel RJ, Fung JW, Chan JY, Bleeker GB, Ypenburg C, et al. Tissue Doppler Velocity is Superior to
45 Strain Imaging in Predicting Long-term Cardiovascular Events After Cardiac Resynchronization Therapy. *Heart*
46 2009;95:1085-90.
47
- 48 129. Lumens J, Leenders GE, Cramer MJ, De Boeck BW, Doevendans PA, Prinzen FW, et al. Mechanistic evaluation of
49 echocardiographic dyssynchrony indices: patient data combined with multiscale computer simulations. *Circ*
50 *Cardiovasc Imaging*. 2012;5(4):491-9.
51

- 1 **130.** Leenders GE, Lumens J, Cramer MJ, De Boeck BW, Doevendans PA, Delhaas T, et al. Septal deformation patterns
2 delineate mechanical dyssynchrony and regional differences in contractility: analysis of patient data using a computer
3 model. *Circ Heart Fail.* 2012;5(1):87-96.
4
- 5 **131.** Calle S, Kamoen V, De Buyzere M, De Pooter J, Timmermans F. A Strain-Based Staging Classification of Left Bundle
6 Branch Block-Induced Cardiac Remodeling. *JACC Cardiovasc Imaging.* 2021;14(9):1691-1702.
7
- 8 **132.** Vernooij K, Verbeek XA, Peschar M, Crijns HJ, Arts T, Cornelussen RN, et al. Left bundle branch block induces
9 ventricular remodelling and functional septal hypoperfusion. *Eur Heart J.* 2005;26(1):91-8.
10
- 11 **133.** Duchenne J, Claus P, Pagourelias ED, Mada RO, Van Puyvelde J, Vunckx K, et al. Sheep can be used as animal
12 model of regional myocardial remodeling and controllable work. *Cardiol J.* 2019;26(4):375-384.
13
- 14 **134.** Voigt JU, Lindenmeier G, Exner B, Regenfus M, Werner D, Reulbach U, et al. Incidence and characteristics of
15 segmental postsystolic longitudinal shortening in normal, acutely ischemic, and scarred myocardium. *J Am Soc*
16 *Echocardiogr.* 2003;16(5):415-23.
17
- 18 **135.** Lumens J, Tayal B, Walmsley J, Delgado-Montero A, Huntjens PR, Schwartzman D, et al. Differentiating
19 Electromechanical From Non-Electrical Substrates of Mechanical Discoordination to Identify Responders to Cardiac
20 Resynchronization Therapy. *Circ Cardiovasc Imaging.* 2015;8(9):e003744.
21
- 22 **136.** Aalen JM, Remme EW, Larsen CK, Andersen OS, Krogh M, Duchenne J, et al. Mechanism of Abnormal Septal
23 Motion in Left Bundle Branch Block: Role of Left Ventricular Wall Interactions and Myocardial Scar. *JACC Cardiovasc*
24 *Imaging.* 2019;12(12):2402-2413.
25
- 26 **137.** Badano LP, Cucchini U, Muraru D, Al Nono O, Sarais C, Iliceto S. Use of three-dimensional speckle tracking to
27 assess left ventricular myocardial mechanics: inter-vendor consistency and reproducibility of strain measurements.
28 *Eur Heart J Cardiovasc Imaging.* 2013;14(3):285-93.
29
- 30 **138.** Morton G, Schuster A, Jogiya R, Kutty S, Beerbaum P, Nagel E. Inter-study reproducibility of cardiovascular
31 magnetic resonance myocardial feature tracking. *J Cardiovasc Magn Reson.* 2012;14(1):43.
32
- 33 **139.** Barreiro-Pérez M, Curione D, Symons R, Claus P, Voigt JU, Bogaert J. Left ventricular global myocardial strain
34 assessment comparing the reproducibility of four commercially available CMR-feature tracking algorithms. *Eur Radiol.*
35 2018;28(12):5137-5147.
36
- 37 **140.** Bernhard B, Grogg H, Zurkirchen J, Demirel C, Hagemeyer D, Okuno T, et al. Reproducibility of 4D cardiac
38 computed tomography feature tracking myocardial strain and comparison against speckle-tracking echocardiography
39 in patients with severe aortic stenosis. *J Cardiovasc Comput Tomogr.* 2022;S1934-5925(22)00003-X.
40
- 41 **141.** Boogers MM, Van Kriekinge SD, Henneman MM, Ypenburg C, Van Bommel RJ, Boersma E, et al. Quantitative
42 Gated SPECT-Derived Phase Analysis on Gated Myocardial Perfusion SPECT Detects Left Ventricular Dyssynchrony and
43 Predicts Response to Cardiac Resynchronization Therapy. *J Nucl Med* 2009;50:718-25.
44
- 45 **142.** Tang H, Tang S, Zhou W. A Review of Image-guided Approaches for Cardiac Resynchronisation Therapy. *Arrhythm*
46 *Electrophysiol Rev.* 2017;6(2):69-74.
47
- 48 **143.** Acosta J, Fernández-Armenta J, Borràs R, Anguera I, Bisbal F, Martí-Almor J, et al. Scar Characterization to Predict
49 Life-Threatening Arrhythmic Events and Sudden Cardiac Death in Patients With Cardiac Resynchronization Therapy:
50 The GAUDI-CRT Study. *JACC Cardiovasc Imaging.* 2018;11(4):561-572.

- 1 **144.** Bleeker GB, Kaandorp TA, Lamb HJ, Boersma E, Steendijk P, de Roos A, et al. Effect of posterolateral scar tissue
2 on clinical and echocardiographic improvement after cardiac resynchronization therapy. *Circulation* 2006;113:969-
3 76.
4
- 5 **145.** Leyva F, Foley PW, Chalil S, Ratib K, Smith RE, Prinzen F, et al. Cardiac resynchronization therapy guided by late
6 gadolinium-enhancement cardiovascular magnetic resonance. *J Cardiovasc Magn Reson* 2011;13:29.
7
- 8 **146.** Aalen JM, Remme EW, Larsen CK, Andersen OS, Krogh M, Duchenne J, et al. Mechanism of Abnormal Septal
9 Motion in Left Bundle Branch Block: Role of Left Ventricular Wall Interactions and Myocardial Scar. *JACC Cardiovasc*
10 *Imaging*. 2019;12(12):2402-2413.
11
- 12 **147.** Steelant B, Stankovic I, Roijackers I, Aarones M, Bogaert J, Desmet W, et al. The Impact of Infarct Location and
13 Extent on LV Motion Patterns: Implications for Dyssynchrony Assessment. *JACC Cardiovasc Imaging*. 2016;9(6):655-
14 64.
15
- 16 **148.** Taylor RJ, Umar F, Panting JR, Stegemann B, Leyva F. Left ventricular lead position, mechanical activation, and
17 myocardial scar in relation to left ventricular reverse remodeling and clinical outcomes after cardiac resynchronization
18 therapy: A feature-tracking and contrast-enhanced cardiovascular magnetic resonance study. *Heart Rhythm*.
19 2016;13(2):481-9.
20
- 21 **149.** Bertini M, Mele D, Malagù M, Fiorencis A, Toselli T, Casadei F, et. Cardiac resynchronization therapy guided by
22 multimodality cardiac imaging. *Eur J Heart Fail* 2016;18:1375-1382.
23
- 24 **150.** Saba S, Marek J, Schwartzman D, Jain S, Adelstein E, White P, et al. Echocardiography-guided left ventricular lead
25 placement for cardiac resynchronization therapy: results of the Speckle Tracking Assisted Resynchronization Therapy
26 for Electrode Region trial. *Circ Heart Fail*. 2013;6(3):427-34.
27
- 28 **151.** Kristensen J, Jensen HK, Fyenbo DB, Bouchelouche K, Nielsen JC. Electrically vs. imaging-guided left ventricular
29 lead placement in cardiac resynchronization therapy: a randomized controlled trial. *Europace*. 2019;21(9):1369-1377.
30
- 31 **152.** Nowak B, Sinha AM, Schaefer WM, Koch KC, Kaiser HJ, Hanrath P, et al. Cardiac resynchronization therapy
32 homogenizes myocardial glucose metabolism and perfusion in dilated cardiomyopathy and left bundle branch block.
33 *J Am Coll Cardiol*. 2003;41(9):1523-8.
34
- 35 **153.** Masci PG, Marinelli M, Piacenti M, Lorenzoni V, Positano V, Lombardi M, et al. Myocardial structural, perfusion,
36 and metabolic correlates of left bundle branch block mechanical derangement in patients with dilated
37 cardiomyopathy: a tagged cardiac magnetic resonance and positron emission tomography study. *Circ Cardiovasc*
38 *Imaging*. 2010;3(4):482-90.
39
- 40 **154.** Thompson K, Saab G, Birnie D, Chow BJ, Ukkonen H, Ananthasubramaniam K, et al. Is septal glucose metabolism
41 altered in patients with left bundle branch block and ischemic cardiomyopathy? *J Nucl Med*. 2006;47(11):1763-8.
42
- 43 **155.** Nelson GS, Berger RD, Fetis BJ, Talbot M, Spinelli JC, Hare JM, et al. Left ventricular or biventricular pacing
44 improves cardiac function at diminished energy cost in patients with dilated cardiomyopathy and left bundle-branch
45 block. *Circulation*. 2000;102:3053-3059
46
- 47 **156.** Deif B, Ballantyne B, Almeahadi F, Mikhail M, McIntyre WF, Manlucu J, et al. Cardiac resynchronization is pro-
48 arrhythmic in the absence of reverse ventricular remodelling: a systematic review and meta-analysis. *Cardiovasc Res*.
49 2018;114(11):1435-1444.
50

- 1 157. Ypenburg C, van Bommel RJ, Borleffs CJ, Bleeker GB, Boersma E, Schalij MJ, et al. Long-term prognosis after
2 cardiac resynchronization therapy is related to the extent of left ventricular reverse remodeling at midterm follow-
3 up. *J Am Coll Cardiol*. 2009;53(6):483-90.
4
- 5 158. Michalski B, Stankovic I, Pagourelis E, Ciarka A, Aaronson M, Winter S, et al. Relationship of Mechanical
6 Dyssynchrony and LV Remodeling With Improvement of Mitral Regurgitation After CRT. *JACC Cardiovasc Imaging*.
7 2022;15(2):212-220.
8
- 9 159. Galli E, Oger E, Aalen JM, Duchenne J, Larsen CK, Sade E, et al. Left atrial strain is a predictor of left ventricular
10 systolic and diastolic reverse remodelling in CRT candidates. *Eur Heart J Cardiovasc Imaging*. 2022;23(10):1373-1382.
11
- 12 160. Sade LE, Atar I, Özin B, Yüce D, Müderrisoğlu H. Determinants of New-Onset Atrial Fibrillation in Patients
13 Receiving CRT: Mechanistic Insights From Speckle Tracking Imaging. *JACC Cardiovasc Imaging*. 2016;9:99-111.
14
- 15 161. Sade LE, Özin B, Atar I, Demir Ö, Demirtaş S, Müderrisoğlu H. Right ventricular function is a determinant of long-
16 term survival after cardiac resynchronization therapy. *J Am Soc Echocardiogr*. 2013;26:706-13.
17
- 18 162. Yuyun MF, Erqou SA, Peralta AO, Hoffmeister PS, Yarmohammadi H, Echouffo Tcheugui JB, et al. Risk of
19 ventricular arrhythmia in cardiac resynchronization therapy responders and super-responders: a systematic review
20 and meta-analysis. *Europace*. 2021;23:1262-1274.
21
- 22 163. Fornwalt BK, Sprague WW, BeDell P, Suever JD, Gerritse B, Merlino JD, et al. Agreement is poor among current
23 criteria used to define response to cardiac resynchronization therapy. *Circulation*. 2010;121(18):1985-91.
24
- 25 164. Boidol J, Średniawa B, Kowalski O, Szulik M, Mazurek M, Sokal A, et al; Triple-Site Versus Standard Cardiac
26 Resynchronisation Trial (TRUST CRT) Investigators. Many response criteria are poor predictors of outcomes after
27 cardiac resynchronization therapy: validation using data from the randomized trial. *Europace*. 2013;15(6):835-44.
28
- 29 165. Birnie DH, Tang AS. The problem of non-response to cardiac resynchronization therapy. *Curr Opin Cardiol*. 2006
30 Jan;21(1):20-6.
31
- 32 166. Lafitte S, Reant P, Zaroui A, Donal E, Mignot A, Bouget H, et al. Validation of an echocardiographic
33 multiparametric strategy to increase responders patients after cardiac resynchronization: a multicentre study. *Eur*
34 *Heart J*. 2009;30(23):2880-7.
35
- 36 167. Yu CM, Bleeker GB, Fung JW, Schalij MJ, Zhang Q, van der Wall EE, et al. Left ventricular reverse remodeling but
37 not clinical improvement predicts long-term survival after cardiac resynchronization therapy. *Circulation*.
38 2005;112(11):1580-6.
39
- 40 168. Linde C, Gold MR, Abraham WT, St John SM, Ghio S, Cerkenvenik J, et al; REsynchronization reVERses Remodeling
41 in Systolic left vEntricular dysfunction Study Group. Long-term impact of cardiac resynchronization therapy in mild
42 heart failure: 5-year results from the REsynchronization reVERses Remod- eling in Systolic left vEntricular dysfunction
43 (REVERSE) study. *Eur Heart J* 2013;34:2592-99.
44
- 45 169. Dickstein K, Normand C, Auricchio A, Bogale N, Cleland JG, Gitt AK, et al. CRT Survey II: a European Society of
46 Cardiology survey of cardiac resynchronisation therapy in 11 088 patients-who is doing what to whom and how? *Eur*
47 *J Heart Fail* 2018;20:1039-1051.
48
- 49 170. Gold MR, Rickard J, Daubert JC, Zimmerman P, Linde C. Redefining the Classifications of Response to Cardiac
50 Resynchronization Therapy: Results From the REVERSE Study. *JACC Clin Electrophysiol*. 2021;7:871-880.
51

- 1 171. Martens P, Nijst P, Verbrugge FH, Dupont M, Tang WHW, Mullens W. Profound differences in prognostic impact
2 of left ventricular reverse remodeling after cardiac resynchronization therapy relate to heart failure etiology. *Heart*
3 *Rhythm*. 2018;15:130-136.
4
- 5 172. Steffel J, Ruschitzka F. Superresponse to cardiac resynchronization therapy. *Circulation*. 2014;130(1):87-90.
6
- 7 173. Parsai C, Bijmens B, Sutherland GR, Baltabaeva A, Claus P, Marciniak M, et al. Toward understanding response to
8 cardiac resynchronization therapy: left ventricular dyssynchrony is only one of multiple mechanisms. *Eur Heart J*.
9 2009;30(8):940-9.
10
- 11 174. Parsai C, Baltabaeva A, Anderson L, Chaparro M, Bijmens B, Sutherland GR. Low-dose dobutamine stress echo to
12 quantify the degree of remodelling after cardiac resynchronization therapy. *Eur Heart J*. 2009;30(8):950-8.
13
- 14 175. Stankovic I, Aarones M, Smith HJ, Vörös G, Kongsgaard E, Neskovic AN, et al. Dynamic relationship of left-
15 ventricular dyssynchrony and contractile reserve in patients undergoing cardiac resynchronization therapy. *Eur Heart*
16 *J*. 2014;35(1):48-55.
17
- 18 176. Voigt JU, Schneider TM, Korder S, Szulik M, Gürel E, Daniel WG, et al. Apical transverse motion as surrogate
19 parameter to determine regional left ventricular function inhomogeneities: a new, integrative approach to left
20 ventricular asynchrony assessment. *Eur Heart J*. 2009;30(8):959-68.
21
- 22 177. Ghani A, Delnoy PP, Smit JJ, Ottervanger JP, Ramdat Misier AR, Adiyaman A, et al. Association of apical rocking
23 with super-response to cardiac resynchronisation therapy. *Neth Heart J*. 2016;24(1):39-46.
24
- 25 178. Stankovic I, Prinz C, Ciarka A, Daraban AM, Mo Y, Aarones M, et al. Long-Term Outcome After CRT in the Presence
26 of Mechanical Dyssynchrony Seen With Chronic RV Pacing or Intrinsic LBBB. *JACC Cardiovasc Imaging*. 2017;10(10 Pt
27 A):1091-1099.
28
- 29 179. Bazoukis G, Thomopoulos C, Tse G, Tsioufis K, Nihoyannopoulos P. Global longitudinal strain predicts responders
30 after cardiac resynchronization therapy-a systematic review and meta-analysis. *Heart Fail Rev*. 2022;27(3):827-836.
31
- 32 180. Menet A, Bernard A, Tribouilloy C, Leclercq C, Gevaert C, Guyomar Y, et al. Clinical significance of septal
33 deformation patterns in heart failure patients receiving cardiac resynchronization therapy. *Eur Heart J Cardiovasc*
34 *Imaging*. 2017;18(12):1388-1397.
35
- 36 181. Salden OAE, Zweerink A, Wouters P, Allaart CP, Geelhoed B, de Lange FJ, et al. The value of septal rebound stretch
37 analysis for the prediction of volumetric response to cardiac resynchronization therapy. *Eur Heart J Cardiovasc*
38 *Imaging*. 2021;22(1):37-45.
39
- 40 182. De Boeck BW, Teske AJ, Meine M, Leenders GE, Cramer MJ, Prinzen FW, et al. Septal rebound stretch reflects
41 the functional substrate to cardiac resynchronization therapy and predicts volumetric and neurohormonal response.
42 *Eur J Heart Fail*. 2009;11(9):863-71.
43
- 44 183. Russell K, Eriksen M, Aaberge L, Wilhelmsen N, Skulstad H, Remme EW, et al. A novel clinical method for
45 quantification of regional left ventricular pressure-strain loop area: a non-invasive index of myocardial work. *Eur Heart*
46 *J*. 2012;33(6):724-33.
47
- 48 184. Duchenne J, Claus P, Pagourelas ED, Mada RO, Van Puyvelde J, Vunckx K, et al. Sheep can be used as animal
49 model of regional myocardial remodeling and controllable work. *Cardiol J*. 2019;26(4):375-384.
50
- 51 185. Cvijic M, Duchenne J, Ünlü S, Michalski B, Aarones M, Winter S, et al. Timing of myocardial shortening determines
52 left ventricular regional myocardial work and regional remodelling in hearts with conduction delays. *Eur Heart J*
53 *Cardiovasc Imaging*. 2018;19(8):941-949.

- 1
2 **186.** Vecera J, Penicka M, Eriksen M, Russell K, Bartunek J, Vanderheyden M, et al. Wasted septal work in left
3 ventricular dyssynchrony: a novel principle to predict response to cardiac resynchronization therapy. *Eur Heart J*
4 *Cardiovasc Imaging*. 2016 Jun;17(6):624-32.
5
6 **187.** Galli E, Leclercq C, Fournet M, Hubert A, Bernard A, Smiseth OA, et al. Value of Myocardial Work Estimation in
7 the Prediction of Response to Cardiac Resynchronization Therapy. *J Am Soc Echocardiogr*. 2018;31(2):220-230.
8
9 **188.** Duchenne J, Larsen CK, Cvijic M, Galli E, Aalen JM, Klop B, et al. Visual Presence of Mechanical Dyssynchrony
10 Combined With Septal Scarring Identifies Responders to Cardiac Resynchronization Therapy. *JACC Cardiovasc*
11 *Imaging*. 2022;15(12):2151-2153.
12
13 **189.** Stassen J, Galloo X, Chimed S, Hirasawa K, Marsan NA, Delgado V, et al. Clinical implications of left atrial reverse
14 remodelling after cardiac resynchronization therapy. *Eur Heart J Cardiovasc Imaging*. 2022;23(6):730-740.
15
16 **190.** Bouwmeester S, Mast TP, Keulards DCJ, de Lepper AGW, Herold IHF, Dekker LR, et al. Left atrial reverse
17 remodeling predicts long-term survival after cardiac resynchronization therapy. *J Echocardiogr* 2022;20(2):115-123.
18
19 **191.** van Everdingen WM, Walmsley J, Cramer MJ, van Hagen I, De Boeck BWL, Meine M, et al. Echocardiographic
20 Prediction of Cardiac Resynchronization Therapy Response Requires Analysis of Both Mechanical Dyssynchrony and
21 Right Ventricular Function: A Combined Analysis of Patient Data and Computer Simulations. *J Am Soc Echocardiogr*.
22 2017;30(10):1012-1020.e2.
23
24 **192.** Burri H, Domenichini G, Sunthorn H, Fleury E, Stettler C, Foulkes I, et al. Right ventricular systolic function and
25 cardiac resynchronization therapy. *Europace*. 2010;12(3):389-94.
26
27 **193.** Leong DP, Höke U, Delgado V, Auger D, Witkowski T, Thijssen J, et al. Right ventricular function and survival
28 following cardiac resynchronisation therapy. *Heart*. 2013;99(10):722-8.
29
30 **194.** Stassen J, van der Bijl P, Galloo X, Hirasawa K, Prihadi EA, Marsan NA, et al. Prognostic Implications of Right
31 Ventricular Free Wall Strain in Recipients of Cardiac Resynchronization Therapy. *Am J Cardiol*. 2022;171:151-158.
32
33 **195.** Campbell P, Takeuchi M, Bourgoun M, Shah A, Foster E, Brown MW, et al; Multicenter Automatic Defibrillator
34 Implantation Trial With Cardiac Resynchronization Therapy (MADIT-CRT) Investigators. Right ventricular function,
35 pulmonary pressure estimation, and clinical outcomes in cardiac resynchronization therapy. *Circ Heart Fail*.
36 2013;6(3):435-42.
37
38 **196.** European Heart Rhythm Association (EHRA); European Society of Cardiology (ESC); Heart Rhythm Society; Heart
39 Failure Society of America (HFSA); American Society of Echocardiography (ASE); American Heart Association (AHA);
40 European Association of Echocardiography (EAE) of ESC; Heart Failure Association of ESC (HFA), Daubert JC, Saxon L,
41 Adamson PB, Auricchio A, Berger RD, Beshai JF, et al. 2012 EHRA/HRS expert consensus statement on cardiac
42 resynchronization therapy in heart failure: implant and follow-up recommendations and management. *Europace*.
43 2012;14(9):1236-86.
44
45 **197.** Biffi M, Massaro G, Diemberger I, Martignani C, Corzani A, Ziacchi M. Cardiac resynchronization therapy in
46 persistent left superior vena cava: Can you do it two-leads-only? *HeartRhythm Case Rep*. 2016;3(1):30-32.
47
48 **198.** Sidhu BS, Sieniewicz B, Gould J, Elliott MK, Mehta VS, Betts TR, et al. Leadless left ventricular endocardial pacing
49 for CRT upgrades in previously failed and high-risk patients in comparison with coronary sinus CRT upgrades. *Europace*
50 2021;23:1577-1585
51

- 1 **199.** Khan FZ, Virdee MS, Palmer CR, Pugh PJ, O'Halloran D, Elvik M, et al. Targeted left ventricular lead placement to
2 guide cardiac resynchronization therapy: the TARGET study: a randomized, controlled trial. *J Am Coll Cardiol*
3 2012;59:1509–1518.
4
- 5 **200.** Döring M, Braunschweig F, Eitel C, Gaspar T, Wetzel U, Nitsche B, et al. Individually tailored left ventricular lead
6 placement: lessons from multimodality integration between three-dimensional echocardiography and coronary sinus
7 angiogram. *Europace* 2013;15:718-727.
8
- 9 **201.** Adelstein E, Alam MB, Schwartzman D, Jain S, Marek J, Gorcsan J, Saba S. Effect of echocardiography-guided left
10 ventricular lead placement for cardiac resynchronization therapy on mortality and risk of defibrillator therapy for
11 ventricular arrhythmias in heart failure patients (from the Speckle Tracking Assisted Resynchronization Therapy for
12 Electrode Region [STARTER] trial). *Am J Cardiol* 2014;113:1518–152.
13
- 14 **202.** Kandala J, Upadhyay GA, Altman RK, Parks KA, Orencole M, Mela T, et al. QRS morphology, left ventricular lead
15 location, and clinical outcome in patients receiving cardiac resynchronization therapy. *Eur Heart J*. 2013;34(29):2252-
16 62.
17

18

19 **Figure legends**

20

21 **Figure 1.** Guideline proposed left ventricular ejection fraction cutoffs for cardiac implantable
22 device implantation in various clinical scenarios

23 *(Recommendations from the 2022 ESC Guidelines for the management of patients with ventricular arrhythmias and*
24 *the prevention of sudden cardiac death are shown in grey boxes, while those shown in blue boxes are from the 2021*
25 *ESC Guidelines on cardiac pacing and cardiac resynchronization therapy)*
26

27 *only imaging parameters are shown; dotted vertical lines represent LVEF cutoffs; CAD – coronary
28 artery disease; CMR – cardiovascular magnetic resonance; CRT-P – cardiac resynchronization
29 therapy; CRT-D – cardiac resynchronization therapy with defibrillator; DCM/HNDCM – dilated
30 cardiomyopathy/hypokinetic non-dilated cardiomyopathy; ICD – implantable cardioverter
31 defibrillator; HCM – hypertrophic cardiomyopathy; HF – heart failure; LGE – late gadolinium
32 enhancement; LV – left ventricular, LVEF – left ventricular ejection fraction; NYHA – New York
33 Heart Association class; OMT – optimal medical therapy; PPM – permanent pacemaker; PPMI –
34 permanent pacemaker indication.
35

36 **Figure 2.** A challenging assessment of left ventricular ejection fraction (LVEF) in a mildly
37 symptomatic (New York Heart Association class II) post-myocarditis patient without arrhythmia,
38 after 11 months of optimal medical therapy.
39

40 The patient was referred for an implantable cardioverter-defibrillator (ICD) consideration after a
41 LVEF of 36% was measured from a foreshortened, out-of-plane image (single-plane) (A). On
42 repeated two- (B) and three-dimensional echocardiographic examinations (C), as well as
43 cardiovascular magnetic resonance imaging (D), LVEF was above 40%. A preventive ICD
44 implantation was not indicated based on the value of LVEF and the absence of additional risk
45 factors.
46

1 **Figure 3.** Echocardiographic findings indicating potentially challenging device implantation.
2 A. A dilated coronary sinus due to persistent left superior vena cava, as demonstrated by an
3 agitated saline study through the patient's left antecubital vein (D) – note that the bubbles are
4 appearing in the coronary sinus (1) before showing in the right heart (2). B. A prominent, mobile,
5 net-like structure in the right atrium (Chiari network) in a patient with second-degree heart block.
6 C. Cor triatriatum dexter in a patient being considered for an implantable cardioverter-
7 defibrillator.

8
9 **Figure 4.** The role of cardiac imaging in the assessment of patients presenting with symptomatic
10 bradycardia

11
12 In patients presenting with symptomatic bradycardia, cardiac imaging is used to assess LV systolic
13 function, but also to detect possible transient causes or previously unrecognized structural
14 abnormalities leading to conduction disorders. If clinical red flags or pre-implantation
15 echocardiography raises suspicion of structural heart disease (SHD) or specific cardiomyopathy,
16 guideline-proposed multimodality imaging protocol should be applied. If SHD is confirmed,
17 disease-specific therapy, if available, should be initiated in addition to device implantation. A
18 description of findings that may complicate device implantation should be included in the cardiac
19 imaging reports. CRT - cardiac resynchronization therapy (-P without defibrillator, -D with
20 defibrillator), LVEF – left ventricular ejection fraction.

21
22 **Figure 5.** Complete atrioventricular block as a consequence of infective endocarditis complicated
23 by an aortic root abscess in a patient with a prosthetic aortic valve.

24
25 Transthoracic echocardiography revealed a large vegetation (A, yellow arrow) and aortic root
26 abscess (white arrows, A and B), which was confirmed by computed tomography (C, white arrows).

27
28 *Computed tomography image courtesy of Radosav Vidakovic, Clinical Hospital Centre Zemun, Serbia*

29
30
31 **Figure 6.** Prosthetic aortic valve endocarditis. Increased focal ¹⁸F-fluorodeoxyglucose (FGD)
32 uptake in the region of prosthetic aortic valve (arrows) on FGD-positron emission tomography
33 (PET, left) and fused PET/computed tomography (right).

34
35 *Image courtesy of Dragana Sobic Saranovic, Center for Nuclear Medicine with PET, University Clinical*
36 *Center of Serbia*

37
38

1 **Figure 7.** Cardiac sarcoidosis on hybrid cardiac magnetic resonance/positron emission
2 tomography

3
4 Late gadolinium enhancement (LGE) cardiac magnetic resonance (CMR) images on the left with
5 hybrid ^{18}F -fluorodeoxyglucose (FDG) CMR/positron emission tomography (PET) images on the
6 right. (A) Subepicardial (near transmural) LGE in the basal anteroseptum extending in to the right
7 ventricular free wall with increased FDG uptake localizing to exactly the same region on fused
8 CMR/PET (maximum standardized uptake value = 3.4; maximum tissue-to-background ratio = 2.3;
9 maximum target-to-normal myocardium ratio = 2.0). (B) Subepicardial LGE in the basal
10 anterolateral wall with increased FDG uptake co-localizing to exactly that region on
11 CMR/PET. (C) Patchy midwall LGE in the anterolateral wall with matched increased FDG uptake on
12 CMR/PET. (D) Multifocal LGE in the lateral wall with matched increased FDG uptake on CMR/PET.

13
14 *Reproduced with permission from Dweck MR et al. JACC Cardiovasc Imaging. 2018;11(1):94-107.*

15
16
17 **Figure 8.** Echocardiographic appearance of transthyretin cardiac amyloidosis and Fabry disease by
18 conventional and speckle-tracking echocardiography.

19
20 While both diseases belong to the spectrum of hypertrophic phenotype (top panels), the pattern
21 of LV longitudinal strain impairment can be strikingly different (bottom panels). In patients with
22 cardiac amyloidosis, there is an 'apical sparing' or a 'cherry-on-top' pattern on the bull's eye plot
23 of global longitudinal strain; in patients with Fabry disease, the impairment of longitudinal strain
24 is usually seen at the basal inferolateral left ventricular wall.

25
26 **Figure 9.** Bone scintigraphy with $^{99\text{m}}\text{Tc}$ -labeled diphosphonates shows no cardiac uptake (A) in a
27 patient without transthyretin amyloidosis (ATTR) and high cardiac uptake (B, arrow) in a patient
28 with ATTR.

29
30 *Image courtesy of Dragana Sobic Saranovic, Center for Nuclear Medicine with PET, University Clinical
31 Center of Serbia*

32
33 **Figure 10.** Atrioventricular (AV) sequential pacing in a patient with hypertrophic obstructive
34 cardiomyopathy and a complete heart block.

35
36 The apical long-axis view shows the systolic anterior motion of the anterior mitral leaflet (A, arrow)
37 causing the left ventricular outflow tract (LVOT) obstruction (B) with a maximum pressure gradient
38 of approximately 80 mmHg (C - yellow arrow). AV sequential pacing with short AV delay resulted
39 in an immediate reduction of LVOT pressure gradient (D – yellow arrow). AV delay was optimized
40 using electrocardiography (ECG) and transthoracic echocardiography. The programmed AV delay
41 was changed gradually until reaching an optimal value with no fusion beats on ECG and no A-wave
42 truncation on the pulsed-wave Doppler of the mitral inflow. LV – left ventricle, LA – left atrium, Ao
43 – aorta.

44

1
2 **Figure 11.** Ultrasound-guided jugular vein puncture and placement of the pacing electrode.

3
4 **Top panels:** (a) Echographic identification of the internal jugular vein (JV) and carotid artery (CA).
5 (b) Compressibility confirms the venous nature of the vessel identified (c) Echography-guided
6 puncture of the internal jugular vein (black arrow: needle pathway; white arrow: needle tip). Using
7 the Seldinger technique, a guidewire is advanced through the needle: echocardiographic guidance
8 confirms the correct position of the wire in the internal jugular vein lumen (short axis view shown
9 in (d)). **Bottom panels:** After identification of the electrode tip in the right atrium (a), the
10 pacemaker is advanced in the right ventricle after crossing the tricuspid valve (b). The lead
11 pathway to the right ventricular apex is monitored under echocardiographic guidance (c).

12
13 *Reproduced and modified with permission from Ferri LA et al. Eur Heart J Acute Cardiovasc Care.*
14 *2016;5(2):125-9.*

15
16
17 **Figure 12.** Multimodality imaging for the identification of tissue characteristics that can be
18 associated with ventricular arrhythmia

19
20 ¹¹C11-HED – 11-carbon-meta-hydroxyephedrine, CAD – coronary artery disease, CMR –
21 cardiovascular magnetic resonance, CT – computed tomography, ¹⁸F-FDG – 18-
22 fluorodeoxyglucose, H/M - heart to mediastinum ratio, ¹²³I-MIBG – 123-Iodine-labeled meta-
23 iodobenzylguanidine, LV – left ventricle, PET – positron emission tomography, Rb – Rubidium,
24 SPECT – single-photon emission computed tomography, Tc – technetium, Tl – thallium.

25 **Figure 13.** Echocardiography and cardiovascular magnetic resonance imaging in arrhythmogenic
26 mitral valve prolapse.

27
28 A. The parasternal long-axis view showing a prolapse of the posterior mitral valve leaflet (arrow).
29 B. Late gadolinium enhancement in the anterolateral LV wall (arrows). C. and D. A late systolic
30 spike (D, arrow) in the lateral mitral annular tissue Doppler velocity signal (“Pickelhaube sign”).

31
32 *CMR image courtesy of Predrag Milicevic, Clinical Hospital Centre Zemun, Belgrade, Serbia*

33
34 **Figure 14.** Echocardiography and cardiovascular magnetic resonance imaging in hypertrophic
35 cardiomyopathy (HCM)

36
37 A. Prominent septal hypertrophy (white line) and dilated left atrium (yellow line). B. Contrast
38 echocardiography for the detection of apical hypertrophy. C. Typical late-peaking, dagger-shaped
39 appearance of continuous-wave Doppler signal in a patient with left ventricular outflow tract
40 obstruction. D. Late gadolinium enhancement (arrows) at the right ventricular insertion points in
41 a patient with symmetric HCM. E. The asterisk (*) indicates an apical left ventricular aneurysm in
42 a patient with HCM and mid-ventricular obstruction. LV – left ventricle, HCM – hypertrophic
43 cardiomyopathy, RV – right ventricle.

1 *CMR images courtesy of Predrag Milicevic, Clinical Hospital Centre Zemun, Belgrade, Serbia*

2

3 **Figure 15.** Echocardiographic assessment of mechanical dyssynchrony.

4

5 Electrical atrioventricular and ventricular conduction delays are visible as prolonged PQ interval or
6 abnormal QRS morphology and width on ECG and result in different mechanical phenomena. **Left:**
7 prolonged atrioventricular conduction may result in a fusion of E and A waves and a reduced left
8 ventricular filling time (LVFT) on transmitral pulsed-wave Doppler measurements. **Middle:** left
9 bundle branch block causes interventricular dyssynchrony that can be assessed as time delay
10 between the onset of right and LV ejection on pulsed wave Doppler recordings of right and LV
11 outflow tracts. **Right:** prolonged intraventricular conduction can be also reflected by mechanical
12 events in the LV which can be assessed by speckle-tracking echocardiography (here septal and
13 lateral strain curves are shown). ECG – electrocardiogram; LV – left ventricle.

14

15 **Figure 16.** The typical sequence of mechanical and electrical events in left bundle branch block
16 (LBBB) on B-mode, M-mode and strain echocardiography.

17

18 An early electrical activation of the septum results in a short initial septal contraction and causes
19 the apex to move septally, while the septum moves leftward (yellow arrow in B-mode, red arrow
20 in M-mode, red strain curve). The delayed activation of the lateral wall pulls then the apex laterally
21 during the ejection phase while stretching the septum (red arrow in B-mode, black strain curve).
22 This typical sequence of the septal-to-lateral apex motion is described as ‘apical rocking’. The
23 septal inward motion is described as ‘septal flash’.

24

25 *Modified with permission from Stankovic I et al. Eur Heart J Cardiovasc Imaging. 2016;17(3):262-9 (upper two*
26 *panels).*

27

28 **Figure 17.** Regional myocardial deformation patterns in ischemic myocardium.

29

30 A. Electrocardiogram of a patient with inferior and infero-lateral infarction. B. Late gadolinium
31 enhancement showing transmural scar in the inferior septum, inferior and inferolateral wall of the
32 left ventricle. C. Echocardiographic assessment of the same patient by speckle-tracking based
33 strain. Myocardial scar causes systolic lengthening and a pronounced post-systolic shortening
34 (arrow) in the affected segments. Furthermore, peak myocardial deformation occurs at different
35 points in time (“dispersion”). LV myocardial dispersion can be quantified by calculating the
36 standard deviation of the segmental time-to-peak values (bull’s eye at the lower right indicating
37 with red and yellow color the segments with the most pronounced post-systolic shortening, PSD -
38 peak strain dispersion).

39

40 **Figure 18.** Scintigraphy with reduced septal tracer uptake in left bundle branch block (LBBB).

41

1 LBBB causes underuse of the early activated septum with thinning of the left ventricular wall and
2 low regional work performed, as well as a thickened lateral wall with a high workload. In positron
3 emission tomography (PET) images, this leads to a reduced tracer uptake in the septum and high
4 uptake values in the lateral wall, indicating LBBB-induced regional myocardial metabolic
5 remodeling. A. A fluorodeoxyglucose-PET in a 50-year-old female with LBBB. B. Same patient after
6 resynchronization therapy, showing metabolic homogeneous uptake in the septum vs lateral wall.
7 *Modified with permission from Nowak B et al. J Am Coll Cardiol. 2003;41(9):1523-8.*

8
9 **Figure 19.** Patient with ischemic dilated cardiomyopathy deemed volumetric non-responder 9
10 months after cardiac resynchronization therapy (CRT).

11
12 Hemodynamic deterioration is evident with the first beat as the CRT is turned off (red arrow).
13 EKG – electrocardiogram, dP/dt – delta Pressure/delta time, LV – left ventricle, LVOT – left
14 ventricular outflow tract, TVI – time velocity integral.

15
16
17 **Figure 20.** Myocardial work analysis in left bundle branch block.

18
19 Combining segmental left ventricular strain measurements with estimated left ventricular
20 pressure allows to construct pressure-strain loops. The area of these loops reflects the performed
21 segmental work per volume unit. Green – segmental loops of the highlighted segment, Red –
22 global loop.

23 A. In the basal segment of the anteroseptal wall of this patient with left bundle branch block, a
24 “figure of eight” formation of the pressure strain loop is found (green loop, corresponding with
25 the segment highlighted in red on the bull’s eye). This aspect reflects negative work, which can be
26 interpreted as “wasted” work compared to the constructive work performed by other parts of the
27 ventricle. B. The pressure-strain loop of the basal segment of the inferolateral wall (green loop
28 corresponding with the segment highlighted in red on the bull’s eye) is bigger than the average
29 (red loop), as it has to compensate for the early activated walls.

30
31
32 **Figure 21.** Coronary vein anatomy displayed in right anterior oblique (RAO) and left anterior
33 oblique (LAO) views.

34
35 Five tributaries of the coronary sinus with broad anastomoses of the inferior vein (IV) and the
36 posterior coronary veins (PV), and of the middle (MCV) and great cardiac vein (GCV, also called the
37 anterior interventricular vein). These two latter share a long anastomotic loop (*). The lateral vein
38 (LV) drains the lateral left ventricular wall. The 35° RAO view enables the visualization of the left

1 ventricle in its basal, medial, and apical segments, whereas in 60° LAO view the left ventricular
2 lateral wall is segmented in anterolateral, posterolateral, and inferolateral regions.

3






4 **Figure 22.** Cardiac resynchronization therapy intraoperative guidance for targeted left ventricular
5 (LV) placement: overlays of the latest mechanically activated segments on fluoroscopy during the
6 left ventricular LV lead implantation by the CARTBox system.

7 The LV is divided in 36 segments which are shown by the wireframe. The small sphere at the basal
8 ring of the wireframe indicates the anterior hinge point of the RV. The colors represent the latest
9 mechanical activation of the lateral wall, which in this case is 269 ms. The lateral branch of the
10 posterior vein (PVL) lies amidst the target area. GCV - great cardiac vein; PV - posterior vein; PVI -
11 inferior branch of the PV.

12

13

1 Table 1. Categories of clinical advice

STRENGTH OF ADVICE	DEFINITION	SYMBOL
	Clinical advice, based on robust published evidence	
	Clinical advice, based on uniform consensus of the writing group	
	May be appropriate, based on published evidence	
	May be appropriate, based on consensus within writing group	
	Area of uncertainty	

2
3

1 **Table 2.** Imaging findings associated with potentially challenging CIED implantation.

	Preferred imaging modalities	Relevance for CIED implantation
Atrial and ventricular septal defects	TTE/TOE, CMR/CT (sinus venosus defects)	- Misplacement of the lead in the left heart during implantation - Risk of paradoxical embolisation during lead extraction for CIED-related infection - Difficult endocardial pacing at the site of repair (fibrosis or prosthetic material)
Persistent left superior vena cava*	TTE with agitated saline injection from the left antecubital vein, CT / CMR	- Left-sided approach frequently challenging - Right-sided approach preferred (if the presence of a right SVC is confirmed by venography or CT/CMR)
Central vein obstruction	Direct and CT venography	- Planning appropriate (technically demanding and riskier) procedures when central veins are actually occluded
Dextrocardia	CXR, fluoroscopy	- Difficult fluoroscopic orientation - The possibility of associated cardiac defects
Severe tricuspid regurgitation	TTE, TOE, CMR	- Difficult lead placement (TR jet, dilated RV)
Mechanical tricuspid valve prosthesis	TTE, TOE	- LV pacing through the coronary sinus or epicardial ventricular pacing is required
Anatomic variants, congenital or acquired anomalies of the coronary sinus	CT, CMR	- Pre-procedural planning in cases with previously failed coronary sinus cannulation
Prominent embryonic remnants	TTE, TOE, CT, CMR	- Possible entrapment of the pacemaker lead within the right atrium

2
3 *in the presence of a dilated coronary sinus, it is advisable to confirm or rule out the presence of persistent
4 left superior vena cava; CIED - cardiovascular implantable electronic devices, CMR – cardiovascular
5 magnetic resonance, CT– computed tomography, CXR -chest X-ray, RV– right ventricle, SVC - superior vena
6 cava, TOE – transoesophageal echocardiography, TR – tricuspid regurgitation, TTE – transthoracic
7 echocardiography.

8
9

1 **Table 3.** Clinical red flags for suspecting some uncommon cardiac or multisystemic diseases in
 2 patients presenting with unexplained conduction disorders

	Clinical red flags	Imaging modalities	Clinical relevance
Cardiac sarcoidosis	- Unexplained AV block in younger patients (<60 years) - Known extracardiac sarcoidosis	TTE, CMR, PET	- Specific treatment - Lower threshold for ICD or CRT-D implantation
Cardiac amyloidosis	- Carpal tunnel syndrome - Spinal stenosis - Peripheral neuropathy - Low voltage (ECG)	TTE, SPECT, CMR	- Specific treatment
Hypertrophic cardiomyopathy	- Positive family history - High voltage (LVH) and/or repolarisation abnormalities on ECG - Systolic heart murmur	TTE, CMR	- Reduction of LVOT pressure gradient with AV sequential pacing - Lower threshold for ICD - Specific treatment
Fabry disease	- Angiokeratoma - Cornea verticillata - Short PR interval - Renal failure, proteinuria - Juvenile/cryptogenic CVI - Neuropathic pain	TTE, CMR	- Specific treatment
Hemochromatosis	- Skin pigmentation - Liver cirrhosis - Skin bronzing - Diabetes mellitus - ↑ transferrin saturation	TTE, CMR: T2-star mapping	- Specific treatment
Chagas disease	- Endemic countries - GIT complications (megaesophagus, megacolon) - Neurologic complications	TTE, CMR	- Specific treatment - Lower threshold for ICD

3
 4 AV – atrioventricular; CMR – cardiovascular magnetic resonance; CRT-D – cardiac
 5 resynchronization therapy with defibrillator; CT – computed tomography; CVI – cerebrovascular
 6 insult; ECG – electrocardiogram; GIT – gastrointestinal tract; ICD – implantable cardioverter
 7 defibrillator; LVH – left ventricular hypertrophy; LVOT – left ventricular outflow tract; PET –
 8 positron emission tomography; SPECT – single photon emission computed tomography; TTE –
 9 transthoracic echocardiography.

10
 11

1 **Table 4:** The spectrum of response to CRT

2

Immediate/short term response

- Coordination of contraction
- Decrease in mitral regurgitation
- Increase in diastolic filling and cardiac output

Mid-to-long term response

- Increase in end organ perfusion, decrease in sympathetic and RAAS activity
- Increase in myocardial perfusion
- Decrease in ventricular volumes
- Decrease in mitral regurgitation
- Increase in LVEF and RV function
- Decrease in ventricular arrhythmias and atrial fibrillation
- Increase in functional capacity and well-being
- Decrease in heart failure hospitalizations
- Decrease in cardiovascular and all cause mortality

3 RAAS – renin-angiotensin-aldosterone system; LVEF – left ventricular ejection fraction; RV – right
4 ventricular.

5

6

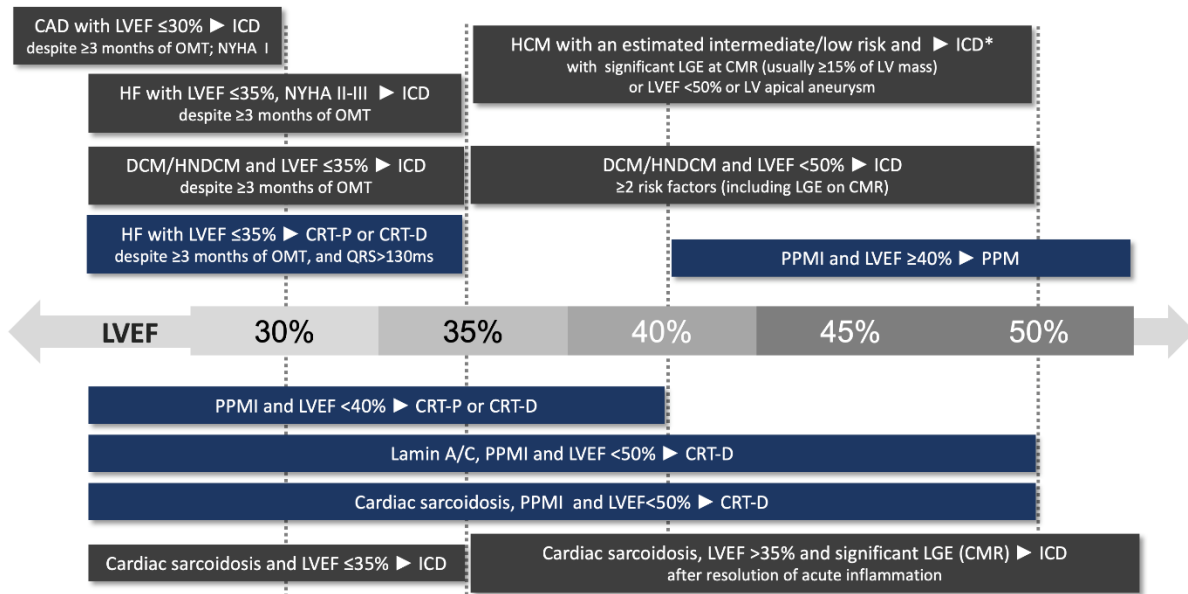


Figure 1
159x84 mm (x DPI)

1
2
3
4

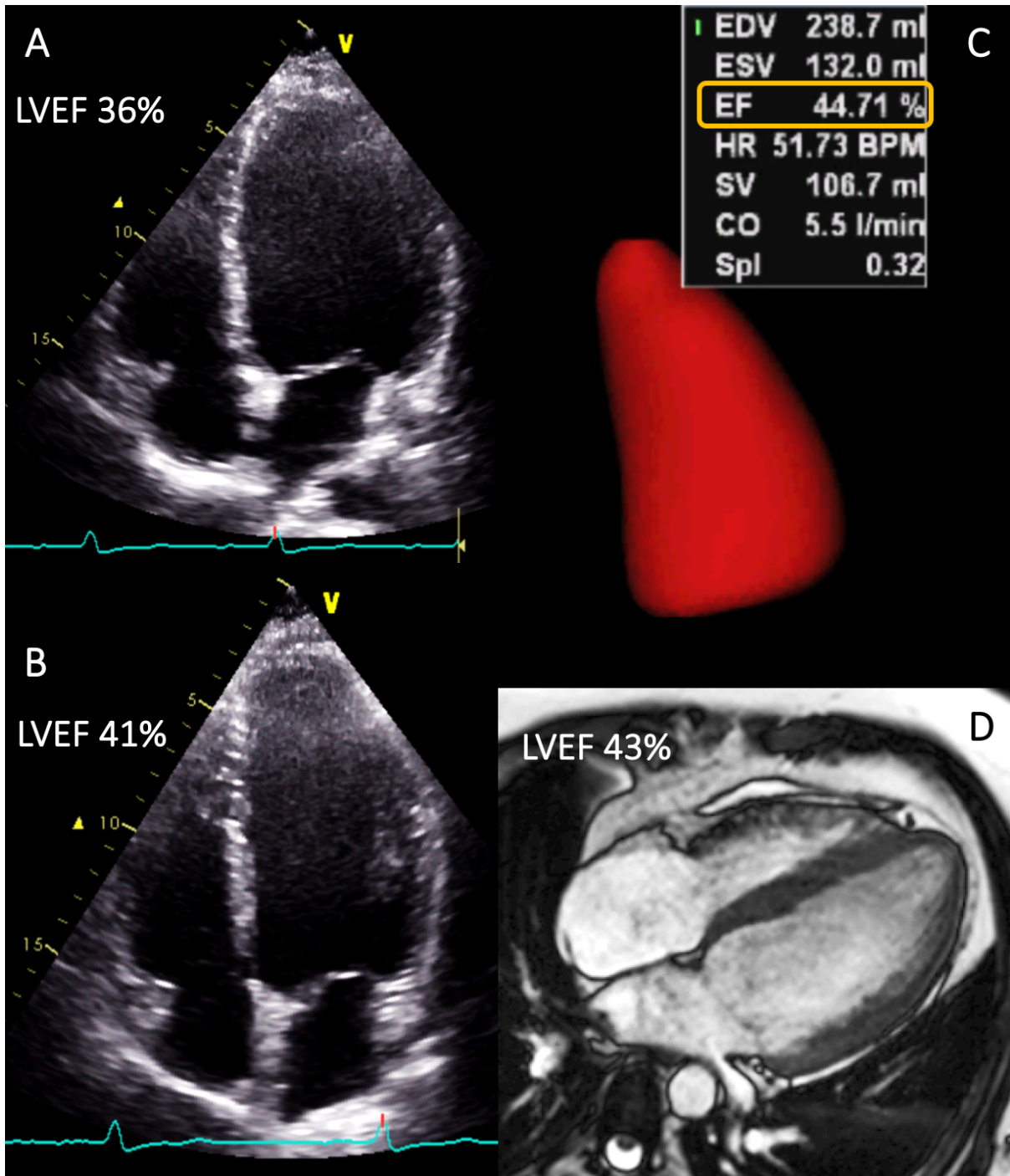


Figure 2
159x185 mm (x DPI)

1
2
3
4

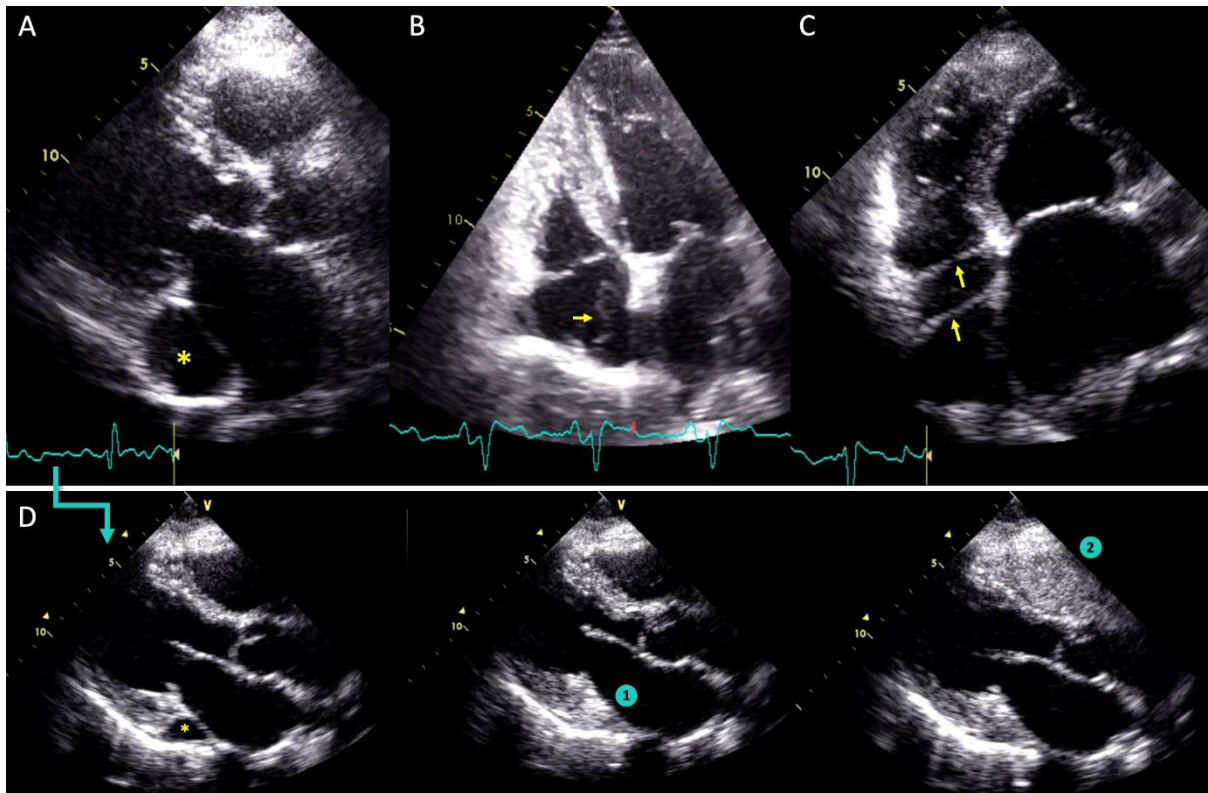
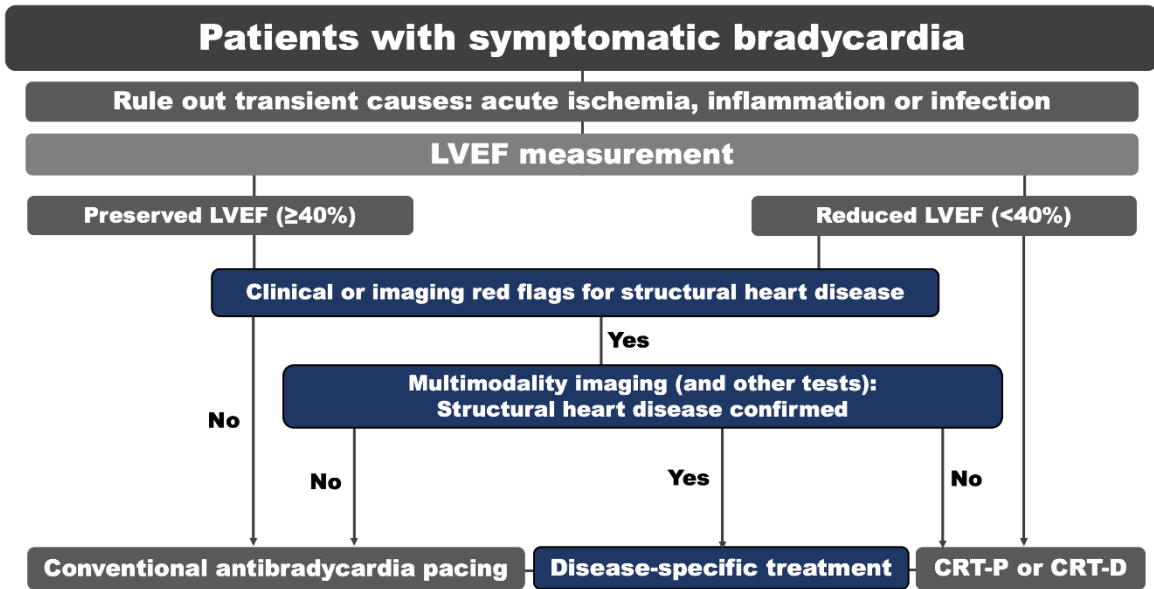


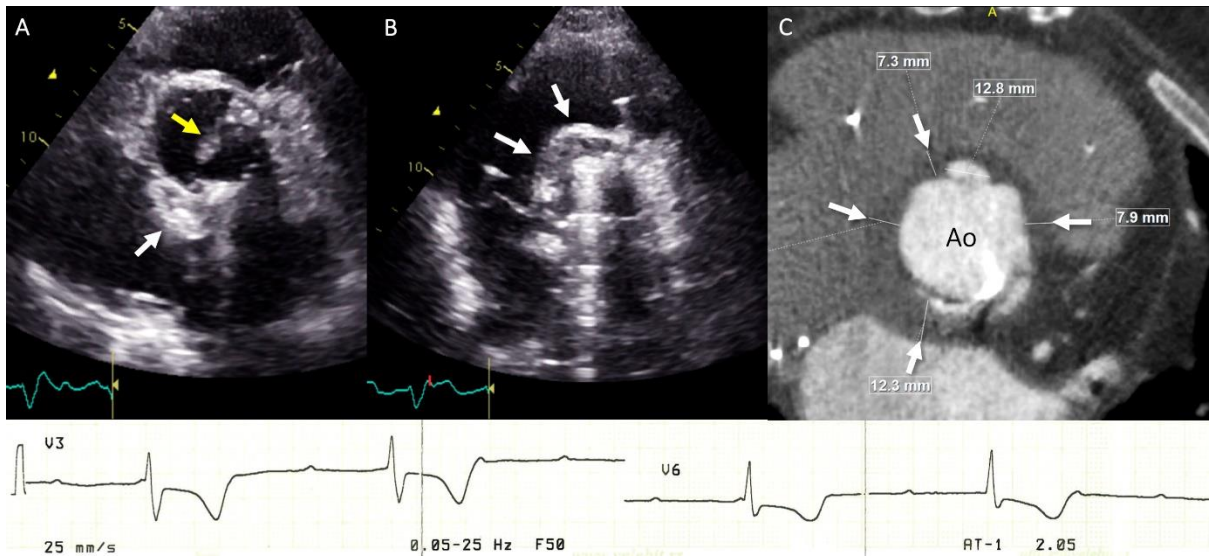
Figure 3
159x104 mm (x DPI)

1
2
3
4



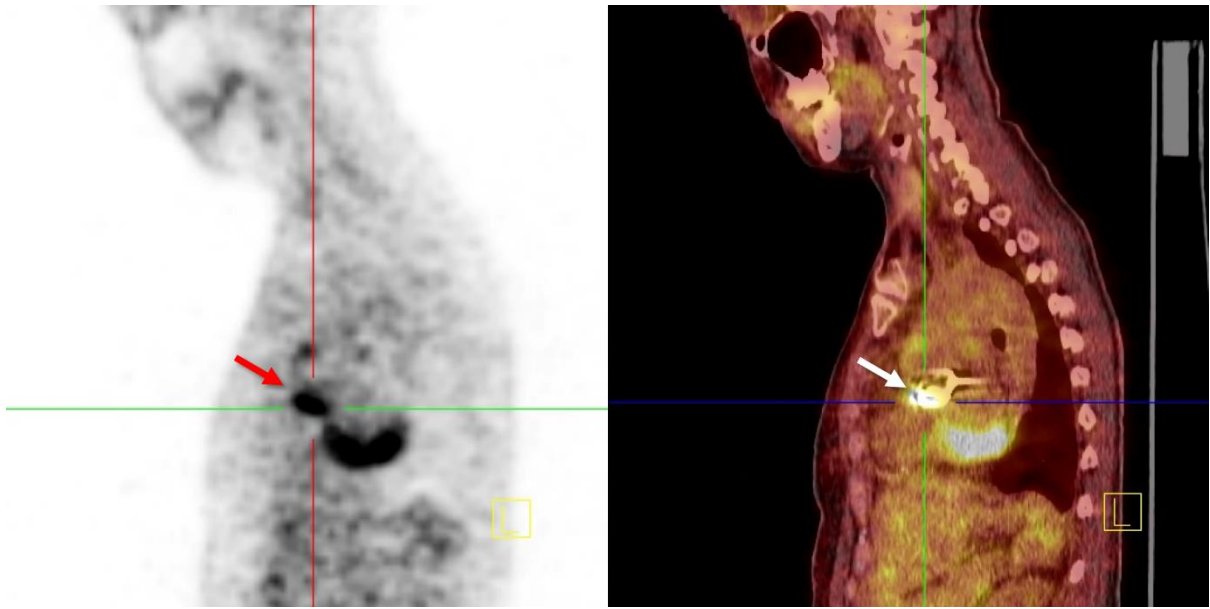
1
2
3
4

Figure 4
159x84 mm (x DPI)



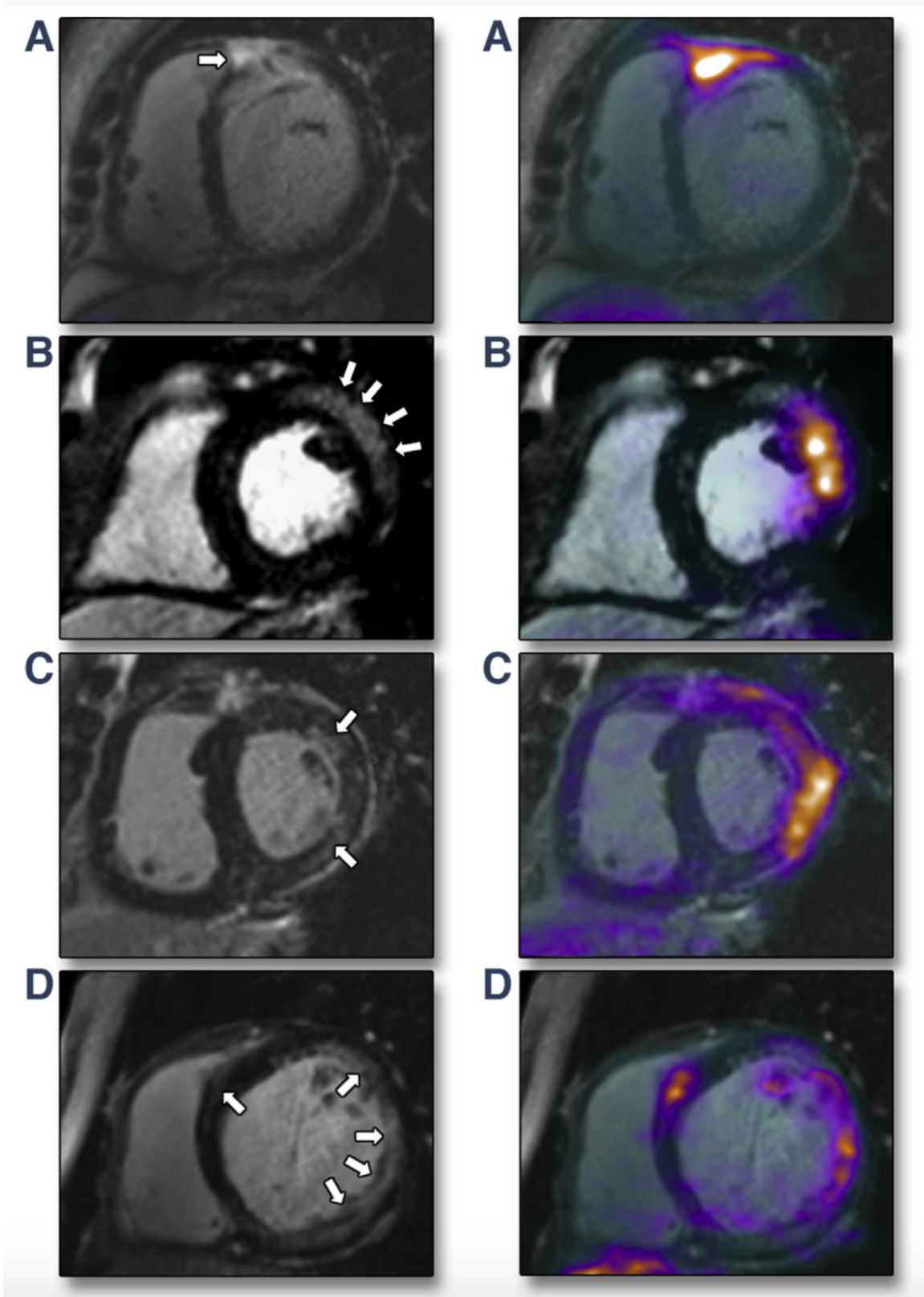
1
2
3
4

Figure 5
159x73 mm (x DPI)



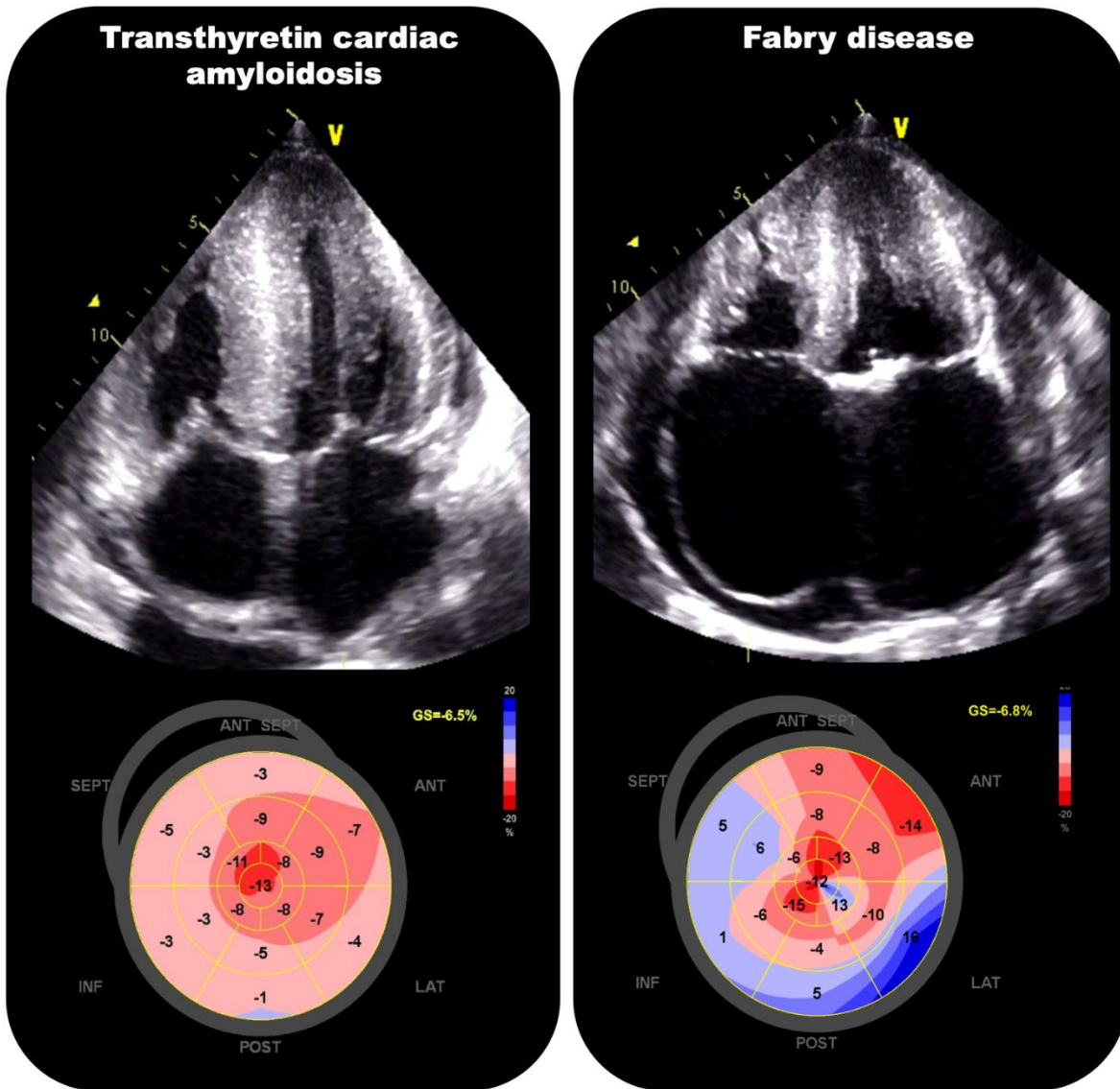
1
2
3
4

Figure 6
159x80 mm (x DPI)



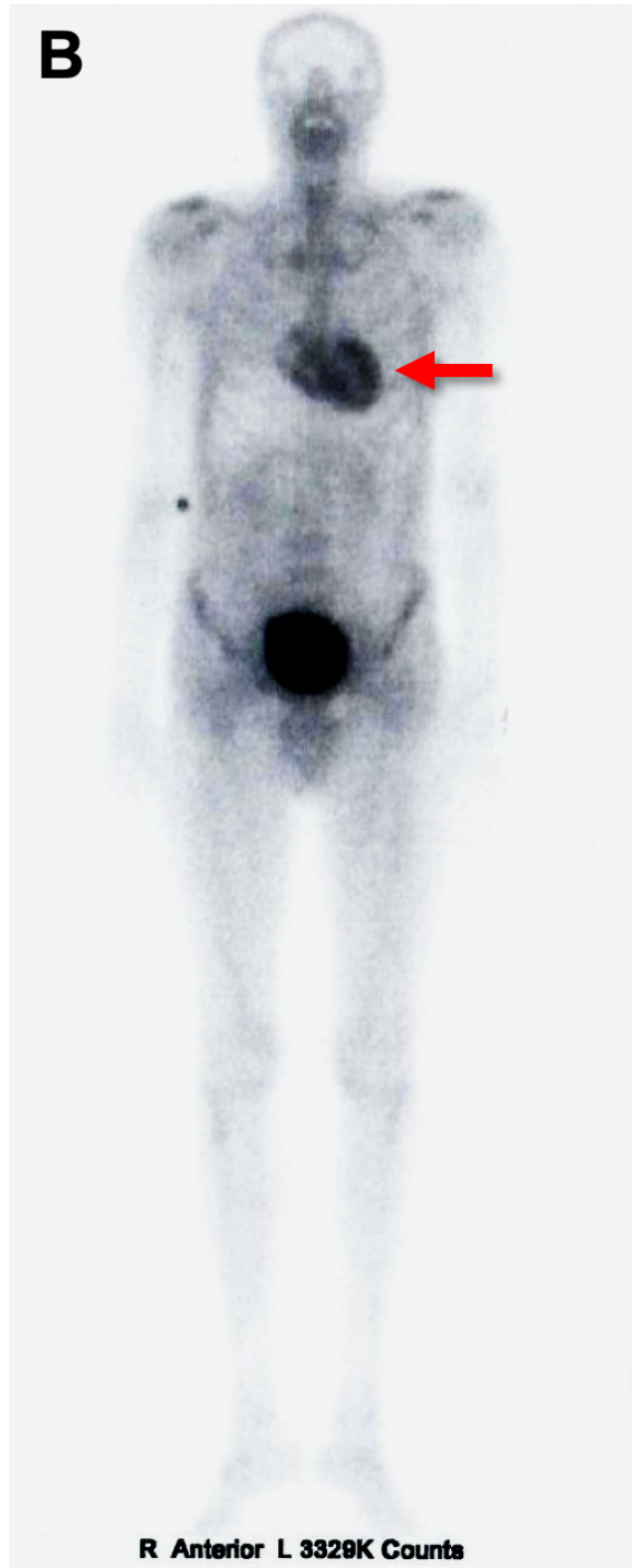
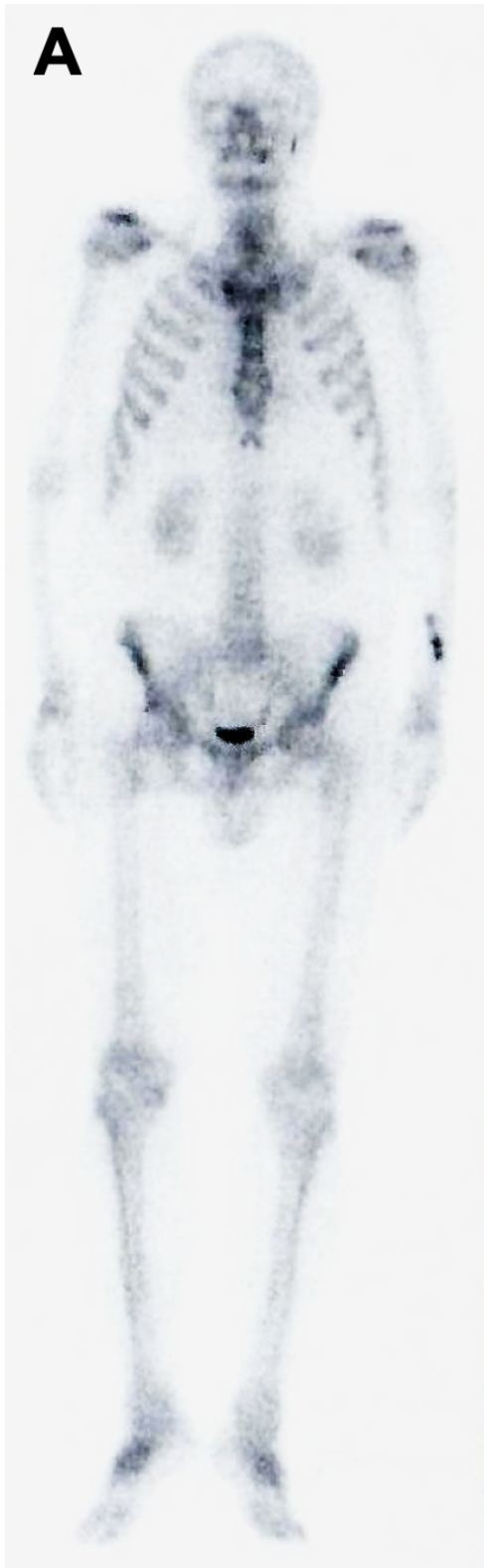
1
2
3

Figure 7
152x213 mm (x DPI)



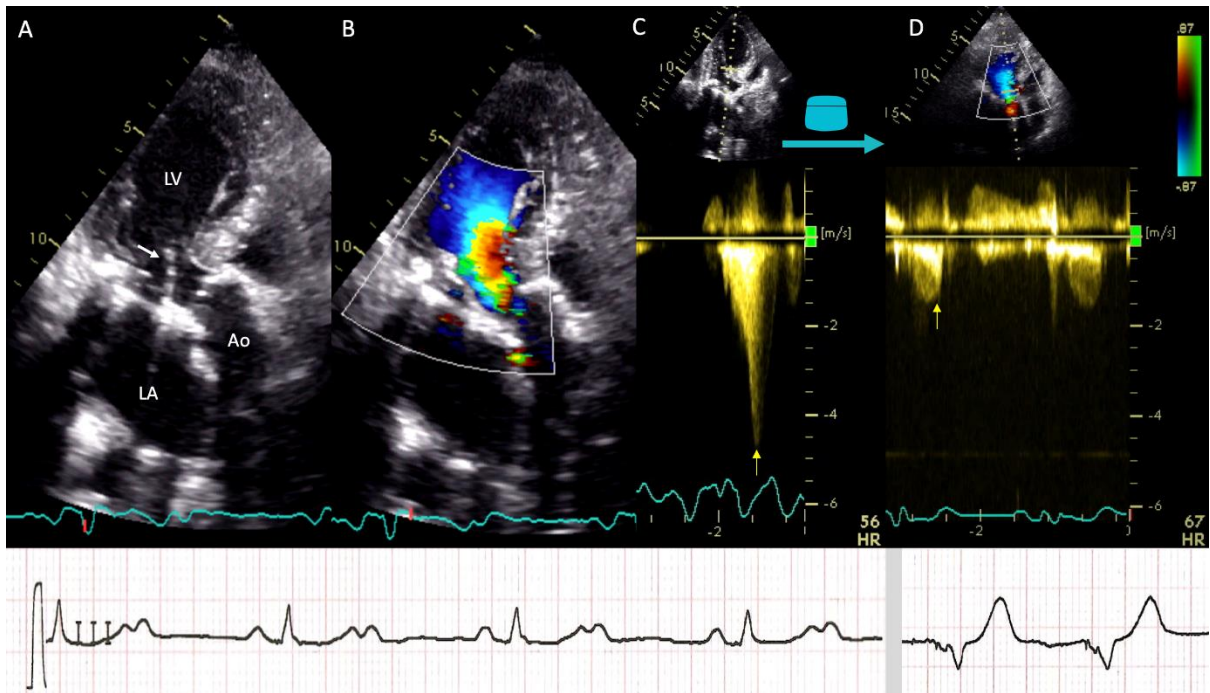
1
2
3
4

Figure 8
159x154 mm (x DPI)



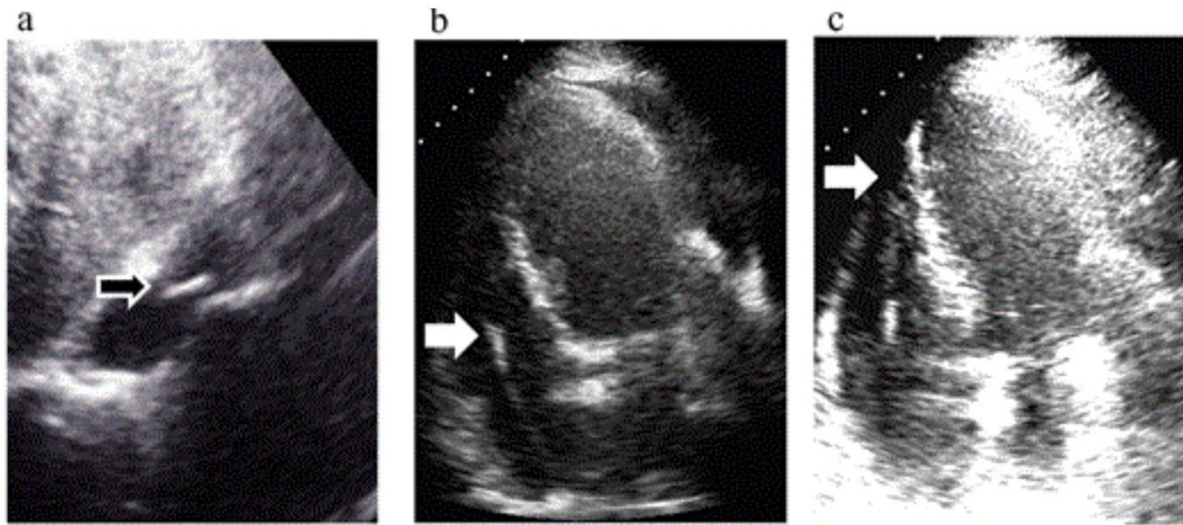
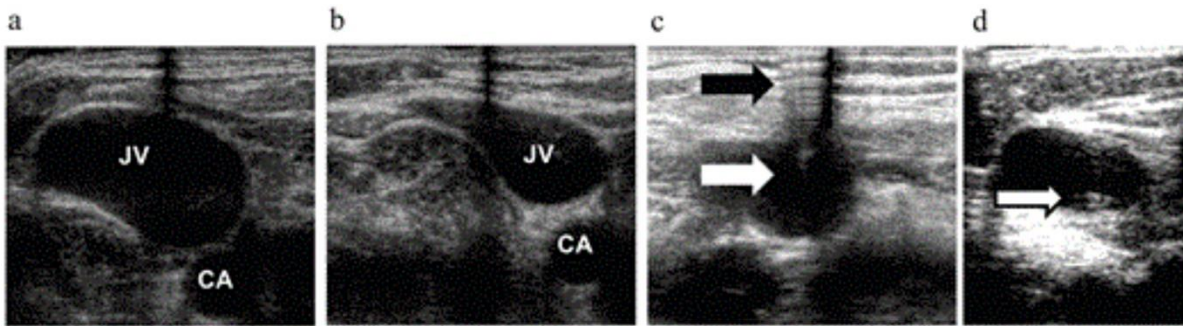
1
2
3
4

Figure 9
159x222 mm (x DPI)



1
2
3
4

Figure 10
159x91 mm (x DPI)



1
2
3
4

Figure 11
159x116 mm (x DPI)

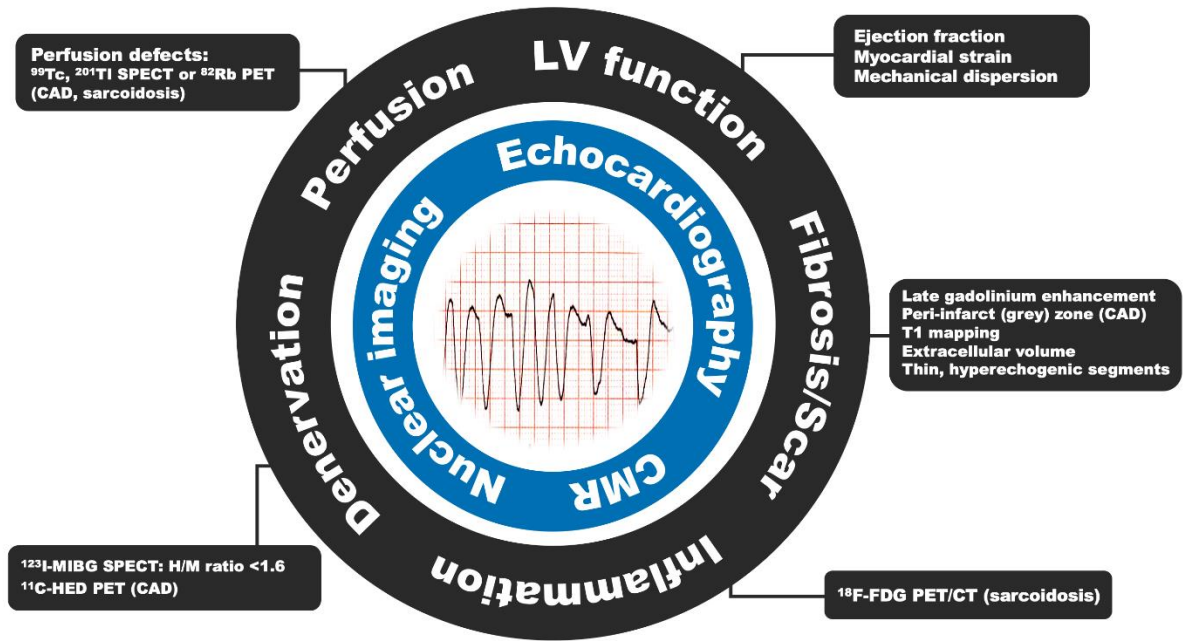


Figure 12
 159x88 mm (x DPI)

1
 2
 3
 4

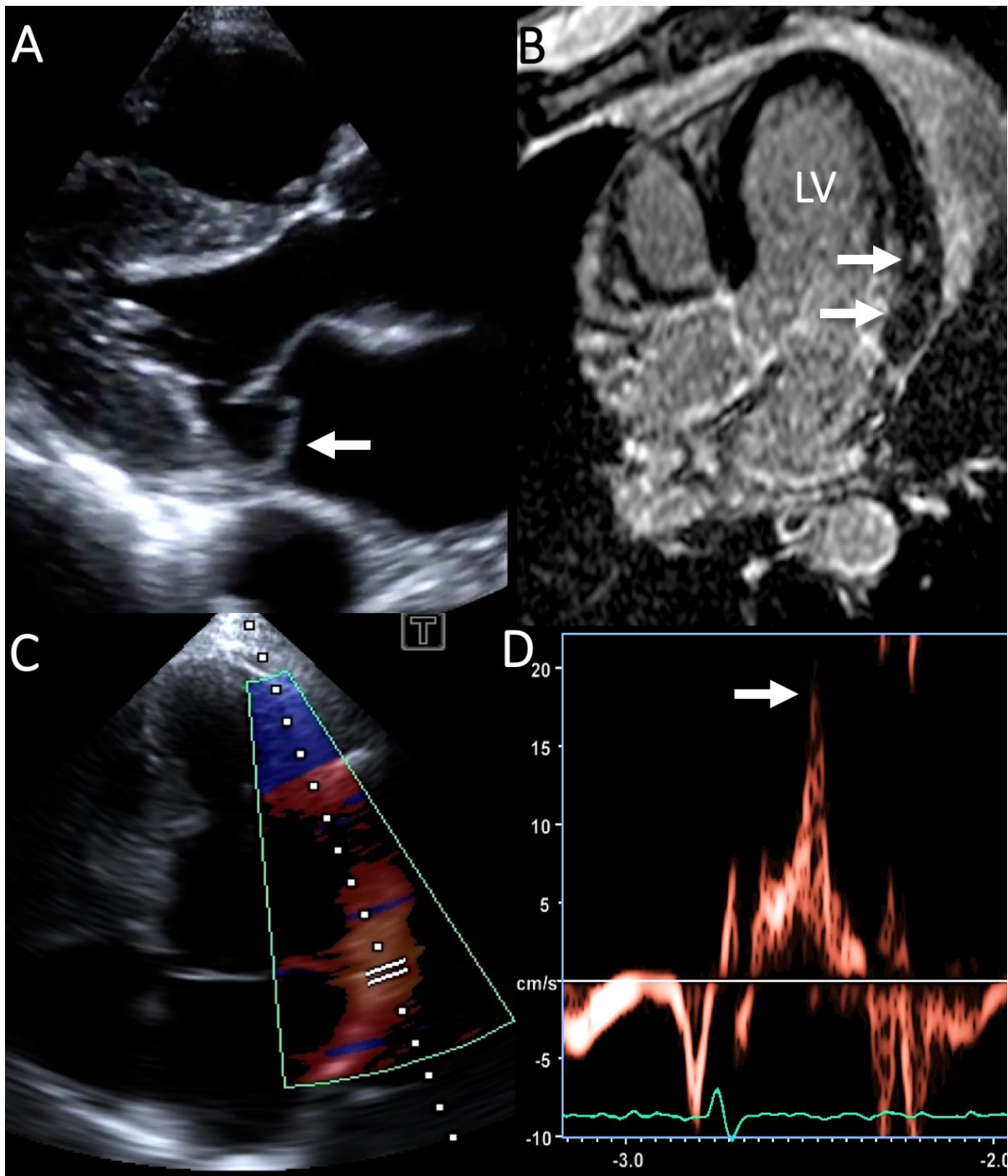


Figure 13
159x186 mm (x DPI)

1
2
3
4

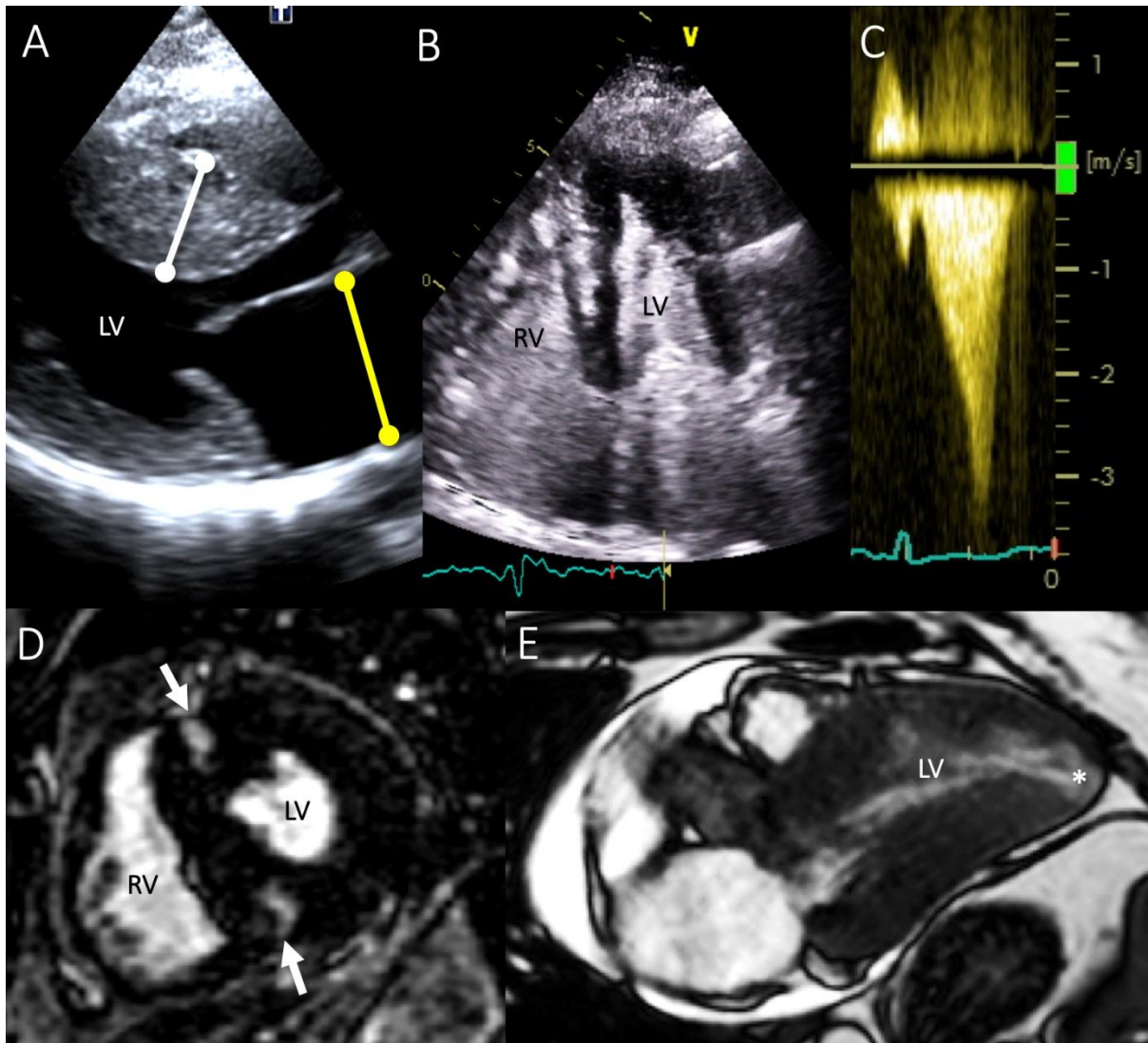
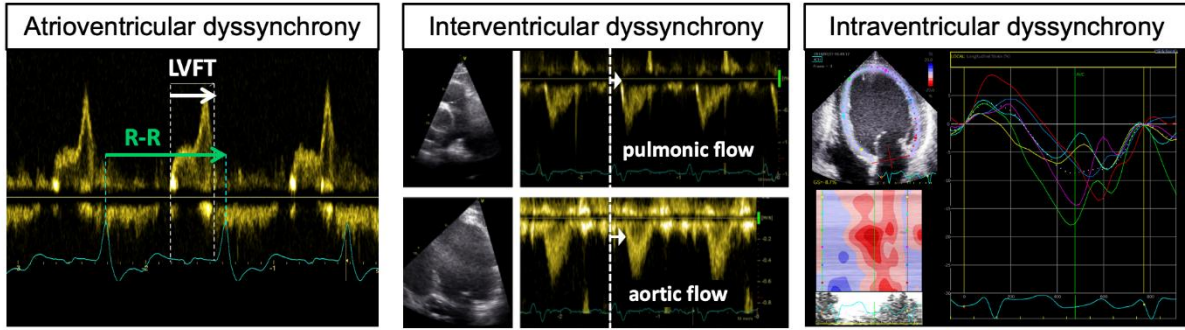


Figure 14
159x144 mm (x DPI)

1
2
3
4



1
2
3
4

Figure 15
159x45 mm (x DPI)

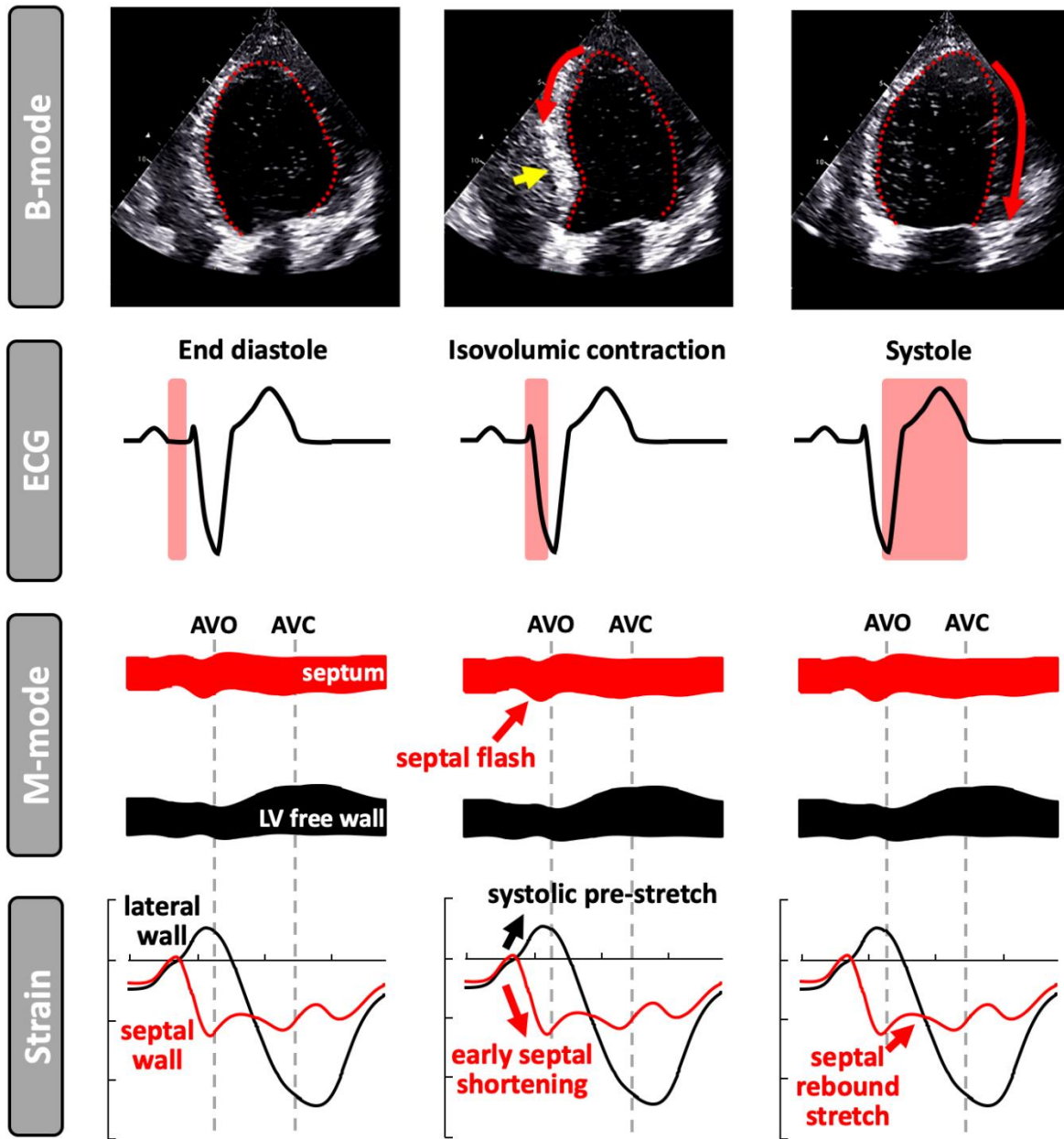
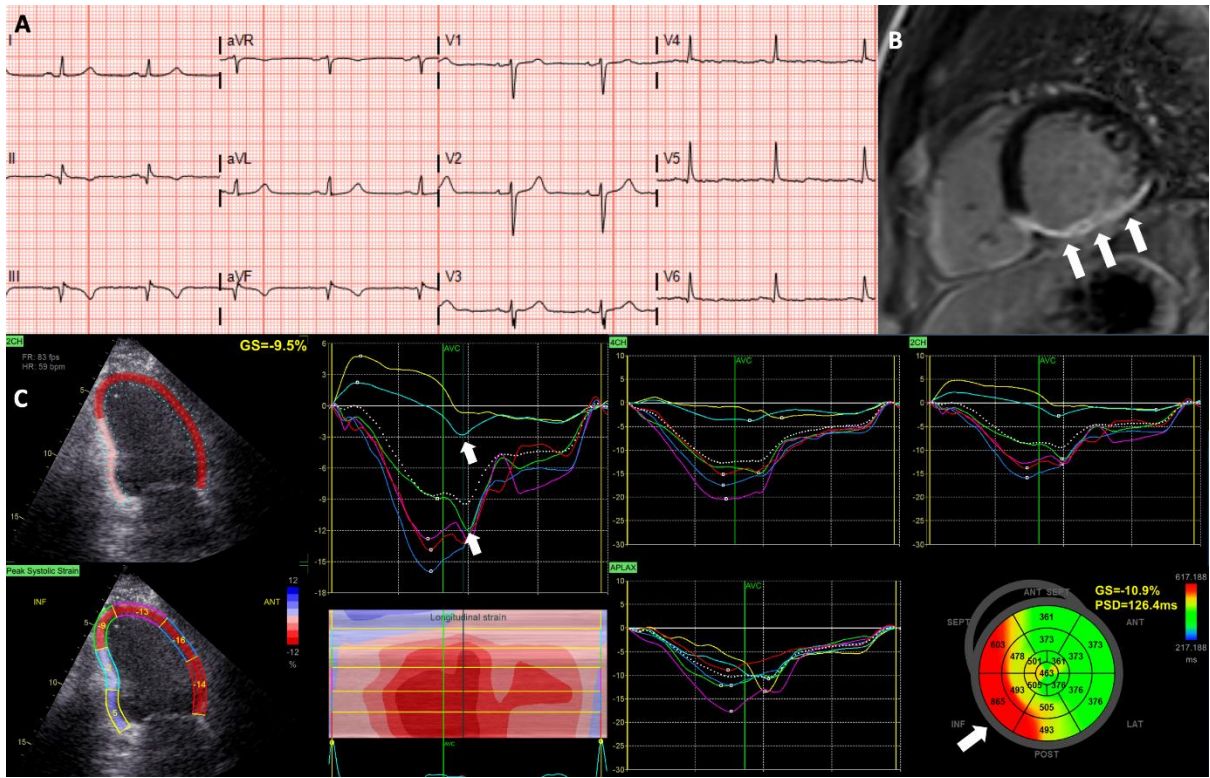


Figure 16
159x171 mm (x DPI)

1
2
3
4



1
2
3
4

Figure 17
159x102 mm (x DPI)

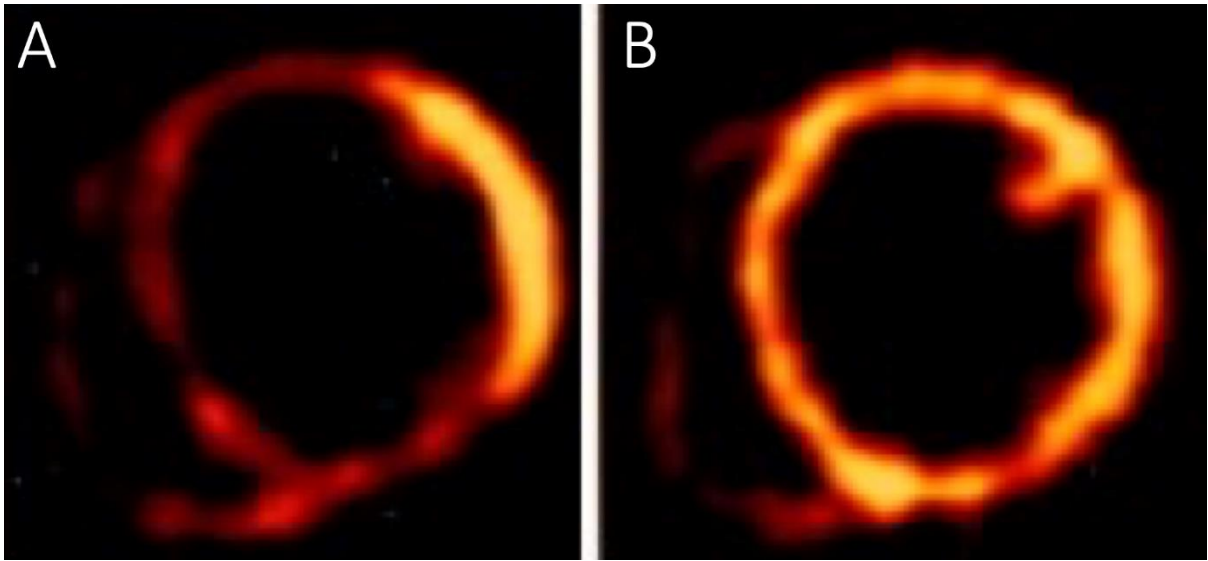


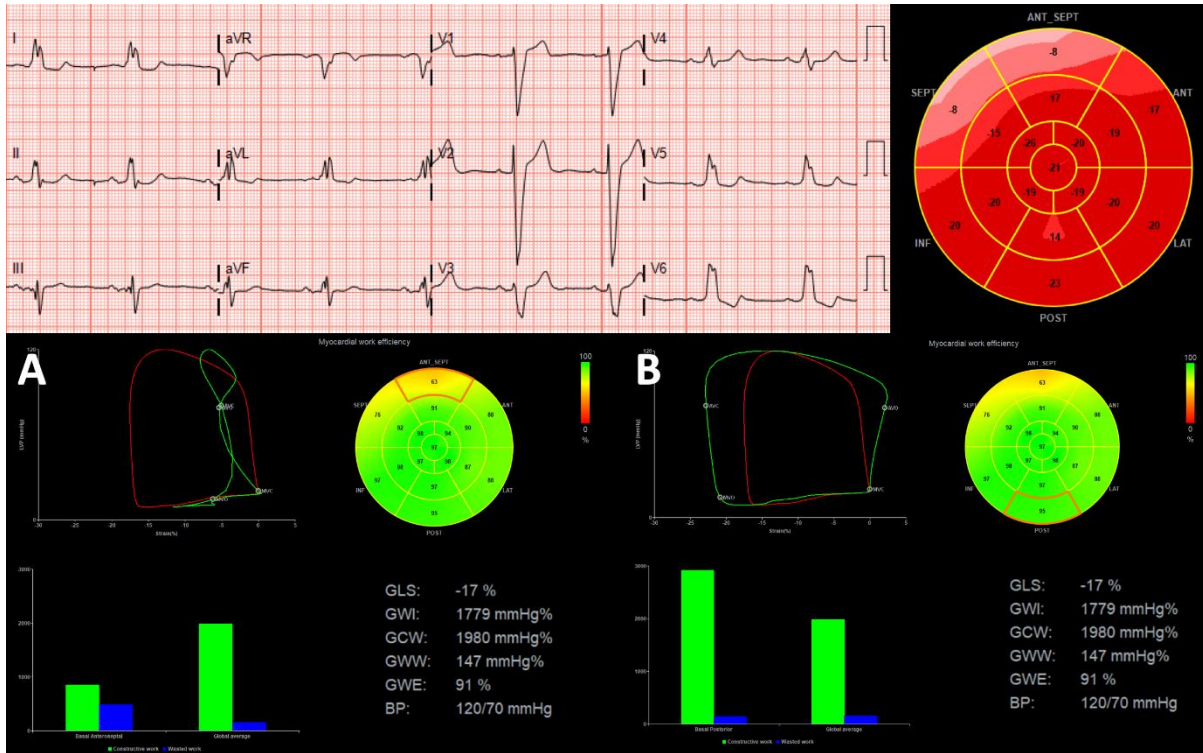
Figure 18
159x73 mm (x DPI)

1
2
3
4



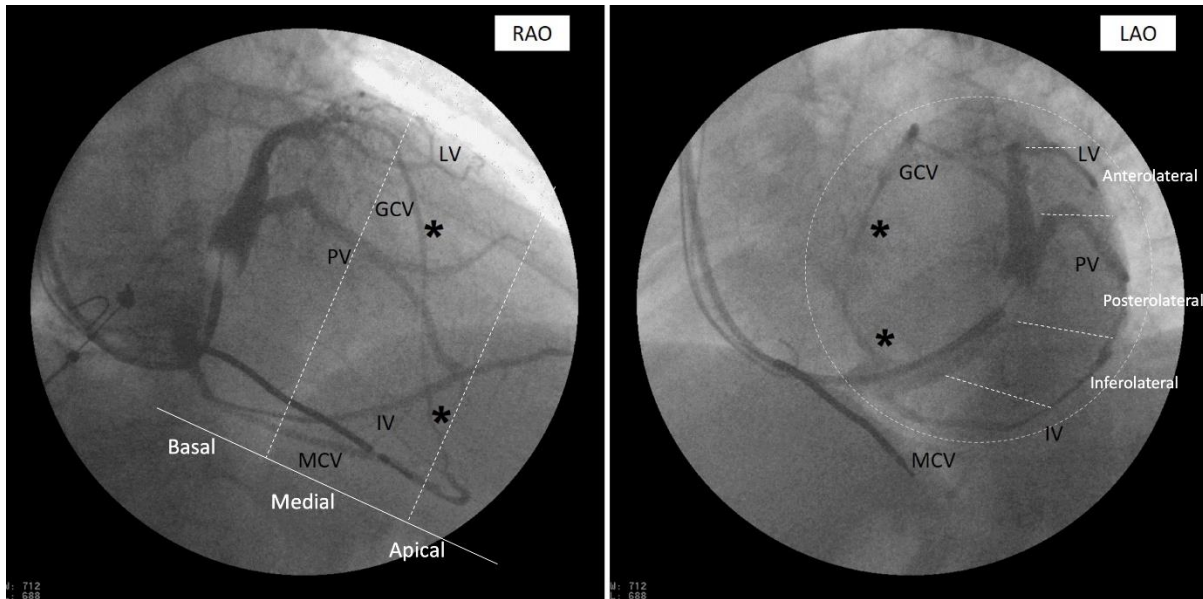
Figure 19
159x191 mm (x DPI)

1
2
3
4



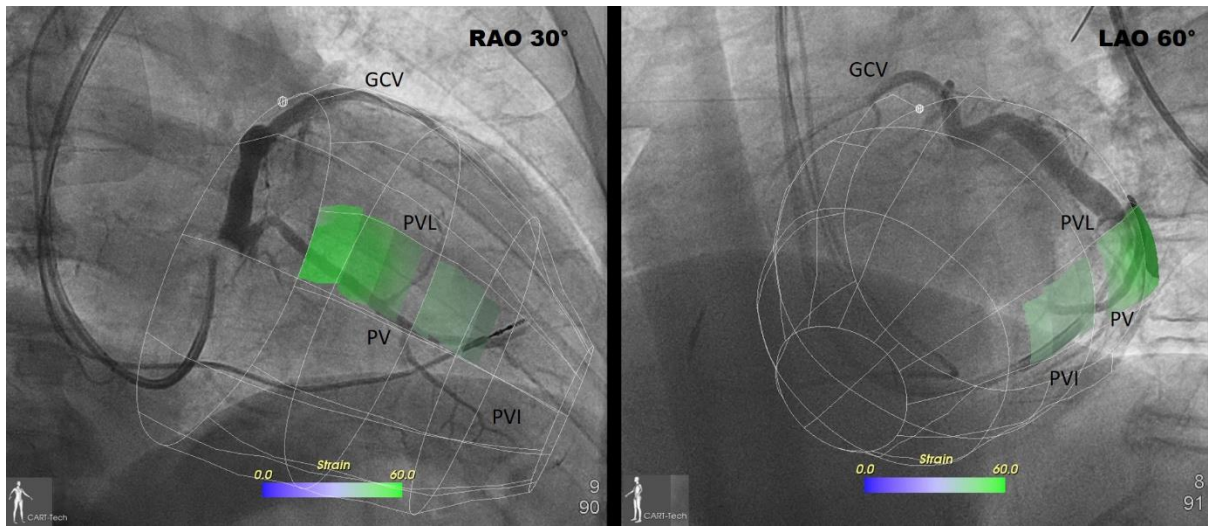
1
2
3
4

Figure 20
159x99 mm (x DPI)



1
2
3
4

Figure 21
159x79 mm (x DPI)



1
2
3

Figure 22
159x69 mm (x DPI)